Oxidant-Induced Mussel-Inspired Modification on PVDF Membrane for Oil/Water Separation

by

Chongdan Luo

A thesis submitted in partial fulfillment of the requirements for the degree of

Master of Science

in
Chemical Engineering

Department of Chemical and Materials Engineering
University of Alberta

Abstract

In this study, an oxidant-induced mussel-inspired modification was implemented to prepare modified polyvinylidene fluoride (PVDF) membrane utilizing the deposition of polydopamine (PDA) coating, which was oxidized by sodium periodate under a slightly acidic condition (pH = 5.0). The surface chemistry and morphologies of the decorated membranes were investigated by FTIR, XPS, EDS, and FESEM. The wettability and permeating properties of the membranes were evaluated by contact angle measurements and filtration tests. The results indicated that the oxidant-assisted PDA coating exhibited outstanding performance in deposition efficiency, hydrophilicity and permeation enhancement as compared with the conventional PDA coating under an autoxidative polymerization process in air (pH = 8.5).

This facile one-step methodology endowed the PVDF membrane with superhydrophilicity and underwater superoleophobicity owing to the hydrophilic functional groups and micro/nano-hierarchical structure formed on the membrane surface and pore walls according to the “Cassie-Baxter” state in the oil/water/solid system. After 2 h reaction, the modified PVDF membrane (pore size 0.45 μm) showed an ultrahigh water flux of 11934 ± 544 L m^{-2} h^{-1} under 0.038 MPa, and even reached 606 L m^{-2} h^{-1} only by gravity. This optimized membrane had an excellent capability to effectively separate oil/water mixtures and oil-in-water emulsions. In addition, the remarkable chemical and mechanical stabilities imply its great potential for the practical application in oil/water separation.

Besides, the oxidant-induced PDA modified PVDF membrane (pore size 0.22 μm) showed the protein resistance against bovine serum albumin (BSA) via a rapid deposition

time of 0.5 h. The wettability and surface zeta potential measurements indicated the improved hydrophilicity and the more negatively charged surface of the modified membrane, which led to the formation of the combined-water layer on the surface and the electrostatic repulsion to inhibit the adsorption or deposition of BSA, thus reducing the protein fouling. The dynamic protein filtration and static protein adsorption tests confirmed the promoted antifouling performance of the modified membrane at a neutral condition.

Preface

Chapter 4 of this thesis has been published as Luo, C.; Liu, Q., "Oxidant-Induced High-Efficient Mussel-Inspired Modification on PVDF Membrane with Superhydrophilicity and Underwater Superoleophobicity Characteristics for Oil/Water Separation", *ACS Applied Materials and Interfaces*, 2017, *9*, 8297-8307. I was responsible for the data collection, analysis as well as the manuscript composition. Liu, Q. was the supervisory author and was involved with concept formation and manuscript edits.

Chapter 5 of this thesis will be submitted for publication to the *Journal of Membrane Science* as Luo, C.; Liu, Q., "Rapid Deposition of the Oxidant-Induced Polydopamine Coating on PVDF Membrane for Protein-Resistant Modification". I was responsible for the data collection, analysis as well as the manuscript composition. Liu, Q. was the supervisory author providing comprehensive guidance and manuscript edits.

Chapter 4 of this thesis was presented at the 7th International Colloids Conference in Sitges, Spain, June, 2017.

Acknowledgement

I would first like to express my sincere gratitude to my supervisor Prof. Qingxia (Chad) Liu for his comprehensive guidance and assistance to my research project during my MSc. program. Prof. Liu has provided enormous support and encouragement, helping me with the promotion of professionalism and thought patterns that will continually influence me in a lifelong process of self-improvement.

I would like to express my appreciation to the support staffs of Canadian Centre for Clean Coal/Carbon and Mineral Processing Technologies (C^5MPT), Ms. Patricia Siferd and Mr. Carl Corbett, for their kind, efficient, and resourceful assistance throughout my research.

I would like to extend my heartfelt appreciation to all my colleagues from C^5MPT for their help and support. It has been a really delightful and pleasant experience working with them.

I would like to thank Ni Yang, Jie Ru, Nathan Gerein, Chen Wang and Shihong Xu for their experienced training and expert technician support in the characterization part of my research work.

I would like to acknowledge the financial support from the Natural Sciences and Engineering Research Council of Canada (NSERC), Canadian Centre for Clean Coal/Carbon and Mineral Processing Technologies (C^5MPT), the Canada Foundation for Innovation (CFI) and the Alberta Advanced Education & Technology Small Equipment Grants Program (AET/SEGP).

Finally, I would also like to convey my profound gratitude to my family and friends for their unconditional love and support.

Table of Contents

List of Tables

List of Figures

List of Symbols

θ_F	The liquid contact angle on a flat solid surface, degree
γ_{SV}	The interfacial energy between solid and vapor, J m^{-2}
γ_{SL}	The interfacial energy between solid and liquid, J m^{-2}
γ_{LV}	The interfacial energy between liquid and vapor, J m^{-2}
R	The ratio of the actual surface area to the projected surface area of the rough surface
θ_{app}	The apparent contact angle of the rough surface, degree
Φ_s	The fraction of the contact area between surface and liquid
γ_o	The interfacial tension between oil and air, N m^{-1}
θ_o	The oil contact angle with solid, degree
γ_{os}	The interfacial tension between oil and solid, N m^{-1}
γ_s	The interfacial tension between solid and air, N m^{-1}
γ_w	The interfacial tension between water and air, N m^{-1}
θ_w	The water contact angle with solid, degree
γ_{ws}	The interfacial tension between water and solid, N m^{-1}
θ_{ow}	The underwater oil contact angle with a flat surface, degree
γ_{ow}	The interfacial tension between oil and water, N m^{-1}
θ_{ow}'	The underwater oil contact angle with a hierarchical rough surface, degree
V (in Chapter 4)	The volume of filtrate, L
A (in Chapter 4)	The effective separation area, m^2
Δt	The permeation time, h

C_f	The oil concentration of filtrates, ppm
C_o	The oil concentration of original oil/water mixtures or oil-in-water emulsions, ppm
DD	The deposition density, mg cm^{-2}
M_1	The weight of the membrane after modification, mg
M_0	The weight of the pristine membrane, mg
A (in Chapter 5)	The area of the membrane, cm^2
ζ	The surface zeta potential, V
ΔE	The streaming potential, V
ΔP	The applied pressure, Pa
ε	The permittivity, F m^{-1}
η	The viscosity of the solution, kg m^{-1} s^{-1}
κ	The conductivity of the solution, S m^{-1}
A_{BSA}	The amount of BSA adsorbed on the surface and pores of membrane per unit area, μg cm^{-2}
C_o	The actual concentration of the initial BSA solution, mg mL^{-1}
V_o	The actual volume of the initial BSA solution, mL
C_{BSA}	The concentration of the BSA solution obtained eventually, mg mL^{-1}
V (in Chapter 5)	The volume of the BSA solution obtained eventually, mL
S	The area of sample, cm^2
J_{w1}	The pure water flux, L m^{-2} h^{-1}
J_{BSA}	The BSA solution flux, L m^{-2} h^{-1}

J_{w2}	The pure water flux after protein permeation, L m^{-2} h^{-1}
F_r	The reversible fouling ratio
F_{ir}	The irreversible fouling ratio
F_r/RFR	The percentage of reversible fouling in total fouling
F_{ir}/RFR	The percentage of irreversible fouling in total fouling

List of Abbreviations

MF	Microfiltration
UF	Ultrafiltration
NF	Nanofiltration
RO	Reverse osmosis
PDA	Polydopamine
DHI	$(dopamine)_2$/5,6-dihydroxyindole
PVDF	Polyvinylidene fluoride
FESEM	Field-emission scanning electron microscope
EDS	Energy dispersive X-Ray spectroscopy
ATR-FTIR	Attenuated total reflectance-fourier transform infrared spectroscopy
XPS	X-Ray photoelectron spectroscopy
SEM	Scanning electron microscope
PTFE	Polytetrafluoroethylene
PU	Polyurethane
PS	Polystyrene
PAM	Polyacrylamide
DA	Dopamine
TEOS	Tetraethoxysilane
PDDA	Poly(diallyldimethylammonium chloride)
PFO	Perfluorooctanoate
CTAB	Cetyltrimethylammonium bromide

PVA	Polyvinyl alcohol
CA	Cellulose acetate
PEI	Polyetherimide
MWCO	Molecular weight cut-off
CM-CS	N,O-carboxymethyl chitosan
PES	Polyethersulfone
TiO_2	Titanium dioxide
SiO_2	Silicon dioxide
Al_2O_3	Aluminium oxide
DMAA	N,N-dimethylacrylamide
BSA	Bovine serum albumin
NVP	N-vinyl-2-pyrrolidinone
AAG	2-acrylamidoglycolic acid monohydrate
AAP	2-acrylamido-2-methyl-1-propanesulfonic acid
PSf	Polysulfone
$CHCl_3$	Chloroform
CCl_4	Carbon tetrachloride
PPHFMM	Polypropylene hollow fiber microporous membrane
CL	Cathodoluminescence
CCD	Charge-coupled device
TOC	Total organic carbon
IC	Inorganic carbon
TC	Total carbon

NDIR	Non-dispersive infrared analysis
KCl	Potassium chloride
NaOH	Sodium hydroxide
UV-Vis-NIR Spectroscopy	Ultraviolet-visible-near infrared spectroscopy
PE	Polyethylene
PP	Polypropylene
Tris-HCl	Tris (hydroxymethyl) aminomethane hydrochloride
rpm	Rate per minute
SDS	Sodium dodecyl sulfate
DI	Deionized
PVP	Poly(N-vinyl pyrrolidine)
MEL	2-methacryloyloxyethyl lipoate
ATRP	Atom transfer radical polymerization
PSBMA	Poly(sulfobetaine methacrylate)
ZrO_2	Zirconium dioxide
IEP	Isoelectric point
PBS	Phosphate buffered saline
DD	Deposition density
RFR	Relative flux reduction
FRR	Flux recovery ratio

Chapter 1 Introduction

1.1 Background

Water scarcity becomes severer as the population and industries expand. The worldwide water consumption will continue increasing to meet various needs in domestic, agriculture, industry, and energy sectors.[1] Meanwhile, large amounts of wastewater are produced every day in the petrochemical, pharmaceutical, metallurgical, chemical and food industries.[2] The treatment and reclamation of wastewater bring about many inevitable challenges, stimulating research interests on developing various technologies to address this issue, such as membrane, flotation, flocculation, adsorption, distillation, and photocatalysis.[3-8] Membrane technology based on separation mechanism is favored over other approaches owing to its advantages including low cost, high energy-efficiency, and large flexibility.[9] Pressure-driven separation techniques can be classified as microfiltration (MF), ultrafiltration (UF), nanofiltration (NF) and reverse osmosis (RO) depending on the pore size of the membranes utilized in different separation processes.[10]

However, the major problem involved in practical applications is the membrane fouling, including the deposition of retained particles, colloids, macromolecules, inorganic and organic matters on the membrane surface or inside the pores.[11] The temporary and permanent fouling decrease the membrane flux and separation efficiency due to the physical and chemical interactions between membrane surface and foulants, especially for the hydrophobic membranes. Therefore, numerous researches have been conducted to improve the antifouling properties of membranes to overcome the challenge of fouling via various modification methods.

1.1.1 Oil/Water Separation

A large quantity of oil-polluted water is generated in oil spill accidents, marine transportation, petrochemical, textile, and food industries, causing serious pollution to the water system.[12] The

harmful sequential impacts of oil-polluted water on ecosystem and health of human body cannot be underestimated. The development of effective oil/water separation techniques becomes a fast rising challenge and attracts worldwide attention. Conventional methods such as gravity separation, skimming, flotation, in situ burning, and chemical dispersal have emerged in recent years.[13-15] However, all of these methods are more or less limited in their efficiency, economy, and energy consumption. Therefore, the advanced materials with excellent capability of oil/water separation accompanying with high efficiency, low cost, and energy-saving have been urgently needed.

The utilization of the membranes with special wettability is considered as the most promising methodology for selective oil/water separation because of the completely opposite affinities of the membranes towards oil and water.[16-18] The wettability of the membrane surface is determined by the surface chemistry and geometrical structure.[19] Two kinds of special wettable membranes with the superhydrophobic/superoleophilic property or the superhydrophilic/superoleophobic property have been fabricated and applied to separate oil and water effectively based on their selective behaviors.

1.1.2 Antifouling Modification

The outstanding intrinsic features of hydrophobic membranes, such as high mechanical strength, thermal stability, and chemical resistance, endow the membranes with better tolerability for separation processes compared with hydrophilic membranes.[20] However, the membrane fouling phenomenon is an inevitable problem during practical applications because of the physical and chemical interactions between membranes and foulants, such as proteins, colloidal particles, and organic compounds, etc., which are hydrophobic in nature as well.[21] The main factors that determine the membrane fouling include hydrophilicity/hydrophobicity balance, surface charge, and surface roughness.

Hydrophilicity modification is a common approach to improve antifouling property of hydrophobic membranes. A modified surface with high hydrophilicity can form a tightly bounded water layer on the surface, diminishing the adsorption of foulants due to the weakening of hydrophobic interaction, resulting in the enhancement of antifouling property.[22]

Surface charges also impact the membrane fouling by the electrostatic force between the surface and the foulants. For instance, the repulsive forces between a charged surface and proteins with the same charge can diminish adsorption and deposition. Thus, numerous efforts have been undertaken to incorporate ionizable functional groups on the membrane surface to reduce fouling.[23-27]

Surface roughness of the membrane is also relative to the antifouling performance. Colloidal particles are inclined to accumulate and deposit on a rougher membrane surface due to the valley structures that may be blocked by the colloidal particles.[28] As for smaller organic molecules, a rougher and heterogeneous surface is more likely to be fouled than a smoother one due to the larger surface area. In general, more attempts are focused on smoothing the membrane surface to diminish fouling.[21]

1.1.3 Mussel-Inspired Modification

Messersmith et al. reported the mussel-inspired methodology that polydopamine (PDA) can be deposited on virtually all types of inorganic or organic substrates under a slightly alkaline condition at the ambient atmosphere.[29] PDA coating layer can act as a versatile platform because of the reactive groups including catechol, amine, and imine, providing many possibilities of subsequent modifications to further promote the functionalization for different purposes.[30] Since 2007, numerous researches have focused on the PDA modifications applied in environmental, biomedical, and energy fields owing to its reactivity, simplicity, and versatility.[31]

The exact polymerization mechanism still remains unclear. Messersmith et al. proposed that the autoxidative polymerization of PDA may be due to the strong adhesion forces of catechol structure and the formation of the cross-linking networks ascribed to the covalent and non-covalent interactions, such as hydrogen bonding, π-π stacking and charge transfer interaction (Figure 1.1a).[29] Lee et al. further revealed that PDA could be formed through two pathways in parallel, i.e. non-covalent self-assembly of $(dopamine)_2$/5,6-dihydroxyindole (DHI) and covalent polymerization of DHI-DHI dimeric and dopamine-DHI-DHI trimeric conjugates (Figure 1.1b).[32] However, Liebscher et al. proposed the covalent structure of monomer units comprised by dihydroxyindole and indoledione with different degrees of saturation and parallel assembled PDA chains via hydrogen-bonding interaction (Figure 1.1c).[33]

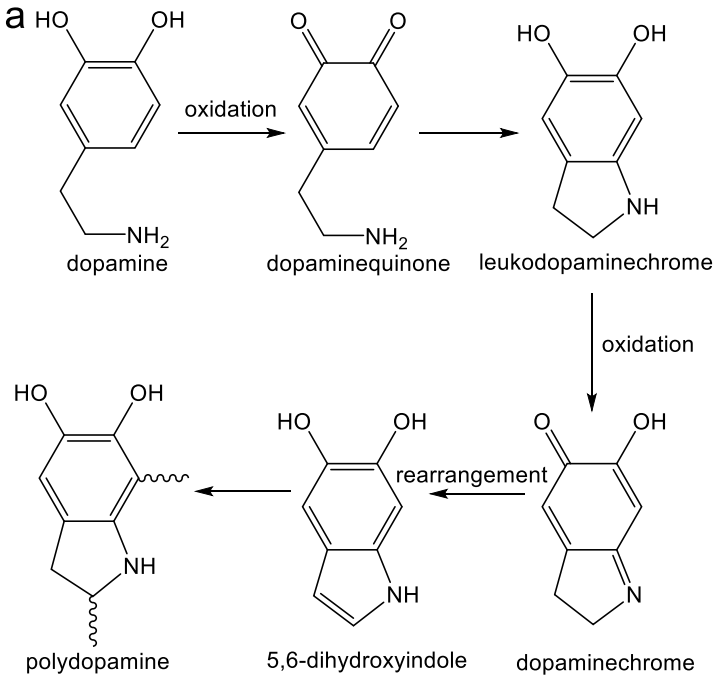

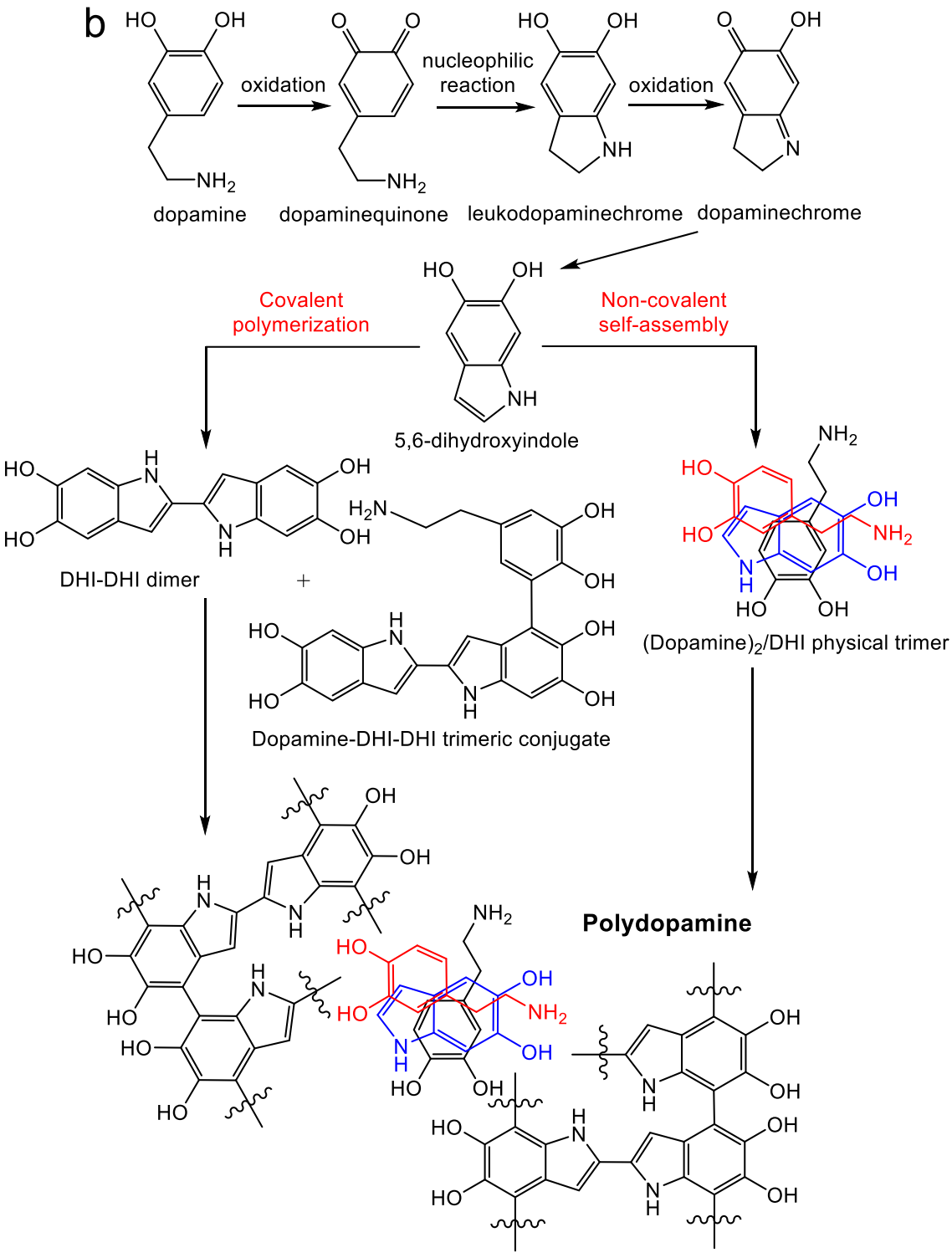
b
oxidation
nucleophilic reaction
oxidation
dopamine
dopaminequinone
leukodopaminechrome
dopaminechrome
5,6-dihydroxyindole
Covalent polymerization
Non-covalent self-assembly
DHI-DHI dimer
+
Dopamine-DHI-DHI trimeric conjugate
(Dopamine)2/DHI physical trimer
Polydopamine

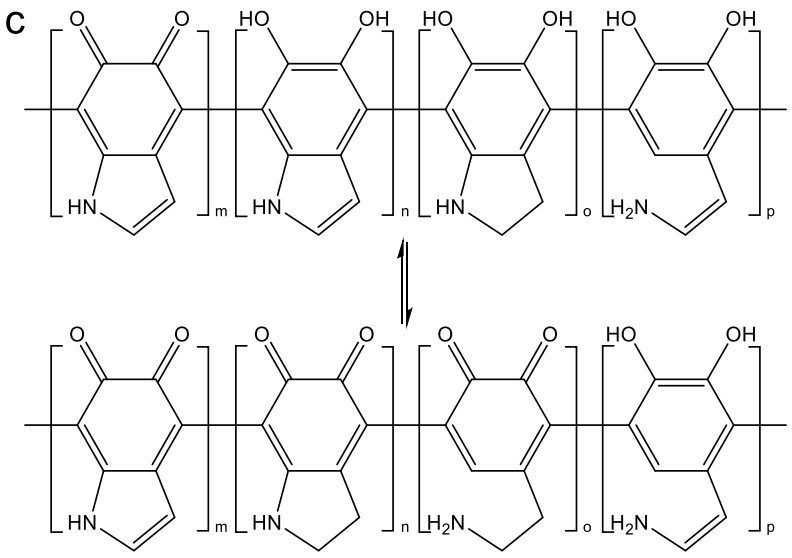

Figure 1.1 Possible mechanisms and structures of PDA proposed by (a) Messersmith, (b) Lee, and (c) Liebscher.

Importantly, PDA coating can be flexibly employed in membrane technology. As a surface modifier, PDA can be directly deposited on the hydrophobic membrane surface to improve the hydrophilicity owing to its hydrophilic functional groups.[34] In addition, PDA has also been served as an intermediate layer to conduct secondary reaction combining with organic or inorganic layers.[35, 36] Another application is to utilize PDA as one of the membrane components. For instance, PDA can facilitate the interfacial compatibility between membrane matrixes and inorganic nanofillers.[37] On the other hand, dopamine-conjugated polymers obtained by pre-decoration can be employed as membrane modifiers or membrane components for various applications.[38, 39]

1.2 Objectives

Mussel-inspired polydopamine coating shows superiorities in membrane science. However, the limitations of the pure PDA coating result in the low-efficiency, instability, poor homogeneity, and deficient hydrophilicity, which significantly restrict its potential applications. The main

objectives of this study are as following:

1. To compare the high-efficient deposition of the PDA coating oxidized by sodium periodate in a weakly acidic condition with the low-efficient conventional autoxidation process on polyvinylidene fluoride (PVDF) membrane.

2. To characterize the membranes by various surface characterization techniques including FESEM, EDS, ATR-FTIR, XPS, and electrokinetic analyzer.

3. To evaluate the improvement of hydrophilicity and water permeation of the modified membranes by contact angle measurements and water flux tests.

4. To investigate the applications of the optimized membranes for oil/water separation and protein resistance.

1.3 References

(1) *Coping with Water Scarcity. Challenge of the Twenty-First Century;* United Nations (UN) Water. Food and Agricultural Association (FAO): 2007.

(2) Padaki, M.; Murali, R. S.; Abdullah, M. S.; Misdan, N.; Moslehyani, A.; Kassim, M. A.; Hilal, N.; Ismail, A. F. Membrane Technology Enhancement in Oil–Water Separation. A Review. *Desalination* **2015***, 357*, 197-207.

(3) Schmidt, C. K.; Brauch, H. N, N-dimethylsulfamide as Precursor for N-nitrosodimethylamine (NDMA) Formation upon Ozonation and Its Fate during Drinking Water Treatment. *Environ. Sci. Technol.* **2008***, 42*, 6340-6346.

(4) Gao, H.; Sun, Y.; Zhou, J.; Xu, R.; Duan, H. Mussel-Inspired Synthesis of Polydopamine-Functionalized Graphene Hydrogel as Reusable Adsorbents for Water Purification. *ACS Appl. Mater. Interfaces* **2013***, 5*, 425-432.

(5) Joss, A.; Zabczynski, S.; Gbel, A.; Hoffmann, B.; Lffler, D.; McArdell, C. S.; Ternes, T. A.;

Thomsen, A.; Siegrist, H. Biological Degradation of Pharmaceuticals in Municipal Wastewater Treatment: Proposing a Classification Scheme. *Water Res.* **2006***, 40*, 1686-1696.

(6) Zhang, C.; Yang, H.; Wan, L.; Liang, H.; Li, H.; Xu, Z. Polydopamine-Coated Porous Substrates as a Platform for Mineralized β-FeOOH Nanorods with Photocatalysis under Sunlight. *ACS Appl. Mater. Interfaces* **2015***, 7*, 11567-11574.

(7) Chen, W.; Su, Y.; Peng, J.; Zhao, X.; Jiang, Z.; Dong, Y.; Zhang, Y.; Liang, Y.; Liu, J. Efficient Wastewater Treatment by Membranes through Constructing Tunable Antifouling Membrane Surfaces. *Environ. Sci. Technol.* **2011***, 45*, 6545-6552.

(8) Zhang, R.; Liu, Y.; He, M.; Su, Y.; Zhao, X.; Elimelech, M.; Jiang, Z. Antifouling Membranes for Sustainable Water Purification: Strategies and Mechanisms. *Chem. Soc. Rev.* **2016***, 45*, 5888-5924.

(9) Drioli, E.; Romano, M. Progress and New Perspectives on Integrated Membrane Operations for Sustainable Industrial Growth. *Ind. Eng. Chem. Res.* **2001***, 40*, 1277-1300.

(10) Charcosset, C. Ultrafiltration, Microfiltration, Nanofiltration and Reverse Osmosis in Integrated Membrane Processes. In *Integrated Membrane Systems and Processes;* John Wiley & Sons: 2015; pp 1.

(11) Rana, D.; Matsuura, T. Surface Modifications for Antifouling Membranes. *Chem. Rev.* **2010***, 110*, 2448-2471.

(12) Chu, Z.; Feng, Y.; Seeger, S. Oil/Water Separation with Selective Superantiwetting/Superwetting Surface Materials. *Angew. Chem., Int. Ed.* **2015***, 54*, 2328-2338.

(13) Ma, Q.; Cheng, H.; Fane, A. G.; Wang, R.; Zhang, H. Recent Development of Advanced Materials with Special Wettability for Selective Oil/Water Separation. *Small* **2016***, 12*, 2186-2202.

(14) Fritt-Rasmussen, J.; Wegeberg, S.; Gustavson, K. Review on Burn Residues from In Situ

Burning of Oil Spills in Relation to Arctic Waters. *Water Air Soil Pollut.* **2015***, 226*, 329.

(15) Kleindienst, S.; Paul, J. H.; Joye, S. B. Using Dispersants after Oil Spills: Impacts on the Composition and Activity of Microbial Communities. *Nat. Rev. Micro.* **2015***, 13*, 388.

(16) Yao, X.; Song, Y.; Jiang, L. Applications of Bio‐Inspired Special Wettable Surfaces. *Adv. Mater.* **2011***, 23*, 719-734.

(17) Lahann, J. Environmental Nanotechnology: Nanomaterials Clean Up. *Nature Nanotech.* **2008***, 3*, 320-321.

(18) Sun, T.; Feng, L.; Gao, X.; Jiang, L. Bioinspired Surfaces with Special Wettability. *Acc. Chem. Res.* **2005***, 38*, 644-652.

(19) Feng, L.; Zhang, Z.; Mai, Z.; Ma, Y.; Liu, B.; Jiang, L.; Zhu, D. A Super-Hydrophobic and Super-Oleophilic Coating Mesh Film for the Separation of Oil and Water. *Angew. Chem., Inter. Ed.* **2004***, 43*, 2012-2014.

(20) Liu, F.; Hashim, N. A.; Liu, Y.; Abed, M. M.; Li, K. Progress in the Production and Modification of PVDF Membranes. *J. Membr. Sci.* **2011***, 375*, 1-27.

(21) Rana, D.; Matsuura, T. Surface Modifications for Antifouling Membranes. *Chem. Rev.* **2010***, 110*, 2448-2471.

(22) Vatanpour, V.; Madaeni, S. S.; Khataee, A. R.; Salehi, E.; Zinadini, S.; Monfared, H. A. TiO_2 Embedded Mixed Matrix PES Nanocomposite Membranes: Influence of Different Sizes and Types of Nanoparticles on Antifouling and Performance. *Desalination* **2012***, 292*, 19-29.

(23) Masuelli, M.; Marchese, J.; Ochoa, N. A. SPC/PVDF Membranes for Emulsified Oily Wastewater Treatment. *J. Membr. Sci.* **2009***, 326*, 688-693.

(24) Shen, L.; Xu, Z.; Liu, Z.; Xu, Y. Ultrafiltration Hollow Fiber Membranes of Sulfonated Polyetherimide/Polyetherimide Blends: Preparation, Morphologies and Anti-Fouling Properties. *J.*

Membr. Sci. **2003***, 218*, 279-293.

(25) Nakao, S.; Osada, H.; Kurata, H.; Tsuru, T.; Kimura, S. Separation of Proteins by Charged Ultrafiltration Membranes. *Desalination* **1988***, 70*, 191-205.

(26) Ulbricht, M.; Richau, K.; Kamusewitz, H. Chemically and Morphologically Defined Ultrafiltration Membrane Surfaces Prepared by Heterogeneous Photo-Initiated Graft Polymerization. *Colloids Surfaces A: Physicochem. Eng. Aspects* **1998***, 138*, 353-366.

(27) Susanto, H.; Ulbricht, M. Photografted Thin Polymer Hydrogel Layers on PES Ultrafiltration Membranes: Characterization, Stability, and Influence on Separation Performance. *Langmuir* **2007***, 23*, 7818-7830.

(28) Elimelech, M.; Zhu, X.; Childress, A. E.; Hong, S. Role of Membrane Surface Morphology in Colloidal Fouling of Cellulose Acetate and Composite Aromatic Polyamide Reverse Osmosis Membranes. *J. Membr. Sci.* **1997***, 127*, 101-109.

(29) Lee, H.; Dellatore, S. M.; Miller, W. M.; Messersmith, P. B. Mussel-Inspired Surface Chemistry for Multifunctional Coatings. *Science* **2007***, 318*, 426-430.

(30) Yang, H.; Luo, J.; Lv, Y.; Shen, P.; Xu, Z. Surface Engineering of Polymer Membranes via Mussel-Inspired Chemistry. *J. Membr. Sci.* **2015***, 483*, 42-59.

(31) Liu, Y.; Ai, K.; Lu, L. Polydopamine and Its Derivative Materials: Synthesis and Promising Applications in Energy, Environmental, and Biomedical Fields. *Chem. Rev.* **2014***, 114*, 5057-5115.

(32) Hong, S.; Na, Y. S.; Choi, S.; Song, I. T.; Kim, W. Y.; Lee, H. Non‐Covalent Self-Assembly and Covalent Polymerization Co-Contribute to Polydopamine Formation. *Adv. Funct. Mater.* **2012***, 22*, 4711-4717.

(33) Liebscher, J.; Mrówczyński, R.; Scheidt, H. A.; Filip, C.; Hădade, N. D.; Turcu, R.; Bende, A.; Beck, S. Structure of Polydopamine: A Never-Ending Story? *Langmuir* **2013***, 29*, 10539-10548.

(34) Xiang, Y.; Liu, F.; Xue, L. Under Seawater Superoleophobic PVDF Membrane Inspired by Polydopamine for Efficient Oil/Seawater Separation. *J. Membr. Sci.* **2015***, 476*, 321-329.

(35) Sui, Y.; Gao, X.; Wang, Z.; Gao, C. Antifouling and Antibacterial Improvement of Surface-Functionalized Poly (vinylidene fluoride) Membrane Prepared via Dihydroxyphenylalanine-Initiated Atom Transfer Radical Graft Polymerizations. *J. Membr. Sci.* **2012***, 394*, 107-119.

(36) Shao, L.; Wang, Z. X.; Zhang, Y. L.; Jiang, Z. X.; Liu, Y. Y. A Facile Strategy to Enhance PVDF Ultrafiltration Membrane Performance via Self-Polymerized Polydopamine Followed by Hydrolysis of Ammonium Fluotitanate. *J. Membr. Sci.* **2014***, 461*, 10-21.

(37) Yang, L.; Phua, S. L.; Toh, C. L.; Zhang, L.; Ling, H.; Chang, M.; Zhou, D.; Dong, Y.; Lu, X. Polydopamine-Coated Graphene as Multifunctional Nanofillers in Polyurethane. *RSC Adv.* **2013***, 3*, 6377-6385.

(38) Charlot, A.; Sciannama, V.; Lenoir, S.; Faure, E.; Jrme, R.; Jrme, C.; Van De Weerdt, C.; Martial, J.; Archambeau, C.; Willet, N. All-in-One Strategy for the Fabrication of Antimicrobial Biomimetic Films on Stainless Steel. *J. Mater. Chem.* **2009***, 19*, 4117-4125.

(39) You, I.; Kang, S. M.; Byun, Y.; Lee, H. Enhancement of Blood Compatibility of Poly (urethane) Substrates by Mussel-Inspired Adhesive Heparin Coating. *Bioconjug. Chem.* **2011***, 22*, 1264-1269.

Chapter 2 Literature Review

2.1 Special Wettable Materials for Oil/Water Separation

Special wettable materials with extremely opposite affinities towards oil and water can be divided into two types: superhydrophobic/superoleophilic materials (oil-removing) and superhydrophilic/superoleophobic materials (water-removing), which both have been designed and fabricated to achieve selective oil/water separation. The wetting behavior of a solid surface is determined by surface chemistry and structure. An appropriate surface architecture can further facilitate the special wettability of materials with the intrinsic chemical characteristic.

The contact angle of a liquid droplet placed on a flat surface is depicted by Young equation (2.1) below:[1]

$$\cos\theta_F = \frac{\gamma_{SV} - \gamma_{SL}}{\gamma_{LV}} \tag{2.1}$$

where θ_F is the liquid contact angle on a flat solid surface, γ_{SV}, γ_{SL}, *and* γ_{LV} are the interfacial energies between solid-vapor, solid-liquid, and liquid-vapor, respectively.

Surface roughness can improve either wettability or nonwettability of surface. The wetting behavior of a droplet on a rough surface can be described by Wenzel equation (2.2).[2]

$$\cos\theta_{app} = \mathrm{R}\ \cos\theta_F = R\frac{\gamma_{SV} - \gamma_{SL}}{\gamma_{LV}} \tag{2.2}$$

where θ_{app} is the apparent contact angle of the rough surface, θ_F is the contact angle of the flat surface made of the same material, R is the ratio of the actual surface area to the projected surface area of the rough surface (R>1).

Cassie-Baxter regime is another model of the wetting behavior of rough surface. The surface with smaller protrusions cannot be filled with liquid due to the trapped air around the surface underneath the liquid. This wetting phenomenon is described by the Cassie-Baxter equation (2.3).[3,4]

$$\cos\theta_{app} = -1+\Phi_s\left(1+R\,\frac{\gamma_{SV}-\gamma_{SL}}{\gamma_{LV}}\right) \quad (2.3)$$

where Φ_s is the fraction of the contact area between surface and liquid.

The schematic illustrations of a liquid droplet on a flat surface, a rough surface (Wenzel regime), and a rough surface with small protrusions (Cassie-Baxter regime) are presented in Figure 2.1.

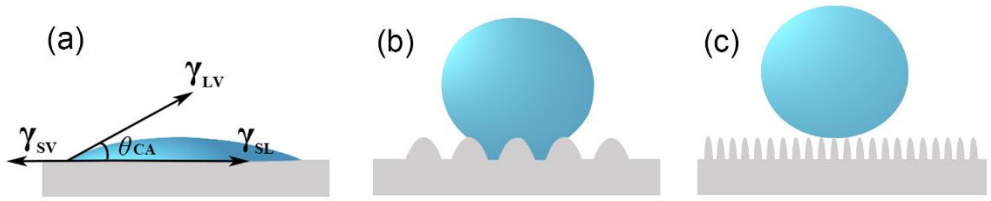

Figure 2.1 Schematic illustrations of a droplet on (a) a flat surface, (b) a rough surface (Wenzel regime), and (c) a rough surface with small protrusions (Cassie-Baxter regime).

2.1.1 Superhydrophobic/Superoleophilic Separation Materials

"Oil-removing" materials with superhydrophobic and superoleophilic property can selectively filter or adsorb oil during the oil/water separation process. Theoretically, a material with a surface energy between those of oil and water shows hydrophobicity and oleophilicity simultaneously according to Young equation (2.1). If enhance the surface roughness, it may exhibit superhydrophobicity and superoleophilicity at the same time.

For example, Feng et al. reported a novel coating mesh with superhydrophobicity and superoleophilicity via a facile spray-and-dry method using polytetrafluoroethylene (PTFE) emulsion as the precursor with the low surface energy property. The diesel oil contact angle on the mesh was 0°, but for water, it was larger than 150°, which allowed the oil phase to rapidly spread and permeate the mesh under gravity force. The mesh with sprayed film showed this special wettability owing to the chemical characteristic of PTFE and the micro/nanostructure.[5] Zhang et al. synthesized a composite film consisting of a porous polyurethane (PU) film and polystyrene (PS) microspheres with a dual-scale structure. The composite film with PS microspheres exhibited

colloidal crystal structure, showing superhydrophobic and superoleophilic property, which could be employed to separate oil and water.[6]

2.1.2 Superhydrophilic/Superoleophobic Separation Materials

In contrast, the "water-removing" materials with superhydrophilic and superoleophobic properties show many advantages compared with the "oil-removing" materials in oil/water separation. Firstly, the "oil-removing" materials have the intrinsic oleophilic feature, which makes them inclined to be fouled by organics due to the hydrophobic interaction; whereas, superoleophobic materials can overcome this shortage with better durability and longer service life. Secondly, "water-removing" materials exhibit superiority in gravity-driven separation because the density of water is higher than that of most oils. To utilize this original property, it becomes much easier to separate oil from water by gravity and thus reduce energy consumption.

However, it is hard to prepare materials with both hydrophilicity and oleophobicity in air because it is theoretically difficult to find a material with a surface energy which is larger than that of water and smaller than that of oil at the same time.[7] There are two methods to achieve this purpose: fabricating hydrophilic and underwater oleophobic materials, and preparing materials with polymers consisting of hydrophilic and oleophobic compositions.

The wetting behaviors of oil and water droplet on a flat surface in air are described as follows according to Young equation:

$$\gamma_o \cos\theta_o + \gamma_{os} = \gamma_s \tag{2.4}$$

$$\gamma_w \cos\theta_w + \gamma_{ws} = \gamma_s \tag{2.5}$$

where γ_o, γ_{os}, and γ_s are the interfacial tensions between oil-air, oil-solid, and solid-air, respectively. γ_w and γ_{ws} are the interfacial tensions between water-air and water-solid, respectively. θ_o and θ_w are the oil and water contact angle with solid, respectively.

Figure 2.2a shows oil droplet contacting with a flat solid surface underwater. The modified Young equation is given in equation (2.6):

$$\cos\theta_{ow} = \frac{\gamma_o \cos\theta_o - \gamma_w \cos\theta_w}{\gamma_{ow}} \quad (2.6)$$

where θ_{ow} is the underwater oil contact angle with a flat surface, γ_{ow} is the interfacial tension between oil and water.

Figure 2.2b displays the underwater oil droplet contacting with a hierarchical rough surface. The contact angle θ_{ow}' can be obtained by equation (2.7).

$$\cos\theta_{ow}' = -1 + \Phi_s(1+\cos\theta_{ow}) \quad (2.7)$$

According to equation , the hydrophilic surface in air can be oleophobic in water spontaneously through calculation.[8] Furthermore, the hydrophilic micro/nano-hierarchical surface can show superoleophobic property underwater because of this "Cassie-Baxter" state in the oil/water/solid system, in which water can be trapped in the hierarchical surface and prevent oil droplet from contacting with surface (Figure 2.2b). As a result, the designed materials with hydrophilic chemical property and micro/nano-hierarchical structures showing superhydrophilicity and underwater superoleophobicity can be utilized to separate oil from water.

Based on this concept, Jiang et al. proposed a polyacrylamide (PAM) hydrogel-coated stainless steel mesh with a micro/nano hierarchically structured surface with nanostructured papillae.[9] Crude oil/water mixture (30% v/v) can be successfully separated utilizing the coated mesh by pouring the mixture into the upper glass tube. Water can permeate through the mesh and be collected in the beaker below driven by gravity only; whereas, oil phase was retained above due to the underwater superoleophobic feature of the coated mesh. Various kinds of oil/water mixtures including oils such as gasoline, diesel, vegetable oil, hexane, and petroleum ether, can be separated via the same process. The as-prepared coated mesh shows a great potential to purify industrial oil-

polluted water.

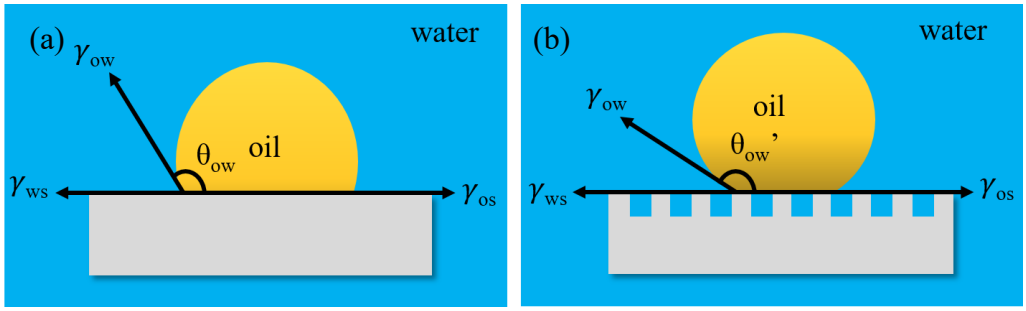

Figure 2.2 Underwater oil contact angle with a (a) flat solid surface, (b) hierarchical rough surface.

Shao et al. found a facile one-step method to fabricate hybrid nanoparticles deposited PVDF membrane by the simultaneous polymerization of dopamine (DA) and hydrolysis of tetraethoxysilane (TEOS) to achieve oil-in-water emulsion separation.[10] The modified PVDF microfiltration membrane showed an ultrahigh water flux (8606 L m^{-1} h^{-1} under 0.9 bar) and excellent antifouling property. The most prominent feature is the stability of the underwater superoleophobicity after rigorous washings and cryogenic bending.[10]

On the other hand, the material with superhydrophilic and superoleophobic property can be obtained by utilizing the polymer with hydrophilic and oleophobic constituents and hierarchical surface architectures. Zhang et al. synthesized a polymer (PDDA-PFO) consisting of poly(diallyldimethylammonium chloride) (PDDA) and sodium perfluorooctanoate (PFO) through the coordination of PFO anions and quaternary ammonium groups, containing hydrophilic and oleophobic groups in the polymer structures.[11] A superhydrophilic and superoleophobic nanocomposite coating with micro/nano-hierarchical structures was fabricated by spray casting of SiO_2 nanoparticles-polymer suspensions on various surfaces. The hydrophilic-oleophobic chemical characteristic and the hierarchical rough architecture of the coating film endowed the substrate with this special wettability. When the hexadecane and water droplets were placed on the surface, they showed spherical shapes initially because of the “Cassie-Baxter” regime at the

solid/liquid/air system, in which air was trapped underneath the droplets. However, after contacting with water droplets, the fluorinated moieties in the coating film rearranged and thus allowed water to complete spread and fill in all the asperities on the surface, resulting in a transformation to the Wenzel state within 9 min. The water contact angle gradually decreased from 165 ± 2° to 0° in 9 min, but the hexadecane contact angle remained at 155 ± 1° constantly.

2.2 Antifouling Modifications of Polymeric Membranes

The interactions between membranes and foulants, such as organic/bio-foulant, inorganic foulant, and multi-foulant, strongly limit the membrane application because of the flux decline and short service life. In order to diminish the membrane fouling, many surface modification methods have been proposed to modify the surface hydrophilicity, surface charge, and surface roughness. Basically, approaches of surface modification can be divided into two types: physical modification and chemical modification. Physical modifications include coating, blending, and fabrication of composite membranes. On the other hand, chemical modifications contain polymer functionalization, polymer grafting, and plasma treatment.

2.2.1 Coating

Hydrophilic materials are physically coated on membrane surface through three mechanisms: (1) adsorption or adhesion of macromolecular layer on the surface via multiple interactions. (2) interpenetration of the functional materials to the base polymer on the interface. (3) mechanical interpenetration of the functional layer to porous membrane.[12] As a result, hydrophobicity of membrane can be diminished with the improvement of hydrophilicity, and thus promote the antifouling properties. However, the stability of the functional layer is the main problem of physical coating.

Many attempts of coating have been implemented to improve fouling resistance of polymeric

membranes.[13-18] For instance, Ahmad Akbari et al. reported that the chitosan-coated polyamide nanofiltration membrane exhibited larger water flux and better antifouling performance against cetyltrimethylammonium bromide (CTAB) than those of the untreated membrane owing to the improvement of hydrophilicity and decrease the surface roughness.[17] Lee et al. also proposed that a neutral hydrophilic polymer polyvinyl alcohol (PVA) can be coated on microfiltration, nanofiltration, and reverse osmosis membranes, leading to the decrease of surface charge and roughness, in order to treat dyeing process wastewater.[18]

2.2.2 Blending

Polymer blending is a widely employed method to promote membrane properties by integrating the merits of constituents in molecular level to meet different demands of applications. It is important to select proper polymeric components with a certain ratio to obtain optimized antifouling membranes. Numerous researches about the blending method have been proposed.[19-23] Nagendran et al. investigated the fabrication of a polymeric ultrafiltration membrane via the blending of cellulose acetate (CA) and polyetherimide (PEI) by phase inversion method.[19] CA/PEI blend membrane showed a larger pore size compared with the pure CA or PEI membranes. The polymeric membranes with different component proportions were also compared in pure water flux, water content, hydraulic resistance, and molecular weight cut-off (MWCO). The higher water flux and better rejection of the blend membrane against several proteins (bovine serum albumin, egg albumin, pepsin, and trypsin) and heavy metal ions (copper, nickel, zinc, and cadmium) revealed the better fouling resistance than that of pure cellulose acetate membrane.

2.2.3 Fabrication of Composite Membranes

Composite membranes consist of two or more components with different chemical or physical features, which can be embodied in the properties of composite materials. N,O-carboxymethyl

chitosan (CM-CS), an amphoteric chitosan derivative, was successfully cross-linked with poly(ethersulfone) (PES) membrane by glutaraldehyde to prepare CM-CS/PES composite microfiltration membrane.[24] The as-prepared membrane was slightly positively charged at a low pH range (3.0-4.7), leading to a better ability to adsorb bovine serum albumin. However, at a higher pH range (6.0-8.0), the CM-CS/PES composite membrane was more negatively charged than CS/PES membrane, showing a better performance of protein resistance.

Inorganic nanoparticles can also serve as an effective antifouling component in composite membranes, such as TiO_2, SiO_2, and Al_2O_3, etc,[25-29] enhancing the hydrophilicity and antifouling property of the base polymeric membranes because of the higher water affinity. Besides, the pore size and porosity of the composite membranes could be larger than those of pure membranes, and hence endow them with higher water flux.

2.2.4 Polymer Functionalization

Bulk modification is an effective and facile approach to obtain modified membranes by functionalizing polymers in casting solution before membrane formation without additional post-modifications. To improve the hydrophilicity of the base polymer component with aromatic backbone structure, the functionalization methods such as carboxylation, sulfonation, amination, and epoxidation are widely used.[30-33] For example, sulfonated polysulfone was synthesized using chlorosulfonic acid, and blended with cellulose acetate and polyethylene glycol 600 in different ratios to fabricate ultrafiltration membranes.[31] Pure water flux, fouling resistance, and water content of membranes with different blending ratios were investigated.

2.2.5 Polymer Grafting

Polymer grafting is another effective approach to modify membrane surface, which can be separated into two types known as “grafting-to” and “grafting-from”. The “grafting-to” method

means polymer chains with functionalized end or side groups may be grafted onto the membrane surface.[34] However, the poor grafting density and the complex procedures limit its application. For "grafting-from" method, immobilized initiators on the membrane surface can initiate the polymerization of monomers from surface by chemical, radiation, photo-induced or plasma-induced techniques.[34-38]

For chemical grafting, Makhlouf et al. reported that free-radical polymerization of acrylic acid monomer grafted on polyamine 6.6 fibers was initiated by benzoyl peroxide as an initiator. The primary free-radical species ($C_6H_5COO•$) and the secondary free-radical species ($C_6H_5•$) were produced by the thermal cleavage of benzoyl peroxide. The hydrophilic and mechanical properties of the modified polyamine 6.6 fibers were significantly improved with the increasing of grafting rate.[35]

For radiation grafting, monomers can be grafted onto the substrate irradiated by the source of radiations. Li et al. irradiated poly(vinylidene fluoride) (PVDF) powder with γ-rays and grafted with N,N-dimethylacrylamide (DMAA) monomers to prepare PVDF-g-PDMAA powder as the material to fabricate antifouling microfiltration membrane.[36] As a result, the modified membrane showed better hydrophilicity and less protein adsorption against bovine serum albumin (BSA) and lysozyme.

Photo-induced graft polymerization is another way to achieve surface modification. Belfort et al. utilized UV-assisted method to graft three hydrophilic monomers, N-vinyl-2-pyrrolidinone (NVP), 2-acrylamidoglycolic acid monohydrate (AAG) and 2-acrylamido-2-methyl-1-propanesulfonic acid (AAP), onto poly(ether sulfone) (PES) and polysulfone (PSf) ultrafiltration membranes by dip technique with 300 nm wavelength lamps. Among all the membranes, PES membrane (50kDa) modified with 5 wt.% AAP showed the highest permeability and BSA

rejection.[37]

Plasma-induced grafting can accomplish adaptable surface within a short time in a facile manner. For example, after remote plasma treatment on the PVDF ultrafiltration membrane with methane/argon gas mixture, it can yield a great deal of oxygen functional groups compared with the unmodified membrane, resulting in the enhancement of flux and hydrophilicity by reducing the foulants adsorption and oil cake formation.[38]

2.2.6 Plasma Treatment

Plasma treatments include plasma sputtering and etching, implantation, and spraying.[39,40] During the plasma sputtering and etching process, plasma is generated by inert gases and the excited ions are accelerated by the electric field towards the substrate. The ions and atoms in the materials escape and sputter off the substrate via elastic and inelastic collisions after energy transfer. For implantation process, radical species created by the plasma gas can recombine with polymer radicals from membrane surface to form oxygen or nitrogen functionalities near the surface. In plasma spraying process, the powders of the sprayed materials are inserted into the plasma area. The powders are melted or partially melted under a high temperature and accelerated towards the substrate to form a coating layer on the surface.

For instance, the antifouling property of the polypropylene hollow fiber microporous membrane (PPHFMM) can be improved by air, NH_3, CO_2, and N_2 plasma treatments.[41-44] The static water contact angles of these plasma-treated membranes obviously decreased with the increasing of treatment time. The antifouling properties of those membranes were improved to some extent.

2.3 References

(1) Genzer, J.; Efimenko, K. Recent Developments in Superhydrophobic Surfaces and Their Relevance to Marine Fouling: A Review. *Biofouling* **2006***, 22*, 339-360.

(2) Wenzel, R. N. Resistance of Solid Surfaces to Wetting by Water. *Ind. Eng. Chem.* **1936***, 28*, 988-994.

(3) Cassie, A.; Baxter, S. Wettability of Porous Surfaces. *Trans. Faraday Soc.* **1944***, 40*, 546-551.

(4) Chu, Z.; Feng, Y.; Seeger, S. Oil/Water Separation with Selective Superantiwetting/Superwetting Surface Materials. *Angew. Chem., Int. Ed.* **2015***, 54*, 2328-2338.

(5) Feng, L.; Zhang, Z.; Mai, Z.; Ma, Y.; Liu, B.; Jiang, L.; Zhu, D. A Super-Hydrophobic and Super-Oleophilic Coating Mesh Film for the Separation of Oil and Water. *Angew. Chem., Inter. Ed.* **2004***, 43*, 2012-2014.

(6) Zhang, J.; Huang, W.; Han, Y. A Composite Polymer Film with Both Superhydrophobicity and Superoleophilicity. *Macromol. Rapid Commun.* **2006***, 27*, 804-808.

(7) Wang, B.; Liang, W.; Guo, Z.; Liu, W. Biomimetic Super-Lyophobic and Super-Lyophilic Materials Applied for Oil/Water Separation: A New Strategy Beyond Nature. *Chem. Soc. Rev.* **2015***, 44*, 336-361.

(8) Liu, M.; Wang, S.; Wei, Z.; Song, Y.; Jiang, L. Bioinspired Design of a Superoleophobic and Low Adhesive Water/Solid Interface. *Adv. Mater.* **2009***, 21*, 665-669.

(9) Xue, Z.; Wang, S.; Lin, L.; Chen, L.; Liu, M.; Feng, L.; Jiang, L. A Novel Superhydrophilic and Underwater Superoleophobic Hydrogel-Coated Mesh for Oil/Water Separation. *Adv. Mater.* **2011***, 23*, 4270-4273.

(10) Wang, Z.; Jiang, X.; Cheng, X.; Lau, C. H.; Shao, L. Mussel-Inspired Hybrid Coatings that Transform Membrane Hydrophobicity into High Hydrophilicity and Underwater Superoleophobicity for Oil-in-Water Emulsion Separation. *ACS Appl. Mater. Interfaces* **2015***, 7*, 9534-9545.

(11) Yang, J.; Zhang, Z.; Xu, X.; Zhu, X.; Men, X.; Zhou, X. Superhydrophilic–Superoleophobic

Coatings. *J. Mater. Chem.* **2012***, 22*, 2834-2837.

(12) Xu, Z.; Huang, X.; Wan, L. *Surface Engineering of Polymer Membranes*; Springer Science & Business Media: 2009.

(13) Nystrm, M. Fouling of Unmodified and Modified Polysulfone Ultrafiltration Membranes by Ovalbumin. *J. Membr. Sci.* **1989***, 44*, 183-196.

(14) Kim, K. J.; Fane, A. G.; Fell, C. The Performance of Ultrafiltration Membranes Pretreated by Polymers. *Desalination* **1988***, 70*, 229-249.

(15) Muppalla, R.; Rana, H. H.; Devi, S.; Jewrajka, S. K. Adsorption of pH-Responsive Amphiphilic Copolymer Micelles and Gel on Membrane Surface as an Approach for Antifouling Coating. *Appl. Surf. Sci.* **2013***, 268*, 355-367.

(16) Lei, J.; Ulbricht, M. Macroinitiator-Mediated Photoreactive Coating of Membrane Surfaces with Antifouling Hydrogel Layers. *J. Membr. Sci.* **2014***, 455*, 207-218.

(17) Akbari, A.; Derikvandi, Z.; Rostami, S. M. M. Influence of Chitosan Coating on the Separation Performance, Morphology and Anti-Fouling Properties of the Polyamide Nanofiltration Membranes. *J. Ind. Eng. Chem.* **2015***, 28*, 268-276.

(18) Kim, I.; Lee, K. Dyeing Process Wastewater Treatment Using Fouling Resistant Nanofiltration and Reverse Osmosis Membranes. *Desalination* **2006***, 192*, 246-251.

(19) Nagendran, A.; Arockiasamy, D. L.; Mohan, D. Cellulose Acetate and Polyetherimide Blend Ultrafiltration Membranes, I: Preparation, Characterization, and Application. *Mater. Manuf. Process.* **2008***, 23*, 311-319.

(20) Nguyen, T. P. N.; Yun, E.; Kim, I.; Kwon, Y. Preparation of Cellulose Triacetate/Cellulose Acetate (CTA/CA)-Based Membranes for Forward Osmosis. *J. Membr. Sci.* **2013***, 433*, 49-59.

(21) Saljoughi, E.; Mohammadi, T. Cellulose Acetate (CA)/Polyvinylpyrrolidone (PVP) Blend

Asymmetric Membranes: Preparation, Morphology and Performance. *Desalination* **2009***, 249*, 850-854.

(22) Kang, S.; Asatekin, A.; Mayes, A. M.; Elimelech, M. Protein Antifouling Mechanisms of PAN UF Membranes Incorporating PAN-g-PEO Additive. *J. Membr. Sci.* **2007***, 296*, 42-50.

(23) Jayalakshmi, A.; Rajesh, S.; Mohan, D. Fouling Propensity and Separation Efficiency of Epoxidated Polyethersulfone Incorporated Cellulose Acetate Ultrafiltration Membrane in the Retention of Proteins. *Appl. Surf. Sci.* **2012***, 258*, 9770-9781.

(24) Zhao, Z.; Wang, Z.; Wang, S. Formation, Charged Characteristic and BSA Adsorption Behavior of Carboxymethyl Chitosan/PES Composite MF Membrane. *J. Membr. Sci.* **2003***, 217*, 151-158.

(25) Bae, T.; Tak, T. Effect of TiO_2 Nanoparticles on Fouling Mitigation of Ultrafiltration Membranes for Activated Sludge Filtration. *J. Membr. Sci.* **2005***, 249*, 1-8.

(26) Li, J.; Xu, Z.; Yang, H.; Yu, L.; Liu, M. Effect of TiO_2 Nanoparticles on the Surface Morphology and Performance of Microporous PES Membrane. *Appl. Surf. Sci.* **2009***, 255*, 4725-4732.

(27) Luo, M.; Zhao, J.; Tang, W.; Pu, C. Hydrophilic Modification of Poly (ether sulfone) Ultrafiltration Membrane Surface by Self-Assembly of TiO_2 Nanoparticles. *Appl. Surf. Sci.* **2005***, 249*, 76-84.

(28) Yu, L.; Xu, Z.; Shen, H.; Yang, H. Preparation and Characterization of PVDF–SiO_2 Composite Hollow Fiber UF Membrane by Sol–Gel Method. *J. Membr. Sci.* **2009***, 337*, 257-265.

(29) Maximous, N.; Nakhla, G.; Wan, W.; Wong, K. Preparation, Characterization and Performance of Al_2O_3/PES Membrane for Wastewater Filtration. *J. Membr. Sci.* **2009***, 341*, 67-75.

(30) Guiver, M. D.; Robertson, G. P. Chemical Modification of Polysulfones: A Facile Method of

Preparing Azide Derivatives from Lithiated Polysulfone Intermediates. *Macromolecules* **1995***, 28*, 294-301.

(31) Malaisamy, R.; Mahendran, R.; Mohan, D.; Rajendran, M.; Mohan, V. Cellulose Acetate and Sulfonated Polysulfone Blend Ultrafiltration Membranes. I. Preparation and Characterization. *J. Appl. Polym. Sci.* **2002***, 86*, 1749-1761.

(32) Van der Bruggen, B. Chemical Modification of Polyethersulfone Nanofiltration Membranes: A Review. *J. Appl. Polym. Sci.* **2009***, 114*, 630-642.

(33) Jayalakshmi, A.; Rajesh, S.; Senthilkumar, S.; Mohan, D. Epoxy Functionalized Poly (ether-sulfone) Incorporated Cellulose Acetate Ultrafiltration Membrane for the Removal of Chromium Ions. *Sep. Purif. Technol.* **2012***, 90*, 120-132.

(34) Stamm, M. *Polymer Surfaces and Interfaces*; Springer: 2008.

(35) Makhlouf, C.; Marais, S.; Roudesli, S. Graft Copolymerization of Acrylic Acid onto Polyamide Fibers. *Appl. Surf. Sci.* **2007***, 253*, 5521-5528.

(36) Yang, X.; Zhang, B.; Liu, Z.; Deng, B.; Yu, M.; Li, L.; Jiang, H.; Li, J. Preparation of the Antifouling Microfiltration Membranes from Poly (N, N-dimethylacrylamide) Grafted Poly (vinylidene fluoride) (PVDF) Powder. *J. Mater. Chem.* **2011***, 21*, 11908-11915.

(37) Kaeselev, B.; Pieracci, J.; Belfort, G. Photoinduced Grafting of Ultrafiltration Membranes: Comparison of Poly (ether sulfone) and Poly (sulfone). *J. Membr. Sci.* **2001***, 194*, 245-261.

(38) Juang, R.; Huang, C.; Hsieh, C. Surface Modification of PVDF Ultrafiltration Membranes by Remote Argon/Methane Gas Mixture Plasma for Fouling Reduction. *J. Taiwan Inst. Chem. Eng.* **2014***, 45*, 2176-2186.

(39) Ayyavoo, J.; Nguyen, T. P. N.; Jun, B.; Kim, I.; Kwon, Y. Protection of Polymeric Membranes with Antifouling Surfacing via Surface Modifications. *Colloids Surf. Physicochem. Eng. Aspects*

2016*, 506*, 190-201.

(40) Chu, P. K.; Chen, J. Y.; Wang, L. P.; Huang, N. Plasma-Surface Modification of Biomaterials. *Mater. Sci. Eng. R Rep.* **2002***, 36*, 143-206.

(41) Yu, H.; Liu, L.; Tang, Z.; Yan, M.; Gu, J.; Wei, X. Surface Modification of Polypropylene Microporous Membrane to Improve Its Antifouling Characteristics in an SMBR: Air Plasma Treatment. *J. Membr. Sci.* **2008***, 311*, 216-224.

(42) Yu, H.; Hu, M.; Xu, Z.; Wang, J.; Wang, S. Surface Modification of Polypropylene Microporous Membranes to Improve Their Antifouling Property in MBR: NH_3 Plasma Treatment. *Sep. Purif. Technol.* **2005***, 45*, 8-15.

(43) Yu, H.; Xie, Y.; Hu, M.; Wang, J.; Wang, S.; Xu, Z. Surface Modification of Polypropylene Microporous Membrane to Improve Its Antifouling Property in MBR: CO_2 Plasma Treatment. *J. Membr. Sci.* **2005***, 254*, 219-227.

(44) Yu, H.; He, X.; Liu, L.; Gu, J.; Wei, X. Surface Modification of Polypropylene Microporous Membrane to Improve Its Antifouling Characteristics in an SMBR: N_2 Plasma Treatment. *Water Res.* **2007***, 41*, 4703-4709.

Chapter 3 Experimental Techniques

3.1 Field-Emission Scanning Electron Microscope (FESEM)

Field-emission scanning electron microscope (FESEM) can extract the topography, composition or crystallographic information of sample surfaces.[1] An electron beam is generated from a field emission gun within a high vacuum column to bombard the object. The secondary electrons are emitted from the surface and caught by the electron detector to produce electronic signals, which can be further amplified and transformed to images with high contrast and high resolution.

Zeiss Sigma 300 VP utilized in this study is equipped with secondary and backscattered electron detectors, an in-lens electron detector, a cathodoluminescence (CL) detector, and a Bruker energy dispersive X-ray spectroscopy (EDS) system. Surface morphologies and the element mappings of the samples were accurately detected by the in-lens detector and the EDS system, respectively.

3.2 Attenuated Total Reflectance-Fourier Transform Infrared Spectroscopy (ATR-FTIR)

An attenuated total reflection accessory is used to characterize, identify and quantify substrates by measuring the change of a totally internally reflected infrared beam which is directed onto the ATR crystal in contact with a sample.[2] An evanescent wave created from the internal reflection will extend into the sample and be attenuated or altered. The attenuated energy from each evanescent wave is passed back to the beam, which then exits at the another end of the crystal and is collected by the detector to generate an infrared spectrum of the sample.

All the spectra of different samples were obtained using Nicolet iS50 ATR-FTIR spectrophotometer with the number of scans of 32, at a resolution of 4 cm^{-1}, and in the range of 1500-4500 cm^{-1}.

3.3 X-Ray Photoelectron Spectroscopy (XPS)

XPS is one of the most widely used techniques to investigate chemical state and quantity of elements from the surfaces of various materials.[3] A beam of monochromatic Al Kα x-rays is utilized to excite the sample surface resulting in the emission of photoelectrons. The information of binding energy and intensity of photoelectron peaks can be acquired by the electron energy analyzer.

The spectra and percent atomic concentration of different membranes were obtained by an AXIS 165 X-ray photoelectron spectrometer (Kratos Analytical) in this research. Survey-scans were collected in the range of binding energy from 0-1100 eV.

3.4 Contact Angle Measurements

Conventionally, the contact angle is measured through a liquid where a liquid-vapor interface contacts with a solid surface, and quantifies the wettability of the solid surface by the liquid phase according to the Young's equation.[4] Several methods can be used to measure the contact angle, such as sessile drop method, Wilhelmy plate method, and Washburn capillary rise method.[5]

In this research, the time-dependent tests of the water contact angles in air of the membranes were conducted with the theta optical tensiometer (Attension, Biolin Scientific T200) via the sessile drop mode. A droplet of DI water from a micro-pipet with a certain volume was placed on the membrane surface. The dynamic process of spread and permeation of the water droplet through the membrane was recorded by the digital camera.

3.5 Optical Microscope

The optical microscope uses visible light and a system of lenses to magnify sample surfaces. The digital images of samples can be captured by the charge-coupled device (CCD) camera, showing the micrographs directly on a computer screen for further analysis.[6]

The optical microscope (Carl-Zeiss, Axioskop 40) was used to observe the feed solution and the filtration solution of the SDS-stabilized hexane-in-water emulsion in this work.

3.6 Total Organic Carbon (TOC) Analysis

Total organic carbon (TOC) value is obtained after removal of the inorganic carbon (IC) from the total carbon (TC). The IC component represents the total quantity of carbon in dissolved carbon dioxide, bicarbonate ions, and carbonate ions. The equation (3.1) below shows the equilibrium state of carbon species in solution, which is driven by the pH condition of the sample.[7]

$$CO_2 + H_2O \Leftrightarrow HCO_3^- + H^+ \Leftrightarrow CO_3^{2-} + 2H^+ \quad (3.1)$$

By the addition of acid and inert-gas sparging, this equilibrium shifts to the left, and hence those inorganic carbon species can be converted to carbon dioxide and released to the air. To detect the TOC component, the TOC-L analyzer (Shimadzu) utilized in this study adopts the 680 ℃ combustion catalytic oxidation method in an oxygen-rich atmosphere, which can oxidize the organic carbon within the solution to produce CO_2. The last stage of the analysis process is to specifically measure the CO_2 generated by the oxidation by the non-dispersive infrared analysis (NDIR) method.[7, 8] This equipment provides an extra wide detection range from 4 μg L^{-1} to 30000 mg L^{-1}.

3.7 Surface Zeta Potential Measurements

SurPASS electrokinetic analyzer is a powerful tool of surface analysis which can investigate the zeta potential of solid surface based on a streaming potential measurement. The surface of polymeric membrane is electrically charged in aqueous solution depending on the chemical properties of the membrane and solution. The surface charge characteristics of membranes are influenced by ionization of surface functional groups, and adsorption of ions, polyelectrolytes, and charged macromolecules.[9] A streaming potential is generated when an electrolyte solution is

forced to flow through a charged surface by hydraulic pressure.[10]

In this work, 1 mM KCl solution was selected as the electrolyte solution. The membrane samples were fixed in the adjustable cell for disk with a diameter of 14 mm. The flow pressure was chosen at 100 mbar. pH of the solution was adjusted by NaOH solution (0.1 M).

3.8 Ultraviolet-Visible-Near Infrared Spectroscopy (UV-Vis-NIR Spectroscopy)

UV-Vis-NIR spectrophotometer is used to characterize materials by measuring the radiation reflection or absorbance of a sample which is illuminated by a radiation with a particular and discrete wavelength in ultra-violet (UV), visible (Vis), or near infrared (NIR) regions. A beam of light passes through a prism and splits into two equally intense beams by a half mirror.[11] One of the beams passes through the sample cuvette containing the solution to be measured. The other beam passes through the reference cuvette containing the solvent only. Collection and comparison are implemented by the electronic detector which measures the intensity of these two beams.[12] The concentration of a certain organic compound can be obtained by detecting the absorbance at some wavelength.

In this research, the concentration of BSA solution was detected by the UV-vis-NIR spectrophotometer (UV-3600, Shimadzu) at the wavelength of 278 nm.

3.9 References

(1) Reichelt, R. Scanning Electron Microscopy. In *Science of Microscopy;* Springer: 2007; pp 133-272.

(2) Hsu, C. S. Infrared Spectroscopy. In *Handbook of Instrumental Techniques for Analytical Chemistry;* Prentice Hall: Englewood Cliffs, NJ, 1997; pp 247-283.

(3) Watts, J. F. X-Ray Photoelectron Spectroscopy. *Vacuum* **1994***, 45*, 653-671.

(4) Adamson, A. W.; Gast, A. P. *Physical Chemistry of Surfaces*; Interscience Publishers: New

York, 1967.

(5) Shang, J.; Flury, M.; Harsh, J. B.; Zollars, R. L. Comparison of Different Methods to Measure Contact Angles of Soil Colloids. *J. Colloid Interface Sci.* **2008***, 328*, 299-307.

(6) Hiraoka, Y.; Sedat, J. W.; Agard, D. A. The Use of a Charge-Coupled Device for Quantitative Optical Microscopy of Biological Structures. *Science* **1987**, 36-41.

(7) Chan, C. C.; Lam, H.; Zhang, X. *Practical Approaches to Method Validation and Essential Instrument Qualification*; John Wiley & Sons: 2011.

(8) Sugimura, Y.; Suzuki, Y. A High-Temperature Catalytic Oxidation Method for the Determination of Non-Volatile Dissolved Organic Carbon in Seawater by Direct Injection of a Liquid Sample. *Mar. Chem.* **1988***, 24*, 105-131.

(9) Elimelech, M.; Chen, W. H.; Waypa, J. J. Measuring the Zeta (Electrokinetic) Potential of Reverse Osmosis Membranes by a Streaming Potential Analyzer. *Desalination* **1994***, 95*, 269-286.

(10) Werner, C.; Krber, H.; Zimmermann, R.; Dukhin, S.; Jacobasch, H. Extended Electrokinetic Characterization of Flat Solid Surfaces. *J. Colloid Interface Sci.* **1998***, 208*, 329-346.

(11) Perkampus, H.; Grinter, H. *UV-VIS Spectroscopy and Its Applications*; Springer: 1992.

(12) Raaman, N. *Phytochemical Techniques*; New India Publishing: 2006.

Chapter 4 Oxidant-Induced High-Efficient Mussel-Inspired Modification on PVDF Membrane with Superhydrophilicity and Underwater Superoleophobicity Characteristics for Oil/Water Separation[1]

4.1 Introduction

Oil/water separation becomes a crucial process to address the oily wastewater problem associated with rapidly expanded industries and massive oil spill accidents.[1-3] Functional filtration materials with special wettability are considered to be one of the most effective tools for oil/water separation.[4-6] Modifications of different porous substrate materials, such as metallic meshes,[7-11] textiles/fabrics,[12-14] and polymer membranes,[15-17] have attracted widespread attention for their excellent selectivity, high efficiency, and long-term reusability. Among them, microfiltration and ultrafiltration polymeric membranes show their unique properties and prominent superiorities for oil/water separation because of high flexibility, lower cost, and smaller pore sizes, which make them suitable for separating surfactant-stabilized oil/water emulsions. However, traditional polymer membranes have some drawbacks, including the unstable mechanical property of hydrophilic polymer membranes (e.g. cellulose derivatives)[18,19] and the fouling affinity of hydrophobic polymer membranes (e.g. polyethylene (PE),[20,21] polypropylene (PP),[22,23] polyvinylidene fluoride (PVDF)[24,25]), which greatly restrict their application in filtration process. Therefore, it is vitally necessary to modify polymer membranes with special wettability and superior performance in terms of permeate flux, separation efficiency, and anti-fouling characteristics.

[1] A version of this chapter was published on ACS Applied Materials & Interfaces: Luo, C.; Liu, Q. Oxidant-Induced High-Efficient Mussel-Inspired Modification on PVDF Membrane with Superhydrophilicity and Underwater Superoleophobicity Characteristics for Oil/Water Separation. *ACS Appl. Mater. Interfaces* **2017**, *9*, 8297-8307. http://pubs.acs.org/doi/abs/10.1021/acsami.6b16206.

Special wettable membranes employed in oil/water separation are typically classified into two different types, i.e., hydrophobic and oleophilic membranes, and hydrophilic and oleophobic membranes.[6] The hydrophobic and oleophilic membranes are easily fouled during the organic phase due to their intrinsic oleophilic properties, while the hydrophilic and oleophobic membranes could overcome this shortcoming. In recent years, considerable efforts have been devoted to hydrophilizing or functionalizing the porous hydrophobic membranes, such as surface coating,[26,27] surface grafting,[28,29] additive blending,[30,31] etc. Among these methods, surface coating is the simplest and most universally used technique to transform membrane hydrophobicity into high hydrophilicity. This method results in excellent fouling resistance and water permeation by depositing a thin hydrophilic layer onto the surface, as well as on the pore walls of the membrane. Additionally, superhydrophilic and underwater superoleophobic feature of filtration membranes could be achieved through the complementary effect of chemistry and surface mechanics inspired by the anti-wetting phenomenon of oil droplets on fish scales.[32] Based on this concept, depositing a superhydrophilic and underwater superoleophobic layer onto the porous filtration membrane through a combination of chemistry and hierarchical structure could be a significantly promising way for oil/water separation, in order to endow the modified membrane with particularly high filtration efficiency under low transmembrane pressure.

Since 2007, mussel-inspired methodology using dopamine, known as “bio-glue”, has drawn much research interest and been adopted to decorate various materials attributed to its universality, simplicity, and economic practicality.[33] It is generally known that the formation of versatile polydopamine (PDA) coating on various substrates can be ascribed to the catechol and amine structures via covalent and non-covalent interaction in an autoxidative polymerization process.[33,34] The exact polymerization mechanism is still unclear so far. Numerous researches reported that the

PDA layer can be efficiently created on all types of surfaces under the optimal condition, i.e., immersing in 2 mg mL^{-1} dopamine tris (hydroxymethyl) aminomethane hydrochloride (Tris-HCl) solution (pH = 8.5) under an ambient atmosphere for a certain period of time.[27,35-38] However, the instability, poor homogeneity, and limited hydrophilicity of pure PDA film restricts its in-service application for oil/water separation without subsequent functionalization.[39,40] Due to the quantities of active catechol groups, PDA can serve as an intermediate layer to react with amine/thiol groups, and metallic nanoparticles for post-modifications.[41] Additional modifications based on the PDA layer are usually intricate and time-consuming.[38,42] Therefore, one-step strategies have been arousing interest because of the convenience and higher preparation efficiency. By one-step co-deposition of PDA and polyethyleneimine (PEI) on PP microfiltration membrane, superhydrophilicity and stability properties can be implemented for efficient oil/water separation.[36] Organic-inorganic hybrid coating on the PVDF microfiltration membrane via simultaneous polymerization of dopamine and hydrolysis of TEOS[37] or binding of TiO_2 nanoparticles[43] are also single-step routes to accomplish emulsion separation. To our knowledge, almost all of the modification approaches require at least 4 hours of deposition for the best results. Except for dopamine, these methods all need additional reactants (e.g. polymer, inorganic nanoparticles, coupling agent, etc.), which are relatively demanding and uneconomical.

Herein, we report a high-efficient, mussel-inspired, one-step method with an unprecedented fast PDA deposition on hydrophobic PVDF microfiltration membrane. This is accomplished via the chemical oxidation effect of sodium periodate under a slightly acidic condition (pH = 5.0), inspired from the recent research carried out by Ponzio *et al*..[44] The formation of hydrophilic and homogeneous PDA nanoparticles on the surface and pore walls endowed the PVDF microfiltration membrane with superhydrophilicity and underwater superoleophobicity by the synergistic effect

between chemistry and hierarchical pattern. Different from the conventional and inefficient autoxidized procedure in the presence of O_2 in a weakly basic buffer solution, the deposition time of the optimized PDA film was dramatically shortened to 2 h. Without post-modifications or additional reactants, the optimally designed superdrophilic and underwater superoleophobic membrane boosted by sodium periodate showed an ultra-high water flux (11934 ± 544 L m^{-2} h^{-1}) under an ultra-low transmembrane pressure (0.038 MPa). Surprisingly, the pure water flux driven only by gravity can even reach 606 L m^{-2} h^{-1}. The prepared modified PVDF membranes were extensively characterized. The special wettability, chemical and mechanical stability, oil/water separation performance, and antifouling ability have been further investigated.

4.2 Experimental Section

4.2.1 Materials

Polyvinylidene fluoride microfiltration membranes (α-PVDF, mean pore size 0.45 μm, diameter 47 mm) were purchased from the Millipore Co. Dopamine hydrochloride, sodium dodecyl sulfate (SDS), hexane, and ethanol were purchased from Sigma-Aldrich. Sodium periodate, tris (hydroxymethyl) aminomethane hydrochloride (Tris-HCl), anhydrous sodium acetate, acetic acid, petroleum ether, and toluene were purchased from Fisher Scientific. All the chemicals were used as received.

4.2.2 Fabrication of Modified Membranes

The PVDF membranes were washed with ethanol and DI water for 15 min under sonication respectively in sequence before modification. The pristine PVDF membranes were pre-wetted with ethanol before immersing in 2 mg mL^{-1} dopamine sodium acetate buffer solution (50 mM, pH = 5.0) with 4 mg mL^{-1} sodium periodate as the oxidant for a designated time (0.5 h, 2 h, 4 h). The vessel was shaken at 150 rpm and covered with an aluminum foil during reaction under ambient

conditions. After the oxidant-induced polymerization, the modified membranes were washed thoroughly with DI water and then dried in an oven at 40 °C overnight before use. The membranes with different deposition time were denoted as PDA-SP-0.5h, PDA-SP-2h, PDA-SP-4h respectively. To investigate the impact of sodium periodate oxidation and the slightly acidic condition on the hydrophilization of PVDF membranes, a control experiment with a notation of PDA-O_2-Tris was designed as the conventional PDA deposition (2 mg mL^{-1} dopamine) on membranes by self-polymerization in Tris-HCl buffer (50 mM, pH = 8.5) in air for 2 h. Another control experiment named PDA-SP-Tris (2 mg mL^{-1} dopamine, Tris-HCl buffer 50 mM, pH = 8.5) was set to indicate the crucial effect of the slightly acidic condition with the same amount of sodium periodate for 2 h. Both control experiments were carried out with the same pre-wetting and drying process.

4.2.3 Characterizations

Surface morphologies and the element mappings of the pristine and modified PVDF membranes were observed by field emission scanning electron microscopy (FESEM, Carl-Zeiss Sigma) and energy-dispersive spectroscopy (EDS), respectively. The surface chemistry was investigated by attenuated total reflectance-Fourier transform infrared spectroscopy (ATR-FTIR, Thermol, Nicolet iS50) and X-ray photoelectron spectrometer (XPS, Kratos, AXIS 165). The water contact angles and underwater-oil contact angles were measured by theta optical tensiometer (Attension, Biolin Scientific T200). The filtration performances were carried out with a vacuum filtration apparatus (Millipore). Micrographs of the feed solution and the filtrate solution of oil-in-water emulsion were obtained by optical microscope (Carl-Zeiss, Axioskop 40). The oil contents in the filtrates of mixtures and emulsions were tested by a total organic carbon analyzer (Shimadzu, TOC–L).

4.2.4 Preparation and Separation of Oil/Water Mixtures and Oil-in-Water Emulsions

The surfactant-free oil/water mixtures were obtained by mixing oil and water in 1/99 (v/v) under 1200 rpm stirring for 3 h and contained different oil components such as hexane, toluene, petroleum ether, and diesel. The surfactant-stabilized oil-in-water emulsions were prepared by dissolving 0.04 mg mL^{-1} of sodium dodecyl sulfate (SDS) in oil/water mixtures under same stirring conditions. All these mixtures and emulsions stayed stable before separation experiments without stratification and precipitation. Note that we chose DI water as an ideal case in our experiments.

The separation experiments were implemented in a vacuum filtration apparatus (Millipore) clamping the optimally modified PVDF membranes in between with an effective separation area of 11.34 cm^2. The prepared mixtures or emulsions were poured into the funnel under a relatively low pressure difference of 0.038 MPa compared with some pressure applied previously. The permeate fluxes of mixtures or emulsions and oil contents in the filtrates were tested. The fluxes and the oil rejection ratios of the modified membranes were defined as equation (4.1) and equation (4.2).

$$\text{Flux (L m}^{-2}\text{ h}^{-1}\text{)} = \frac{V}{A\Delta t} \tag{4.1}$$

$$\text{Oil rejection ratio (\%)} = (1-\frac{C_f}{C_o})\times 100 \tag{4.2}$$

where V (L) is the volume of filtrate, A (m^2) is the effective separation area, Δt (h) is the permeation time, C_f (ppm) is the oil concentration of filtrates, and C_o (ppm) is the oil concentration of original oil/water mixtures or oil-in-water emulsions.

4.2.5 Stability Test

In order to detect the chemical stability of the optimally modified PVDF membranes in both neutral and harsh pH environments, we compared the color and water contact angle variations of the PDA-SP-2h, PDA-O_2-Tris and PDA-SP-Tris membranes after being rinsed with the neutral

(pH = 7), strong acidic (pH = 2) and strong basic (pH = 12) solutions for 12 h. The mechanical stabilities of these membranes were also investigated by subjected to one minute of sonication. The treatment was replicated twice.

The oil antifouling performance is an essential indicator to evaluate the reusability and durability of an oil/water separation membrane, which would be a direct reflection of the variations of separation efficiency by reuse. The flux recovery property was detected through recording the flux every 2 minutes by a three-cyclic experiment of SDS-stabilized petroleum ether-in-water emulsion separation. Between two cycles, the optimally modified PVDF membranes were only rinsed with DI water for 10 min to clean the residue for the next measurement.

4.3 Results and Discussion

4.3.1 Surface Morphology and Chemistry

The modified membrane is required to satisfy two crucial conditions: hydrophilicity and hierarchical surface pattern to achieve the purpose of excellent oil/water separation with superhydrophilic and underwater superoleophobic property. Superhydrophilic surface with micro/nano-hierarchical structure can be water-affinitive and trap water in the slots on the coating layer to decrease the contact area between the oil droplet and the membrane surface. This endows the membrane with a low-adhesive superoleophobic feature simultaneously via the oil/water/solid system in the "Cassie-Baxter" regime.[32]

Using this methodology, PDA generates nanoparticle structure with the addition of sodium periodate under acidic conditions (pH = 5.0) in the chemical oxidation process. The surface morphologies of the membranes were revealed by FESEM images in Figure 4.1 and Figure 4. S1 in the Supporting Information. The images at 5k magnification of PDA coating PVDF substrates oxidized by O_2 (in Tris-HCl buffer solution) and sodium periodate (in sodium acetate buffer

solution) for 2 h were shown in Figure 4.1c and Figure 4.1e respectively. This exhibits pore structure originating from pristine PVDF substrate (Figure 4.1a). At 50k magnification, several clustered PDA particles attached on the top surface of the PVDF in pure dopamine solution after two-hour deposition (Figure 4.1d). The particle size was variably distributed from 30 to 115 nm. These particles were attached to each other forming aggregates with the size about 0.1-0.5 μm. However, as shown in Figure 4.1f, a homogeneous and rough PDA nanoparticle coating layer formed conformally on the smooth surface of the PVDF membrane as well as on the internal pore channels. The porous construction of the pristine membrane was retained with a sufficient coverage of PDA nanoparticles coating on the membrane pore surface. The PDA nanoparticles showed a uniform size distribution with a mean size of 35 nm. This micro/nano-structured hydrophilic layer can trap abundant water while forming a thin water layer on the surface to prevent oil permeation. This leads to the superhydrophilic and underwater superoleophobic characteristic of the modified membranes.

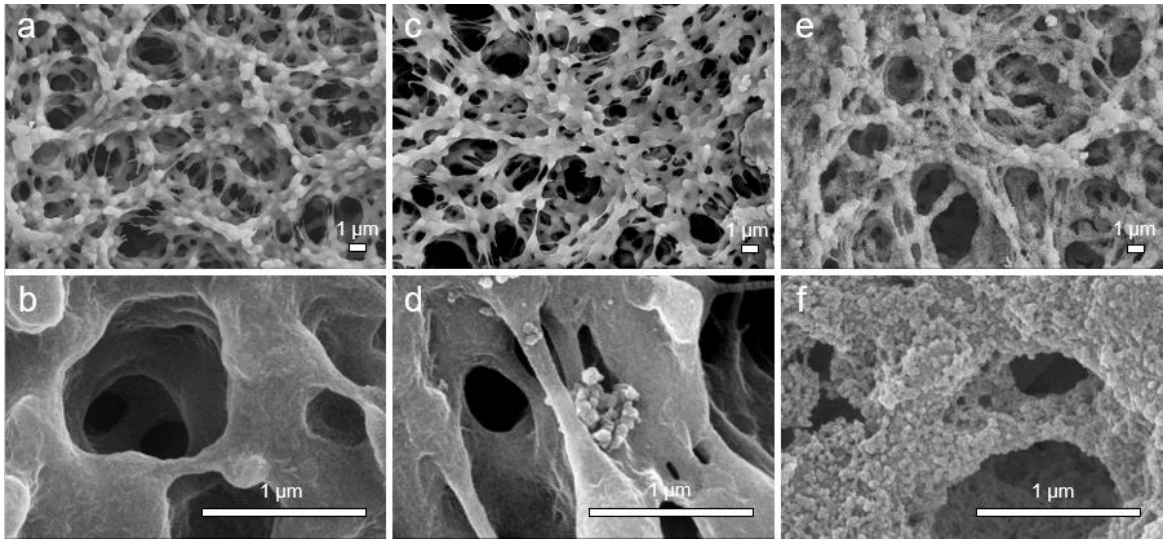

Figure 4.1 FESEM top-view images of the (a, b) pristine PVDF membrane, (c, d) dopamine/O_2-modified PVDF membrane (pH = 8.5, 2 h), and (e, f) dopamine/sodium periodate-modified PVDF membrane (pH = 5.0, 2 h). The scale bars are 1 μm in all images at different magnifications.

Deposition time and pH conditions have significant effects on the formation of PDA nanoparticles on the PVDF substrate. Surface morphologies of the PDA deposited PVDF membranes oxidized by sodium periodate in sodium acetate buffer solution (50 mM, pH = 5.0) for 0.5 h and 4 h were illustrated in Figure 4. S1 in the Supporting Information. For 0.5 h reaction time, smaller PDA nanoparticles could be found on the surface and internal pore channels (Figure 4. S1a and Figure 4. S1b). Whereas, increasing the reaction time to 4 h may result in undesirable blocking of the pores and reduction of water flux because of the thicker PDA layer with coagulation structure (Figure 4. S1c and Figure 4. S1d). The images of PDA formation with sodium periodate oxidation in the conventional Tris-HCl buffer solution at pH = 8.5 were also presented in Figure 4. S1e and Figure 4. S1f as a control group, showing that there were no PDA nanoparticles sufficiently covering the substrate compared with that in the slightly acidic environment (Figure 4.1e and Figure 4.1f). Figure 4. S1f exhibited an uneven size distribution of PDA particles from 45 to 250 nm. The FESEM results demonstrated that the optimized coating condition for PDA nanoparticles deposited on PVDF membrane was in the presence of sodium periodate at acidic media (pH = 5.0) for 2 h. The thicknesses of the pristine and modified PVDF membranes were shown in Figure 4. S2 (in the Supporting Information). The thickness of the pristine PVDF membrane was about 94.04 ± 0.19 μm. With the exist of sodium periodate and the increasing deposition time, the PDA nanoparticle layer showed a thicker trend. The optimally modified membrane (PDA-SP-2h) had a thickness about 95.56 ± 1.36 μm as shown in Figure 4. S2e.

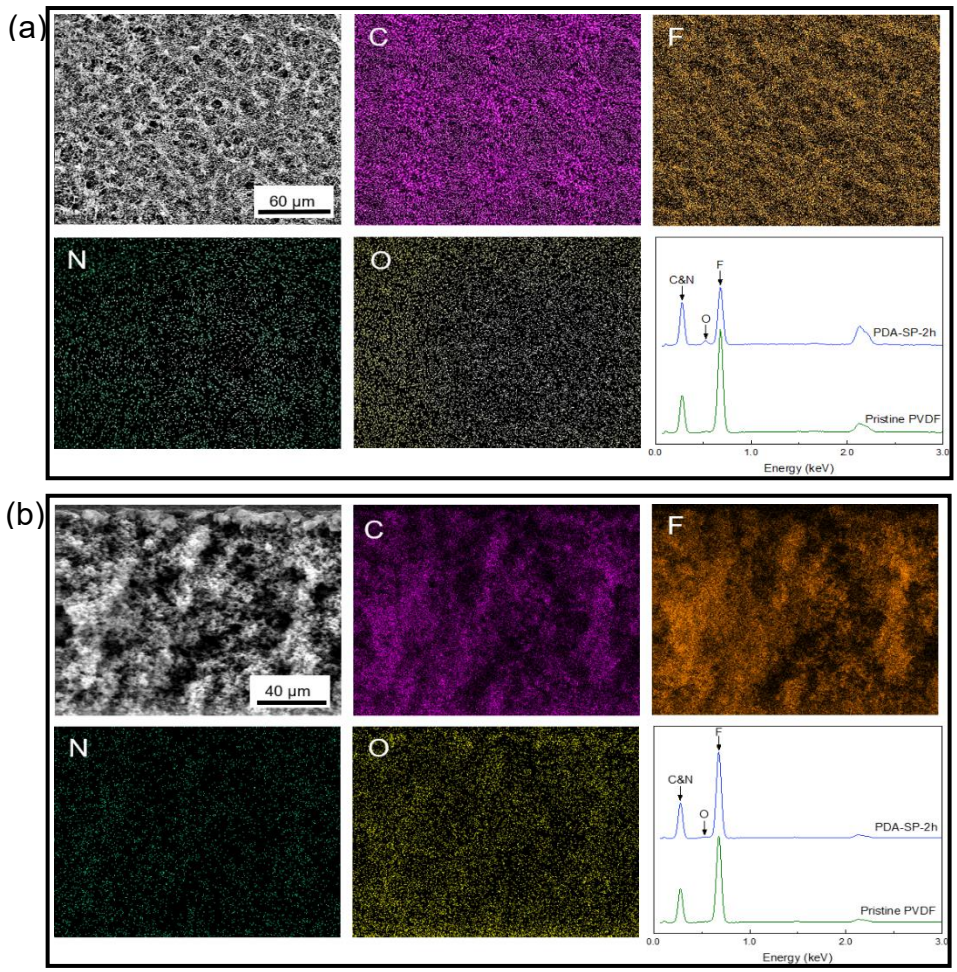

Figure 4.2 FESEM images, EDS mappings and spectra of (a) top surface and (b) cross-section of the dopamine/sodium periodate-modified PVDF membrane (pH = 5.0, 2 h). Pink, orange, green, yellow dots represent elemental C, F, N and O, respectively.

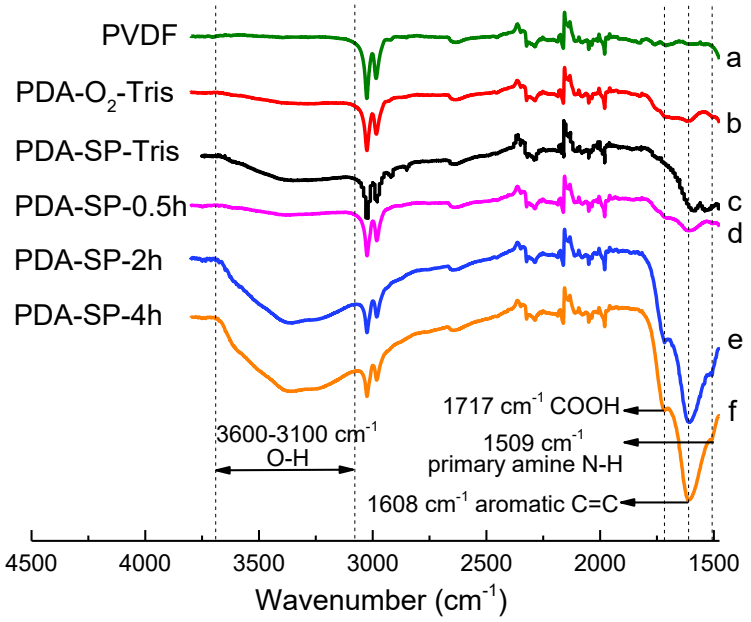

Figure 4.3 ATR-FTIR spectra of the (a) pristine PVDF membrane, (b) dopamine/O_2-modified PVDF membrane (pH = 8.5, 2 h), (c) dopamine/sodium periodate-modified PVDF membrane (pH = 8.5, 2 h), and dopamine/sodium periodate-modified PVDF membrane (pH = 5.0) for (d) 0.5 h, (e) 2 h, and (f) 4 h.

The EDS mappings and spectra of this optimal reaction condition shown in Figure 4.2 indicated that the elements N, O distributed homogenously on the top surface and cross-section of the modified PVDF membrane, ascribed to the deposition of hydrophilic PDA nanoparticles on the membrane surface and inner pores, which could achieve superhydrophilicity and high water permeation.

The chemical components of pristine PVDF membrane and as-prepared membranes with controlled conditions were further investigated by ATR-FTIR and XPS measurements. ATR-FTIR spectra in Figure 4.3 showed two apparent absorption peaks at 1509 cm^{-1} and 1608 cm^{-1} for PDA-SP-2h and PDA-SP-4h modified PVDF membranes, assigned to primary amine N-H bending vibrations and aromatic C=C resonance vibrations derived from PDA structure, respectively.

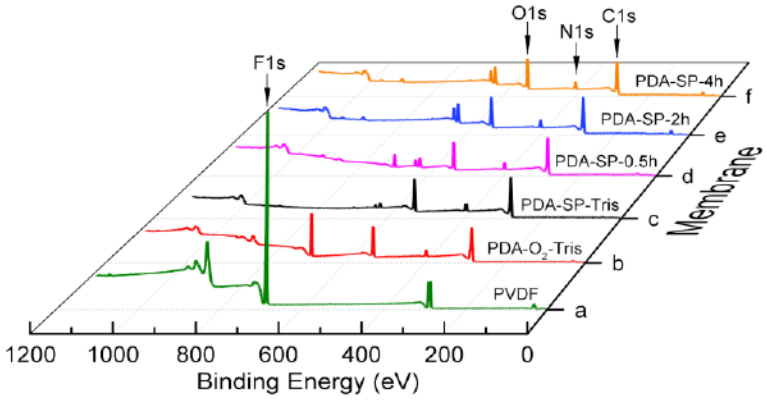

Figure 4.4 XPS spectra of the (a) pristine PVDF membrane, (b) dopamine/O_2-modified PVDF membrane (pH = 8.5, 2 h), (c) dopamine/sodium periodate-modified PVDF membrane (pH = 8.5, 2 h), and dopamine/sodium periodate-modified PVDF membrane (pH = 5.0) for (d) 0.5 h, (e) 2 h, and (f) 4 h.

Additionally, the spectra of PDA-SP-2h and PDA-SP-4h showed a new absorption peak around 1717 cm^{-1}, ascribed to carbonyl/carboxyl groups,[44] which was absent in PVDF membranes decorated with PDA in Tris-HCl buffer solution oxidized by O_2 or sodium periodate. As the FTIR result of the PVDF membrane treated by 2 mg mL^{-1} dopamine in Tris-HCl buffer solution oxidized by O_2 for 24 h (Figure 4. S3) and some results reported by others,[35,37,38,44] the band of carbonyl/carboxyl group was not detectable in the FTIR spectra of different substrates modified by PDA in Tris-HCl buffer solution by O_2 for various reaction time. Therefore, sodium periodate oxidation at acidic pH led to the formation of hydrophilic carboxyl groups on the substrates during the deposition process of PDA, endowing the membranes with superhydrophilicity properties, which is unprecedented for PDA-modified membranes obtained by the conventional method.

Table 4.1 Elemental Composition of the Pristine and Modified Membrane Surfaces Examined by XPS

membrane	composition (at %)				atomic ratio	
	C	F	O	N	N/C	O/C
Pristine PVDF	48.27	51.73				
PDA-O_2-Tris	64.44	15.86	14.95	4.75	0.07	0.23
PDA-SP-Tris	72.03	0.70	19.40	7.87	0.11	0.27
PDA-SP-0.5h	71.79	5.71	16.87	5.63	0.08	0.23
PDA-SP-2h	71.26	0.65	20.57	7.52	0.11	0.29
PDA-SP-4h	71.61	0.07	21.62	6.70	0.09	0.30

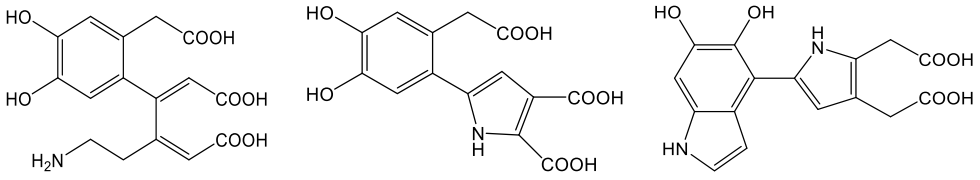

Figure 4.5 Structural components of the sodium periodate-oxidized PDA.[44] (Reprinted (adapted) with permission from Ponzio *et al*.[44] Copyright 2016 American Chemical Society.)

The XPS result presented in Figure 4.4 demonstrated that all F 1s peaks of decorated membranes decreased or even disappeared because of the coating, whereas the peaks of N 1s and O 1s appeared. For PDA-SP-2h and PDA-SP-4h, the percent atomic concentrations of O 1s were relatively higher than those of others in Table 4.1, and even higher than that of the PDA produced by autoxidation in alkaline condition for 24 h (Figure 4. S4 and Table 4. S1 in the Supporting Information). These results were in agreement with the spectra given by the ATR-FTIR measurement, showing that more carboxylic groups or quinonoid structures formed during the oxidation process. The O/C ratios of PDA-SP-2h and PDA-SP-4h were markedly higher than that of the stoichiometric value of dopamine (O/C = 0.25),[33] indicating the significant oxidation effect of sodium periodate during the deposition process of PDA. The N/C ratio of PDA-SP-4h is slightly

smaller compared with that of PDA-SP-2h and can be ascribed to the loss of the amine groups in dopamine side chains and pyrrole moieties due to the oxidative breakdown.[44] Structures of products generated by the degradation of o-quinone and the oxidative breakdown of the side-chain triggered by sodium periodate to yield carboxyl functions according to the melanin degradation mechanisms were shown in Figure 4.5.[44,45]

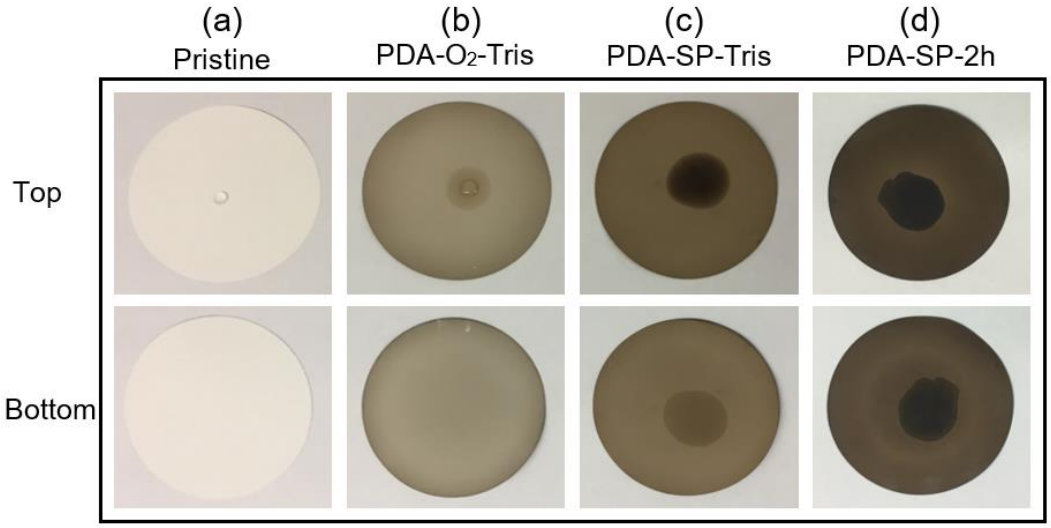

Figure 4.6 Photographs of a 10 μL water droplet on the top surfaces (above) and the reverse sides (below) of the (a) pristine PVDF membrane, (b) dopamine/O_2-modified PVDF membrane (pH = 8.5, 2 h), (c) dopamine/sodium periodate-modified PVDF membrane (pH = 8.5, 2 h), and (d) dopamine/sodium periodate-modified PVDF membrane (pH = 5.0, 2 h).

4.3.2 Wettability of the Modified Membranes.

The wettability characteristics of the decorated PVDF membrane with optimized coating condition compared with the pristine PVDF membrane and control groups in contact with water droplets in air and with oil droplets underwater were presented in Figure 4.6 and Figure 4.7. In the case of PDA-decorated PVDF membranes oxidized by sodium periodate (Figure 4.6c and Figure 4.6d), the water drop would immediately spread along and permeate through the membranes

simultaneously once the droplets contacted with the membrane surfaces.

However, the pristine membrane (Figure 4.6a) and the autoxidized PDA-deposited membrane (Figure 4.6b) were not able to soak water drop. According to the accurate measurements of the water contact angle in Figure 4.7a, the water contact angle of the pristine hydrophobic PVDF membrane is around 113° in air. The conventional PDA-modified surfaces using dissolved oxygen are usually hydrophilic with a minimum water contact angle about 40-60° after 24-hour immersion in dopamine solution (2 mg mL^{-1}) in alkaline pH.[33,35] For 2-hour immersion, the pure PDA-deposited membrane (PDA-O_2-Tris) showed a stable contact angle about 97°. The PDA-modified membrane with chemical oxidation in alkaline condition (PDA-SP-Tris) displayed an instant contact angle about 33°, and then slowly declined to 0° in 22 s. However, the modified membrane employing the facile and optimal methodology notated as PDA-SP-2h exhibited excellent superhydrophilicity with an instant contact angle of 19°. At that time, the water droplet would immediately spread, permeated through the membrane in approximately 11 s to reach a contact angle of 0°, and completely soaked into the membrane.

As indicated in Figure 4.8, the pure water flux of the autoxidized PDA-deposited membrane (Figure 4.8a) at 0.038 MPa was about 331 ± 12 L m^{-2} h^{-1}, which was very low due to the poor hydrophilicity. However, the pure water fluxes of the PDA-modified membranes oxidized by sodium periodate in Tris-HCl buffer solution (pH= 8.5) and sodium acetate buffer solution (pH = 5.0) under the same pressure were as high as 9536 ± 429 L m^{-2} h^{-1} and 11934 ± 544 L m^{-2} h^{-1}, respectively (Figure 4.8b and Figure 4.8c). It is noted that the appreciable superhydrophilicity and the unprecedentedly high water flux of PDA-SP-2h were attributed to the hydrophilic and hierarchical coating on the surface and pore channels, as well as the negligible pore blocking of

PDA coating. This demonstrated the vital effect of sodium periodate in the slightly acidic environment. Thus, the dramatically improved hydrophilicity could enable water to permeate through the membrane much faster than others operated even under higher pressure.[46-48] Significantly, the pure water flux of the PDA-SP-2h was about 606 L m^{-2} h^{-1} solely driven by gravity, which was actually higher than those of many modified PVDF membranes operated under gravity[37] or extra pressure.[42,43]

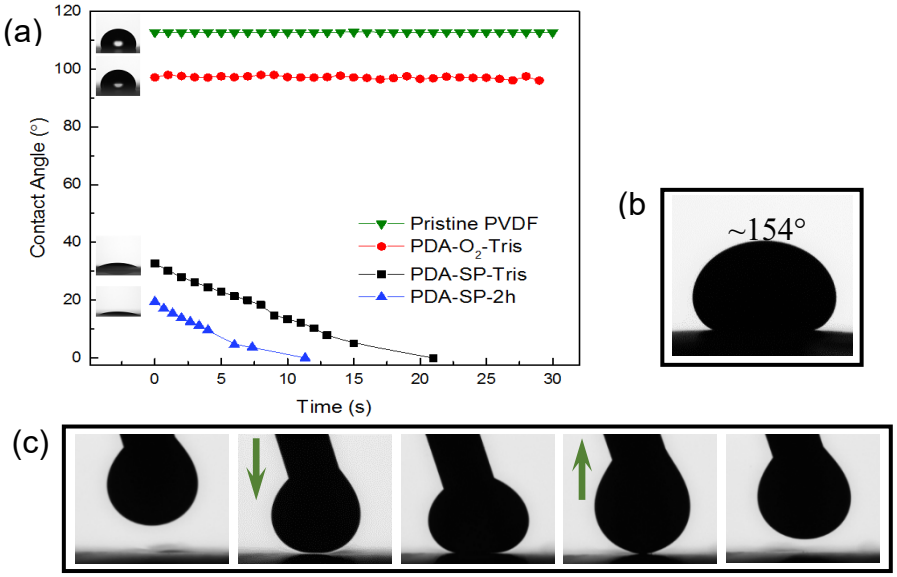

Figure 4.7 (a) Water contact angle in air of the pristine PVDF membrane, the dopamine/O_2-modified PVDF membrane (pH = 8.5, 2 h), the dopamine/sodium periodate-modified PVDF membrane (pH = 8.5, 2 h), and the dopamine/sodium periodate-modified PVDF membrane (pH = 5.0, 2 h). (The water droplet is about 5 μL). (b) Underwater oil contact angle and (c) dynamic underwater oil-adhesion of the dopamine/sodium periodate-modified PVDF membrane (pH = 5.0, 2 h). (The chloroform droplet is about 10 μL).

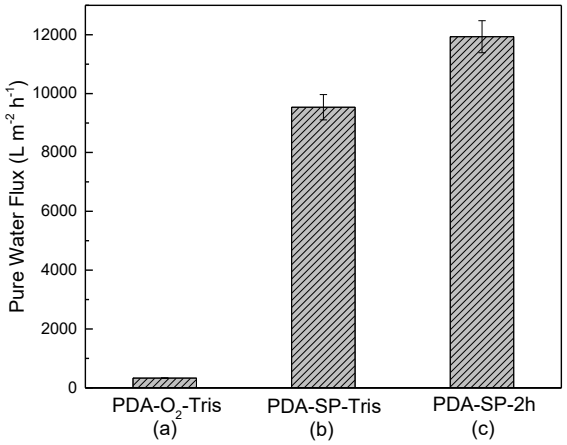

Figure 4.8 Pure water flux of the (a) dopamine/O_2-modified PVDF membrane (pH = 8.5, 2 h), (b) dopamine/sodium periodate-modified PVDF membrane (pH = 8.5, 2 h), and (c) dopamine/sodium periodate-modified PVDF membrane (pH = 5.0, 2 h).

Spontaneously, the superhydrophilicity feature can endow the modified PVDF membrane with the underwater superoleophobicity owing to the complementary effect of chemistry and mechanics of the "Cassie-Baxter" state at the oil/water/solid interface in the micro/nano-structures. Chloroform was selected to be used as an oil phase to detect the underwater superoleophobicity and dynamic underwater-oil-adhesion of the optimally modified membrane notated as PDA-SP-2h because its density is higher than that of water. The underwater oil contact angle was about 154° shown in Figure 4.7b, and no significant deformation and residual oil were observed during the dynamic contact process when an oil droplet was forced to contact with the membrane surface and then lifted up using an injection syringe (Figure 4.7c). This revealed the superoleophobicity and the low underwater-oil-adhesion of the decorated membrane surface by our optimized method. The excellent underwater superoleophobicity and the rather low oil-adhesion properties qualify this modified membrane for efficient oil/water separation.

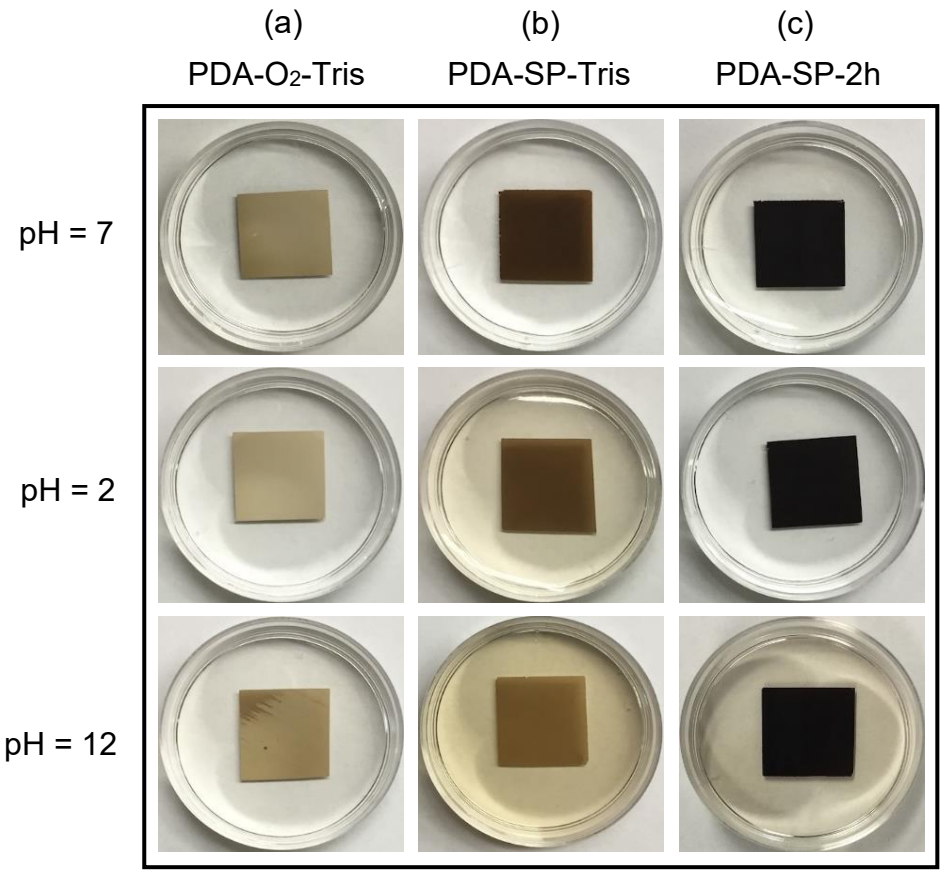

Figure 4.9 Photographs of the (a) dopamine/O_2-modified PVDF membrane (pH = 8.5, 2 h), (b) dopamine/sodium periodate-modified PVDF membrane (pH = 8.5, 2 h), and (c) dopamine/sodium periodate-modified PVDF membrane (pH = 5.0, 2 h), after being rinsed by solutions with different pH values for 12 h. All membranes were cut into square pieces (1.4 cm × 1.4 cm), rinsed by different solutions with the same volume of 5 mL.

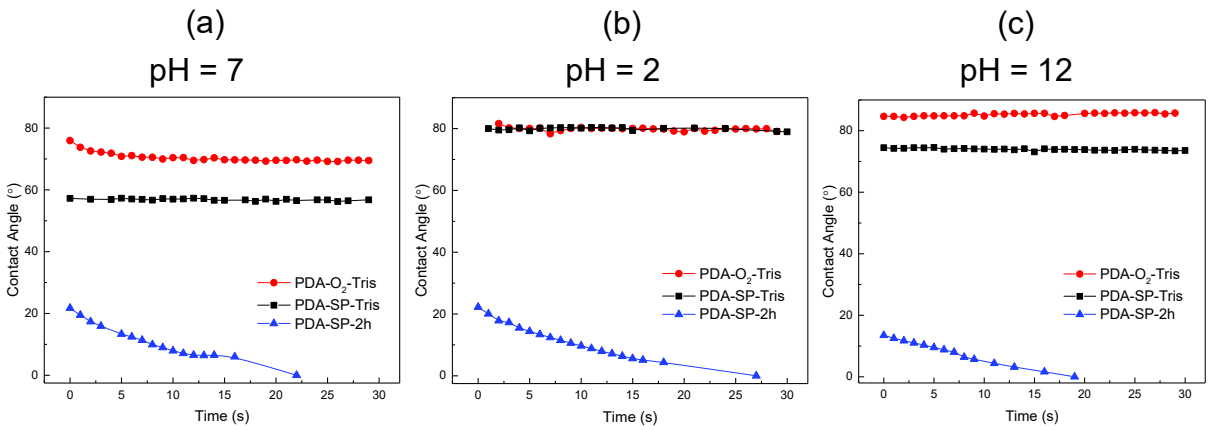

Figure 4.10 Water contact angle of the dopamine/O_2-modified PVDF membrane (pH = 8.5, 2 h), the dopamine/sodium periodate-modified PVDF membrane (pH = 8.5, 2 h), and the dopamine/sodium periodate-modified PVDF membrane (pH = 5.0, 2 h), after being rinsed by (a) neutral, (b) strong acidic, and (c) strong basic solutions for 12 h. (The water droplet is about 5 μL).

4.3.3 Stability of the Modified Membranes.

The freshly formed PDA coating layers display stability in neutral, slightly acidic and slightly basic solutions, whereas most of PDA can be dissolved and detached from the substrates in strong acidic and basic solutions due to the noncovalent interactions between PDA film and substrates.[49,50] To investigate the potential application of the optimally modified membrane (PDA-SP-2h) in neutral and harsh pH environments compared with the control experiments named as PDA-O_2-Tris and PDA-SP-Tris, respectively, all the membranes were rinsed by the neutral (pH = 7), strong acidic (pH = 2) and strong basic (pH = 12) solution for 12 h.

As presented in Figure 4.9, the solutions with different pH values which were used to rinse the autoxidized PDA-deposited membrane (Figure 4.9a) did not turn yellow due to the few PDA nanoparticles attached on the membrane surfaces shown in Figure 4.1c and Figure 4.1d. The solutions with pH = 2 and pH = 12 containing the modified membranes labeled as PDA-SP-Tris

turned to yellow, and the membranes were obviously bleached in the strong acidic and basic environments after being rinsed for 12 h (Figure 4.9b). By comparison, the membranes obtained under optimal preparation were more stable without apparent fade in the same conditions. The steadier PDA coating on the substrates (Figure 4.9c) revealed the crucial role of sodium periodate and the slightly acidic environment. As displayed in Figure 4.10, no noticeable declines of the water contact angle of the optimally prepared membranes (PDA-SP-2h) demonstrated that the excellent superhydrophilicity feature remained unchanged after being subjected to different chemical stresses. Whereas the evident hydrophilicity loss of the modified membranes notated as PDA-SP-Tris could be observed under the same treatment.

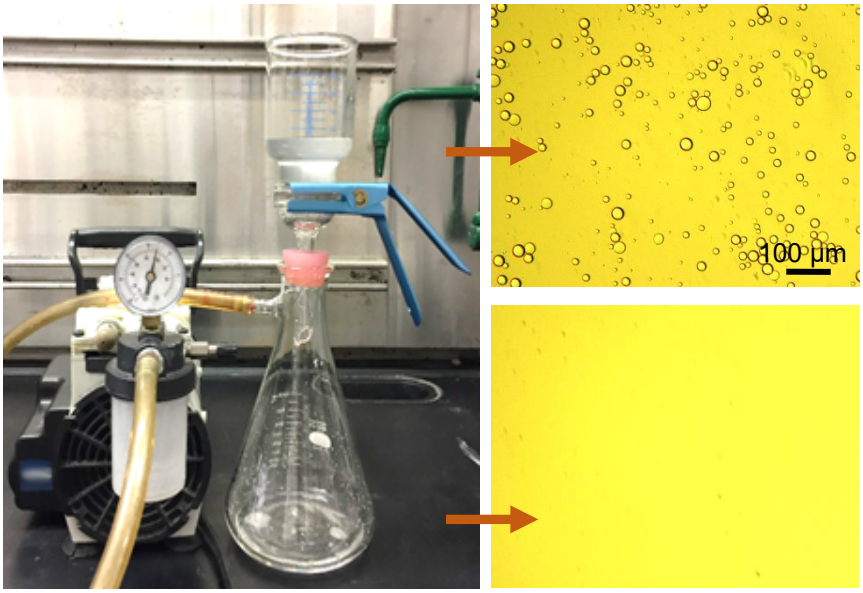

Figure 4.11 Photograph of the oil/water separation apparatus under 0.038 MPa and the micrographs of SDS-stabilized hexane-in-water emulsion and the filtrate using the dopamine/sodium periodate-modified PVDF membrane (pH = 5.0, 2 h).

The mechanical stabilities of these membranes were also detected after destructive disturbance (one-minute sonication, twice). As shown in Figure 4. S5 in the Supporting Information, the

contact angle of the optimally prepared membranes (PDA-SP-2h) indicated excellent hydrophilicity after treated with physical stress. However, the control group (PDA-SP-Tris) became less hydrophilic due to the poor mechanical stability.

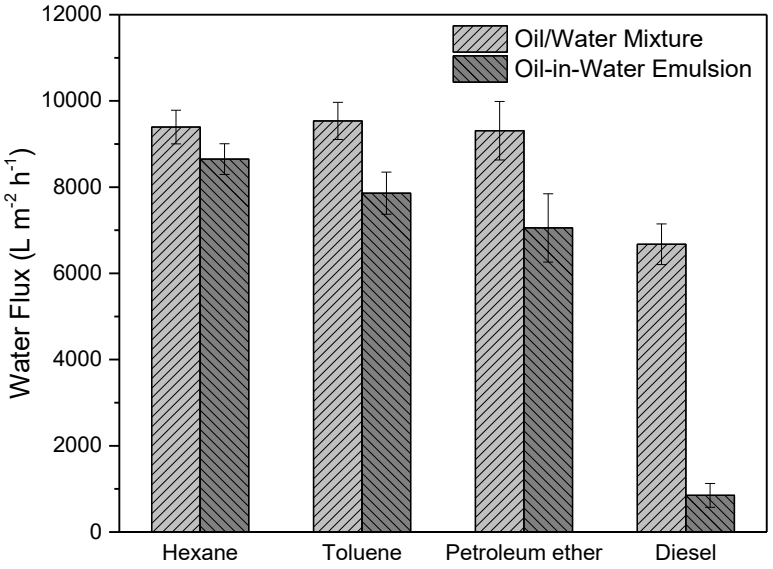

Figure 4.12 Water flux of different oil/water mixtures and oil-in-water emulsions permeated through the dopamine/sodium periodate-modified PVDF membrane (pH = 5.0, 2 h).

4.3.4 Separation of Oil/Water Mixtures and Oil-in-Water Emulsions with the Optimally Modified Membranes.

The superhydrophilicity and underwater superoleophobicity feature may endow the dopamine/sodium periodate-modified membrane (pH = 5.0, 2 h) with an excellent ability to separate oil/water mixtures and oil-in-water emulsions. To assess the separation performance, we prepared a series of oil/water mixtures and oil-in-water emulsions to permeate through the membranes in a vacuum filtration apparatus under a relatively low pressure difference of 0.038 MPa with an effective separation area of 11.34 cm^2 (Figure 4.11) to evaluate the water permeation

fluxes and oil rejection ratios. Figure 4.11 also showed the optical microscopy images of the feed solution (top right) and the filtrate solution (bottom right) of the SDS-stabilized hexane-in-water emulsion as an example. Numerous oil droplets with a size of 2-32 μm distributed in the oil-in-water emulsion, but no oil droplets could be observed in the transparent filtrate solution, illustrating that the oil phase could be separated from the emulsifier-stabilized emulsion.

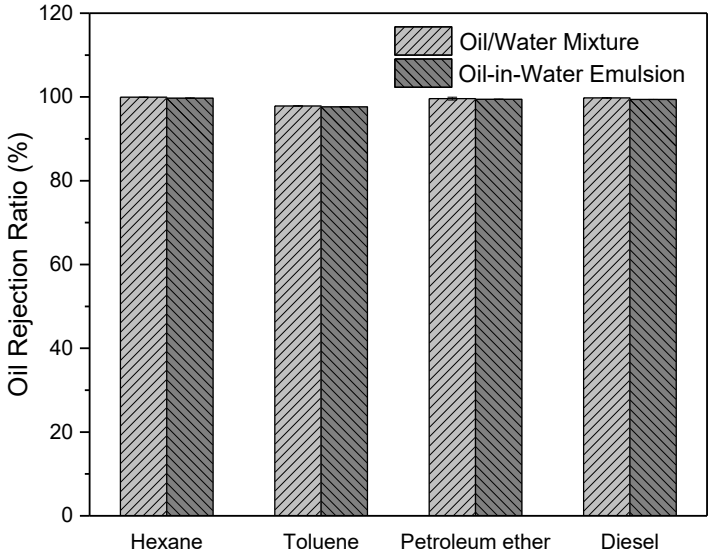

Figure 4.13 Oil rejection ratios of different oil/water mixtures and oil-in-water emulsions permeated through the dopamine/sodium periodate-modified PVDF membrane (pH = 5.0, 2 h).

As shown in Figure 4.12, for oil/water mixtures such as hexane/water, toluene/water, petroleum ether/water, and diesel/water, the water permeation fluxes were 9394 ± 391 L m^{-2} h^{-1}, 9537 ± 431 L m^{-2} h^{-1}, 9308 ± 679 L m^{-2} h^{-1}, and 6675 ± 473 L m^{-2} h^{-1}, respectively. For those emulsions contain surfactant e.g. SDS/hexane/water, SDS/toluene/water, SDS/petroleum ether/water, and SDS/diesel/water, the flux were 8649 ± 356 L m^{-2} h^{-1}, 7860 ± 488 L m^{-2} h^{-1}, 7055 ± 792 L m^{-2} h^{-1}, and 850 ± 276 L m^{-2} h^{-1}, respectively, which were comparatively lower than that of the corresponding surfactant-free oil/water mixtures due to the interference of surfactant.

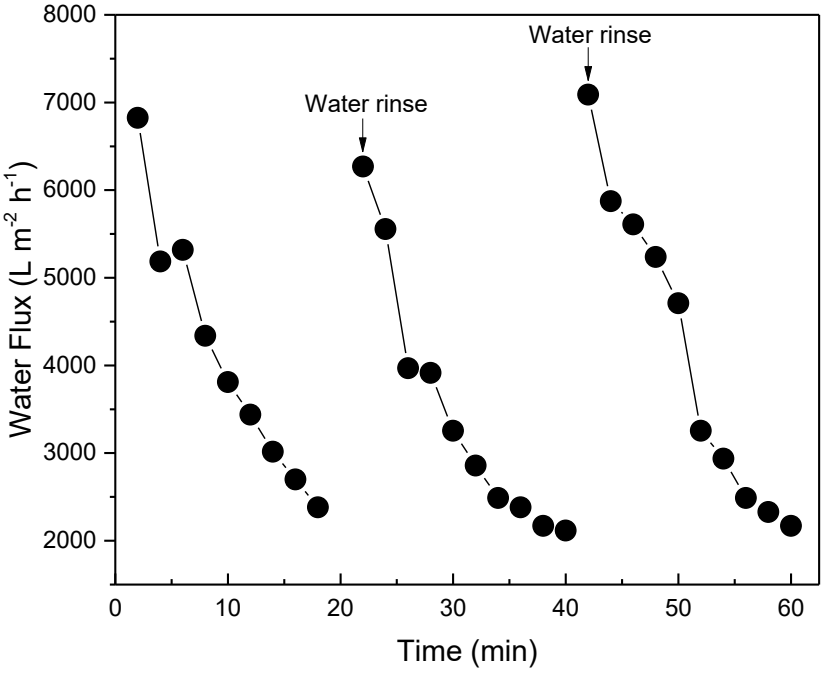

Figure 4.14 Variation of the water flux and flux recovery of SDS-stabilized petroleum ether-in-water emulsion treated by the dopamine/sodium periodate-modified PVDF membrane (pH = 5.0, 2 h) under constant pressure of 0.038 MPa.

The oil contents of the filtrates of these mixtures and emulsions were measured by a total organic carbon (TOC) analyzer and the oil rejection ratios are exhibited in Figure 4.13. For these oil/water mixtures containing hexane, toluene, petroleum ether and diesel, the oil rejection ratios were 99.93 ± 1.20%, 97.85 ± 0.77%, 99.62 ± 33.86%, and 99.77 ± 0.70%, respectively. While for those oil-in-water emulsions, the oil rejection ratios were 99.71 ± 1.80%, 97.64 ± 4.38%, 99.44 ± 0.89%, and 99.41 ± 0.42% respectively for each corresponding oil type. All the results revealed higher permeation fluxes and better separation efficiencies than those of some other modified filtration membranes.[51,52]

To evaluate the oil antifouling performance and reusability of the dopamine/sodium periodate-modified membrane (pH = 5.0, 2 h), a three-cyclic filtration experiment was implemented by

employing SDS-stabilized petroleum ether-in-water emulsion to permeate through the membrane under a constant pressure of 0.038 MPa. As shown in Figure 4.14, the filtration time for each cycle was 20 min and the real-time flux was measured every 2 minutes. The membranes were rinsed with DI water for 10 min between two cycles before the next measurement. The water permeation flux decreased sharply in the first 4 min resulted from the oil accumulation on the membrane surface.[53,54] This phenomenon may be caused by the oil cake layer formed under transmembrane pressure. Then the flux declined relatively slowly in every filtration cycle. However, the oil residue on the surface could be rinsed off by DI water, and the water flux could be recovered to the initial level. The oil rejection ratios of the second and the third cycle (98.60% and 98.47%, respectively) indicated that the optimally modified membrane has an excellent reusability and oil antifouling ability, revealing the practical ability for a long-term oil/water separation process.

4.4 Conclusions

We demonstrate a facile single-step high-efficient mussel-inspired methodology to modify hydrophobic PVDF microfiltration membrane with superhydrophilicity and underwater superoleophobicity properties for in-service application for oil/water separation. The deposition time for forming a layer of homogeneous and superhydrophilic PDA coating was greatly reduced under chemical oxidation of sodium periodate in the slightly acidic condition (pH = 5.0). The optimally designed membrane shows ultra-high pure water permeability under ultra-low transmembrane pressure, and even exhibits an appreciable pure water flux only driven by gravity. The excellent oil/water separation ability and anti-fouling performance allow the as-prepared membrane to be an effective tool to accomplish long-term and efficient separations. Furthermore, the extraordinary chemical and mechanical stability of the optimally modified membrane makes it suitable for applications in severe environments.

4.5 References

(1) Fakhru'l-Razi, A.; Pendashteh, A.; Abdullah, L. C.; Biak, D. R. A.; Madaeni, S. S.; Abidin, Z. Z. Review of Technologies for Oil and Gas Produced Water Treatment. *J. Hazard. Mater.* **2009**, *170*, 530-551.

(2) Schrope, M. Deep Wounds. *Nature* **2011**, *472*, 152-154.

(3) Ivshina, I. B.; Kuyukina, M. S.; Krivoruchko, A. V.; Elkin, A. A.; Makarov, S. O.; Cunningham, C. J.; Peshkur, T. A.; Atlas, R. M.; Philp, J. C. Oil Spill Problems and Sustainable Response Strategies through New Technologies. *Environ. Sci.: Processes Impacts* **2015**, *17*, 1201-1219.

(4) Chu, Z.; Feng, Y.; Seeger, S. Oil/Water Separation with Selective Superantiwetting/Superwetting Surface Materials. *Angew. Chem., Int. Ed.* **2015**, *54*, 2328-2338.

(5) Ma, Q.; Cheng, H.; Fane, A. G.; Wang, R.; Zhang, H. Recent Development of Advanced Materials with Special Wettability for Selective Oil/Water Separation. *Small* **2016**, *12*, 2186-2202.

(6) Xue, Z.; Cao, Y.; Liu, N.; Feng, L.; Jiang, L. Special Wettable Materials for Oil/Water Separation. *J. Mater. Chem. A* **2014**, *2*, 2445-2460.

(7) Kota, A. K.; Kwon, G.; Choi, W.; Mabry, J. M.; Tuteja, A. Hygro-Responsive Membranes for Effective Oil-Water Separation. *Nat. Commun.* **2012**, *3*, 1025-1030.

(8) Liu, N.; Chen, Y.; Lu, F.; Cao, Y.; Xue, Z.; Li, K.; Feng, L.; Wei, Y. Straightforward Oxidation of a Copper Substrate Produces an Underwater Superoleophobic Mesh for Oil/Water Separation. *ChemPhysChem* **2013**, *14*, 3489-3494.

(9) Zhang, F.; Zhang, W. B.; Shi, Z.; Wang, D.; Jin, J.; Jiang, L. Nanowire‐Haired Inorganic Membranes with Superhydrophilicity and Underwater Ultralow Adhesive Superoleophobicity for High‐Efficiency Oil/Water Separation. *Adv. Mater.* **2013**, *25*, 4192-4198.

(10) Wang, F.; Lei, S.; Xue, M.; Ou, J.; Li, C.; Li, W. Superhydrophobic and Superoleophilic

Miniature Device for the Collection of Oils from Water Surfaces. *J. Phys. Chem. C* **2014**, *118*, 6344-6351.

(11) Feng, L.; Zhang, Z.; Mai, Z.; Ma, Y.; Liu, B.; Jiang, L.; Zhu, D. A Super‐Hydrophobic and Super‐Oleophilic Coating Mesh Film for the Separation of Oil and Water. *Angew. Chem., Int. Ed.* **2004**, *43*, 2012-2014.

(12) Li, J.; Yan, L.; Zhao, Y.; Zha, F.; Wang, Q.; Lei, Z. One-Step Fabrication of Robust Fabrics with Both-Faced Superhydrophobicity for the Separation and Capture of Oil from Water. *Phys. Chem. Chem. Phys.* **2015**, *17*, 6451-6457.

(13) Wang, J.; Chen, Y. Oil-Water Separation Capability of Superhydrophobic Fabrics Fabricated via Combining Polydopamine Adhesion with Lotus-Leaf-Like Structure. *J. Appl. Polym. Sci.* **2015**, *132*, 42614.

(14) Xue, C.; Ji, P.; Zhang, P.; Li, Y.; Jia, S. Fabrication of Superhydrophobic and Superoleophilic Textiles for Oil-Water Separation. *Appl. Surf. Sci.* **2013**, *284*, 464-471.

(15) Kwon, G.; Kota, A.; Li, Y.; Sohani, A.; Mabry, J. M.; Tuteja, A. On-Demand Separation of Oil-Water Mixtures. *Adv. Mater.* **2012**, *24*, 3666-3671.

(16) Gao, X.; Xu, L.; Xue, Z.; Feng, L.; Peng, J.; Wen, Y.; Wang, S.; Zhang, X. Dual‐Scaled Porous Nitrocellulose Membranes with Underwater Superoleophobicity for Highly Efficient Oil/Water Separation. *Adv. Mater.* **2014**, *26*, 1771-1775.

(17) Zhu, Y.; Zhang, F.; Wang, D.; Pei, X. F.; Zhang, W.; Jin, J. A Novel Zwitterionic Polyelectrolyte Grafted PVDF Membrane for Thoroughly Separating Oil from Water with Ultrahigh Efficiency. *J. Mater. Chem. A* **2013**, *1*, 5758-5765.

(18) Khulbe, K.; Hamad, F.; Feng, C.; Matsuura, T.; Khayet, M. Study of the Surface of the Water Treated Cellulose Acetate Membrane by Atomic Force Microscopy. *Desalination* **2004**, *161*, 259-

262.

(19) Tang, C.; Ye, S.; Liu, H. Electrospinning of Poly (styrene-co-maleic anhydride) (SMA) and Water-Swelling Behavior of Crosslinked/Hydrolyzed SMA Hydrogel Nanofibers. *Polymer* **2007***, 48*, 4482-4491.

(20) Al-Obeidani, S.; Al-Hinai, H.; Goosen, M.; Sablani, S.; Taniguchi, Y.; Okamura, H. Chemical Cleaning of Oil Contaminated Polyethylene Hollow Fiber Microfiltration Membranes. *J. Membr. Sci.* **2008***, 307*, 299-308.

(21) Mueller, J.; Davis, R. H. Protein Fouling of Surface-Modified Polymeric Microfiltration Membranes. *J. Membr. Sci.* **1996***, 116*, 47-60.

(22) Yu, H.; Xie, Y.; Hu, M.; Wang, J.; Wang, S.; Xu, Z. Surface Modification of Polypropylene Microporous Membrane to Improve Its Antifouling Property in MBR: CO_2 Plasma Treatment. *J. Membr. Sci.* **2005***, 254*, 219-227.

(23) Yang, Y.; Li, Y.; Li, Q.; Wan, L.; Xu, Z. Surface Hydrophilization of Microporous Polypropylene Membrane by Grafting Zwitterionic Polymer for Anti-Biofouling. *J. Membr. Sci.* **2010***, 362*, 255-264.

(24) Ochoa, N.; Masuelli, M.; Marchese, J. Effect of Hydrophilicity on Fouling of an Emulsified Oil Wastewater with PVDF/PMMA Membranes. *J. Membr. Sci.* **2003***, 226*, 203-211.

(25) Yamato, N.; Kimura, K.; Miyoshi, T.; Watanabe, Y. Difference in Membrane Fouling in Membrane Bioreactors (MBRs) Caused by Membrane Polymer Materials. *J. Membr. Sci.* **2006***, 280*, 911-919.

(26) Du, J. R.; Peldszus, S.; Huck, P. M.; Feng, X. Modification of Poly (vinylidene fluoride) Ultrafiltration Membranes with Poly (vinyl alcohol) for Fouling Control in Drinking Water Treatment. *Water Res.* **2009***, 43*, 4559-4568.

(27) Xi, Z.; Xu, Y.; Zhu, L.; Wang, Y.; Zhu, B. A Facile Method of Surface Modification for Hydrophobic Polymer Membranes Based on the Adhesive Behavior of Poly (DOPA) and Poly (dopamine). *J. Membr. Sci.* **2009***, 327*, 244-253.

(28) Chen, J.; Li, J.; Chen, C. Surface Modification of Polyvinylidene Fluoride (PVDF) Membranes by Low-Temperature Plasma with Grafting Styrene. *Plasma Sci. Technol.* **2009***, 11*, 42.

(29) Liu, F.; Du, C.; Zhu, B.; Xu, Y. Surface Immobilization of Polymer Brushes onto Porous Poly (vinylidene fluoride) Membrane by Electron Beam to Improve the Hydrophilicity and Fouling Resistance. *Polymer* **2007***, 48*, 2910-2918.

(30) Fontananova, E.; Jansen, J. C.; Cristiano, A.; Curcio, E.; Drioli, E. Effect of Additives in the Casting Solution on the Formation of PVDF Membranes. *Desalination* **2006***, 192*, 190-197.

(31) Oh, S.; Kim, N.; Lee, Y. Preparation and Characterization of PVDF/TiO_2 Organic-Inorganic Composite Membranes for Fouling Resistance Improvement. *J. Membr. Sci.* **2009***, 345*, 13-20.

(32) Liu, M.; Wang, S.; Wei, Z.; Song, Y.; Jiang, L. Bioinspired Design of a Superoleophobic and Low Adhesive Water/Solid Interface. *Adv. Mater.* **2009***, 21*, 665-669.

(33) Lee, H.; Dellatore, S. M.; Miller, W. M.; Messersmith, P. B. Mussel-Inspired Surface Chemistry for Multifunctional Coatings. *Science* **2007***, 318*, 426-430.

(34) Hong, S.; Na, Y. S.; Choi, S.; Song, I. T.; Kim, W. Y.; Lee, H. Non-Covalent Self-Assembly and Covalent Polymerization Co-Contribute to Polydopamine Formation. *Adv. Funct. Mater.* **2012***, 22*, 4711-4717.

(35) Xiang, Y.; Liu, F.; Xue, L. Under Seawater Superoleophobic PVDF Membrane Inspired by Polydopamine for Efficient Oil/Seawater Separation. *J. Membr. Sci.* **2015***, 476*, 321-329.

(36) Yang, H.; Liao, K.; Huang, H.; Wu, Q.; Wan, L.; Xu, Z. Mussel-Inspired Modification of a

Polymer Membrane for Ultra-High Water Permeability and Oil-in-Water Emulsion Separation. *J. Mater. Chem. A* **2014**, *2*, 10225-10230.

(37) Wang, Z.; Jiang, X.; Cheng, X.; Lau, C. H.; Shao, L. Mussel-Inspired Hybrid Coatings that Transform Membrane Hydrophobicity into High Hydrophilicity and Underwater Superoleophobicity for Oil-in-Water Emulsion Separation. *ACS Appl. Mater. Interfaces* **2015**, *7*, 9534-9545.

(38) Yang, H.; Pi, J.; Liao, K.; Huang, H.; Wu, Q.; Huang, X.; Xu, Z. Silica-Decorated Polypropylene Microfiltration Membranes with a Mussel-Inspired Intermediate Layer for Oil-in-Water Emulsion Separation. *ACS Appl. Mater. Interfaces* **2014**, *6*, 12566-12572.

(39) Kang, S. M.; Hwang, N. S.; Yeom, J.; Park, S. Y.; Messersmith, P. B.; Choi, I. S.; Langer, R.; Anderson, D. G.; Lee, H. One-Step Multipurpose Surface Functionalization by Adhesive Catecholamine. *Adv. Funct. Mater.* **2012**, *22*, 2949-2955.

(40) Liu, Y.; Chang, C.; Sun, T. Dopamine-Assisted Deposition of Dextran for Nonfouling Applications. *Langmuir* **2014**, *30*, 3118-3126.

(41) Yang, H.; Lan, Y.; Zhu, W.; Li, W.; Xu, D.; Cui, J.; Shen, D.; Li, G. Polydopamine-Coated Nanofibrous Mats as a Versatile Platform for Producing Porous Functional Membranes. *J. Mater. Chem.* **2012**, *22*, 16994-17001.

(42) Shao, L.; Wang, Z. X.; Zhang, Y. L.; Jiang, Z. X.; Liu, Y. Y. A Facile Strategy to Enhance PVDF Ultrafiltration Membrane Performance via Self-Polymerized Polydopamine Followed by Hydrolysis of Ammonium Fluotitanate. *J. Membr. Sci.* **2014**, *461*, 10-21.

(43) Shi, H.; He, Y.; Pan, Y.; Di, H.; Zeng, G.; Zhang, L.; Zhang, C. A Modified Mussel-Inspired Method to Fabricate TiO_2 Decorated Superhydrophilic PVDF Membrane for Oil/Water Separation. *J. Membr. Sci.* **2016**, *506*, 60-70.

(44) Ponzio, F.; Barthes, J.; Bour, J.; Michel, M.; Bertani, P.; Hemmerlé, J.; d'Ischia, M.; Ball, V. Oxidant Control of Polydopamine Surface Chemistry in Acids: A Mechanism-Based Entry to Superhydrophilic-Superoleophobic Coatings. *Chem. Mater.* **2016***, 28*, 4697-4705.

(45) Ito, S.; Wakamatsu, K. Chemical Degradation of Melanins: Application to Identification of Dopamine‐Melanin. *Pigm. Cell Res.* **1998***, 11*, 120-126.

(46) Kang, G.; Cao, Y. Application and Modification of Poly (vinylidene fluoride) (PVDF) Membranes-A Review. *J. Membr. Sci.* **2014***, 463*, 145-165.

(47) Liu, F.; Hashim, N. A.; Liu, Y.; Abed, M. M.; Li, K. Progress in the Production and Modification of PVDF Membranes. *J. Membr. Sci.* **2011***, 375*, 1-27.

(48) Yang, H.; Luo, J.; Lv, Y.; Shen, P.; Xu, Z. Surface Engineering of Polymer Membranes via Mussel-Inspired Chemistry. *J. Membr. Sci.* **2015***, 483*, 42-59.

(49) Wei, H.; Ren, J.; Han, B.; Xu, L.; Han, L.; Jia, L. Stability of Polydopamine and Poly (DOPA) Melanin-Like Films on the Surface of Polymer Membranes under Strongly Acidic and Alkaline Conditions. *Colloids Surf., B* **2013**, *110*, 22-28.

(50) Dreyer, D. R.; Miller, D. J.; Freeman, B. D.; Paul, D. R.; Bielawski, C. W. Elucidating the Structure of Poly (dopamine). *Langmuir* **2012**, *28*, 6428-6435.

(51) Zhang, W.; Zhu, Y.; Liu, X.; Wang, D.; Li, J.; Jiang, L.; Jin, J. Salt-Induced Fabrication of Superhydrophilic and Underwater Superoleophobic PAA-g-PVDF Membranes for Effective Separation of Oil-in-Water Emulsions. *Angew. Chem., Int. Ed.* **2014**, *53*, 856-860.

(52) Ju, J.; Wang, T.; Wang, Q. Superhydrophilic and Underwater Superoleophobic PVDF Membranes via Plasma-Induced Surface PEGDA for Effective Separation of Oil-in-Water Emulsions. *Colloids Surf., A* **2015**, *481*, 151-157.

(53) Zhang, W.; Shi, Z.; Zhang, F.; Liu, X.; Jin, J.; Jiang, L. Superhydrophobic and Superoleophilic

PVDF Membranes for Effective Separation of Water-in-Oil Emulsions with High Flux. *Adv. Mater.* **2013**, *25*, 2071-2076.

(54) Zhu, Y.; Wang, D.; Jiang, L.; Jin, J. Recent Progress in Developing Advanced Membranes for Emulsified Oil/Water Separation. *NPG Asia Mater.* **2014**, *6*, e101.

4.6 Supporting Information

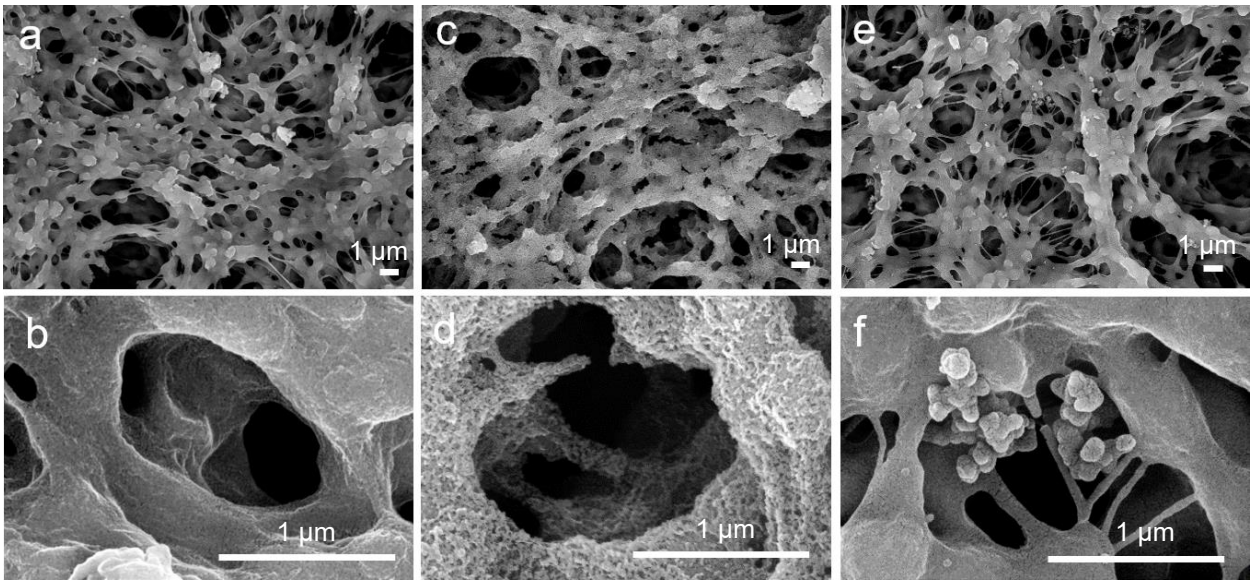

Figure 4. S1 Surface morphologies of the (a-d) dopamine/sodium periodate-modified PVDF membrane (pH = 5.0) for (a, b) 0.5 h, and (c, d) 4 h, and (e, f) dopamine/sodium periodate-modified PVDF membrane (pH = 8.5, 2 h). The scale bars are 1 μm in all images at different magnifications.

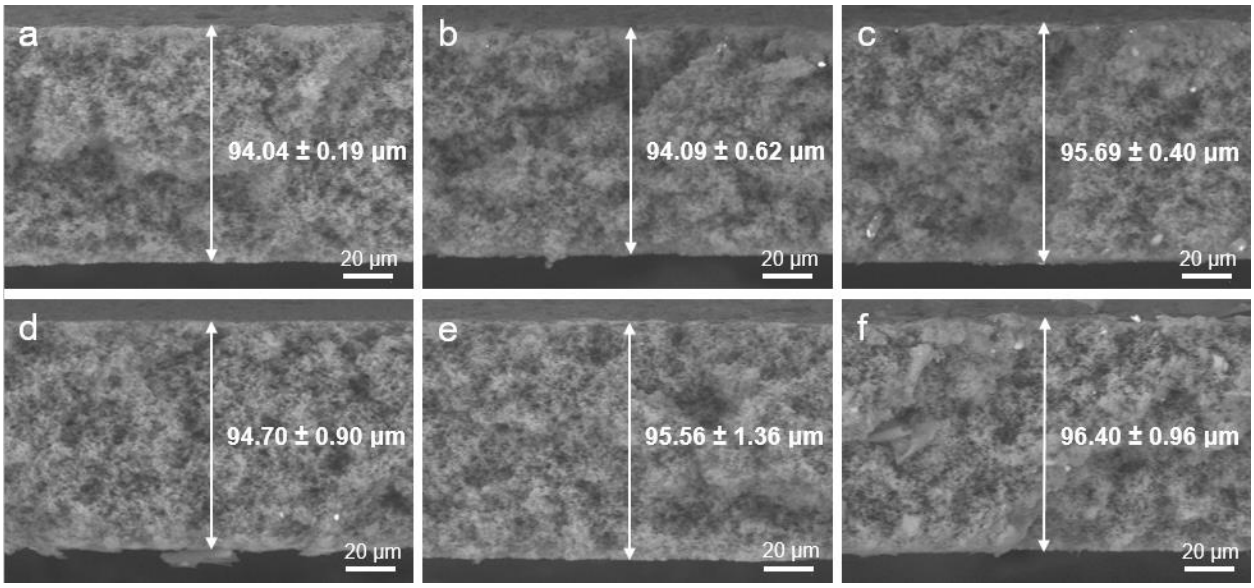

Figure 4. S2 FESEM images and thickness of the cross-section of the (a) pristine PVDF membrane, (b) dopamine/O_2-modified PVDF membrane (pH = 8.5, 2 h), (c) dopamine/sodium periodate-modified PVDF membrane (pH = 8.5, 2 h), (d-f) dopamine/sodium periodate-modified PVDF membrane (pH = 5.0) for (d) 0.5 h, (e) 2 h, and (f) 4 h.

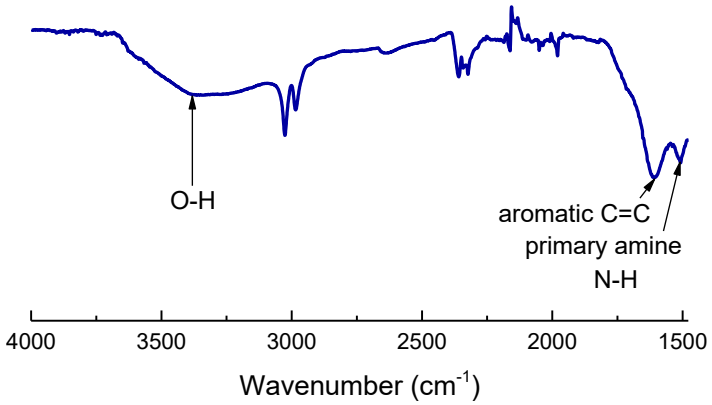

Figure 4. S3 ATR-FTIR spectra of the dopamine/O_2-modified PVDF membrane (pH = 8.5, 24 h).

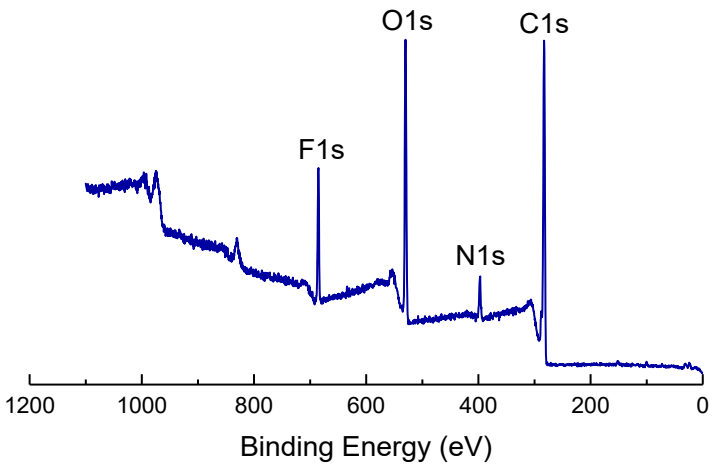

Figure 4. S4 XPS spectra of the dopamine/O_2-modified PVDF membrane (pH = 8.5, 24 h).

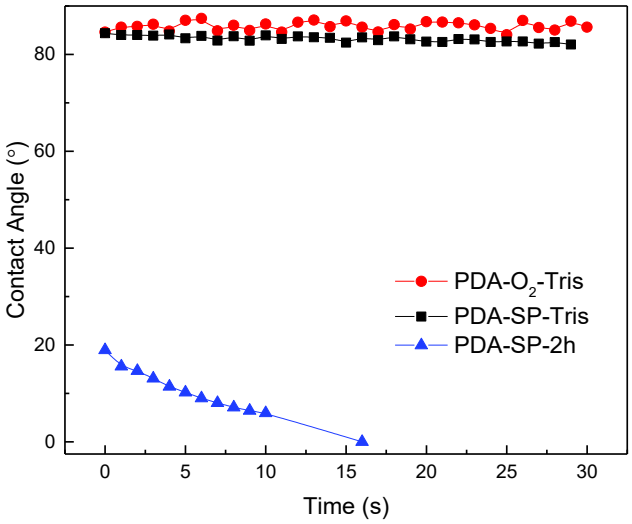

Figure 4. S5 Water contact angle of the dopamine/O_2-modified PVDF membrane (pH = 8.5, 2 h), the dopamine/sodium periodate-modified PVDF membrane (pH = 8.5, 2 h), and the dopamine/sodium periodate-modified PVDF membrane (pH = 5.0, 2 h) after sonication treatment.

Table 4. S1 Elemental Composition of the Dopamine/O_2-Modified PVDF Membrane Surface (pH = 8.5, 24 h) Examined by XPS

membrane	composition (at %)				atomic ratio	
	C	F	O	N	N/C	O/C
PDA-O_2-Tris-24h	72.71	5.84	16.97	4.48	0.06	0.23

Chapter 5 Rapid Deposition of the Oxidant-Induced Polydopamine Coating on PVDF Membrane for Protein-Resistant Modification[2]

5.1 Introduction

Membrane-based technology has shown superiorities over many conventional approaches for water separation and purification due to its operating flexibility, removal efficiency, energy conservation, and cost reduction.[1,2] However, fouling phenomenon of the porous membrane is a key challenge in the separation process caused by the electrostatic force and the hydrophobic interaction between the membrane surfaces and organic foulants.[3] In particular, hydrophobic membranes manufactured with polymers such as polytetrafluoroethylene (PTFE), polyvinylidene fluoride (PVDF), polypropylene (PP) and polyethylene (PE) display the high susceptibility to protein fouling due to the intrinsic hydrophobicity.[4,5] As a consequence, membrane fouling generally results in the increase of transmembrane pressure, the reduction of flux, and the decrease of durability.[6] The hydrophilic modification is commonly employed to improve the antifouling property of those hydrophobic membranes,[7-9] leading to the formation of a thin water layer on the modified hydrophilic surface, which acts as a barrier against proteins from adsorbing onto the membranes via repulsive hydration forces.[10-13] The modification methods of polymeric membranes can be divided into several types: coating,[14-16] blending,[17-19] composite,[20-22] grafting,[23-25] chemical modification,[26-28] and combined methods.[29-31] However, most of these approaches are suffering from some shortages, such as low efficiency, poor flexibility, and high cost, which limit their practical applications to some extent. Thus, methodologies with higher efficiency, better universality, and lower cost are expected to prepare membranes with antifouling property.

Messersmith et al. reported the mussel-inspired chemistry that dopamine can self-polymerize

[2] A version of this chapter will be submitted to the *Journal of Membrane Science*.

under a slightly alkaline condition with oxygen, forming a versatile polydopamine (PDA) coating layer on virtually all types of surfaces.[32] However, the pure PDA layer is insufficient to achieve antifouling modification because of its instability and limited hydrophilicity. It is noteworthy that PDA coating layer can be utilized as an intermediate layer for subsequent functionalization because of the quantities of active catechol groups. Zhu *et al.* reported that the antifouling property of PP membrane can be improved by immobilizing poly(N-vinyl pyrrolidine) (PVP) on the PDA-pretreated membrane via hydrogen-bonding interactions.[33] Zwitterionic copolymers can also be incorporated onto the poly(ether sulfone) (PES) hollow fiber membrane through the introduction of 2-methacryloyloxyethyl lipoate (MEL) containing sufficient grafting sites to react with PDA anchored on the membrane.[34] The initiators of atom transfer radical polymerization (ATRP) were immobilized onto the PDA-modified membrane to accomplish surface zwitterionization by poly(sulfobetaine methacrylate) (PSBMA).[35] The deposition of hydrophilic inorganic components, such as SiO_2, TiO_2, and ZrO_2, can be facilitated with the PDA intermediate layer by promoting the binding force and distribution of particles on hydrophobic membranes.[36-38] But, those methods mentioned above contain multiple steps to achieve the hydrophilicity and antifouling enhancement, which are quite time-consuming and low-efficient.

Therefore, many researches have been aimed at the one-step methodology to enhance antifouling characteristic by PDA coating. For example, dextran molecules were co-deposited with PDA onto various substrates in the polymerization process.[39] PSBMA could also be co-deposited with PDA onto the PP porous membrane in a one-pot mixture of dopamine/PSBMA solution.[40] Besides, antifouling improvement could also be accomplished by the co-deposition of PDA and low-molecular-weight polyethyleneimine (PEI) via Michael addition and Schiff-base reactions.[41] However, most of the co-deposition processes take a rather long time to obtain the

optimal results. Chemical oxidation is introduced in the polymerization process to dramatically shorten the reaction time and accelerate the deposition of PDA, compared with the autoxidative polymerization process in air. $CuSO_4/H_2O_2$ was utilized as a trigger to generate a mass of reactive oxygen free radicals and thus shortened the reaction time of the co-deposition of PDA and PSBMA to 1 h.[6] More importantly, the $CuSO_4/H_2O_2$-triggered PDA/PSBMA coating showed better uniformity, stability and antifouling properties than those of the conventional PDA coating oxidized by oxygen. In our previous work, a facile one-step method was reported to modify PVDF membrane with superhydrophilicity via the deposition of PDA coating oxidized by sodium periodate in a weakly acidic condition (pH = 5.0) for 2 h to separate oil/water mixtures and oil-in-water emulsions.[42] The as-prepared membrane exhibited high water flux, high oil rejection ratio, great chemical and mechanical stability for oil/water separation.

Herein, we investigate the protein resistance of the dopamine/sodium periodate-modified PVDF membrane in an extremely short reaction time of 0.5 h. Sodium periodate oxidation at pH = 5.0 can markedly accelerate the deposition rate of PDA and significantly enhance the hydrophilicity of the PDA layer. A robust combined-water layer can be formed on the membrane surface to inhibit the adsorption and deposition of bovine serum albumin (BSA). Moreover, sodium periodate can also lead to the formation of carboxyl groups on the membrane surface, which can increase the electrostatic repulsion between the negatively charged surface and BSA. The modified membrane showed a better protein resistance at the neutral condition owing to the enhanced hydrophilicity and the more negatively charged surface.

5.2 Experimental Section

5.2.1 Materials

Polyvinylidene fluoride microfiltration membranes (PVDF, mean pore size 0.22 μm, diameter

47 mm) were purchased from the Millipore Co. Dopamine hydrochloride, bovine serum albumin (BSA, IEP = 4.7, M_w ~66 kDa), phosphate buffered saline (PBS, pH = 7.4, 0.01 M) were purchased from Sigma-Aldrich. Sodium periodate, anhydrous sodium acetate, acetic acid, and tris (hydroxymethyl) aminomethane hydrochloride (Tris-HCl) were purchased from Fisher Scientific. All the chemicals were used as received.

5.2.2 Fabrication of Antifouling Membranes

The PVDF membranes were immersed in 2 mg mL^{-1} dopamine sodium acetate buffer solution (50 mM, pH = 5.0) with 4 mg mL^{-1} sodium periodate for 0.5 h and 2 h, after washed and pre-wetted with ethanol and DI water. A beaker containing the membrane and solution was shaken at 150 rpm while covered with an aluminum foil under ambient conditions. The decorated membranes were rinsed with DI water and dried in an oven at 40 ℃ overnight after modification. The membranes with different deposition time were denoted as PDA-SP-0.5h and PDA-SP-2h, respectively. A control sample named PDA-O_2-Tris was obtained by the conventional deposition method in 2 mg mL^{-1} dopamine Tris-HCl buffer solution (50 mM, pH = 8.5) with a reaction time of 2 h in air via self-polymerization. The control experiment was conducted with the same process of pre-wetting and drying.

5.2.3 Characterizations

Surface morphologies of the pristine and modified PVDF membranes were observed by the field emission scanning electron microscopy (FESEM, Carl-Zeiss Sigma). The charging properties of membrane surfaces were detected by a streaming potential method using the electrokinetic analyzer (SurPASS Anton Paar, GmbH). 1 mM KCl solution was chosen as the electrolyte solution. The water contact angles were measured by the theta optical tensiometer (Attension, Biolin Scientific T200). The absorbance of protein was monitored by the UV-vis-NIR spectrophotometer

(UV-3600, Shimadzu). All the filtration fluxes were tested with a dead-end solvent resistant stirred cell (Millipore XFUF04701).

5.2.4 Deposition Density Measurements

The deposition density (*DD*, mg cm^{-2}) was obtained using the following equation (5.1):

$$DD = \frac{M_1 - M_0}{A} \tag{5.1}$$

where M_1, M_0 and A are the weight of the membrane after modification (mg), the weight of the pristine membrane (mg), and the area of the membrane (17.34 cm^2), respectively. Each result was based on the mean value of three parallel measurements.

5.2.5 Surface Zeta Potential Measurements

Each membrane sample was cut into a circle with a diameter of 14 mm and fixed in the adjustable cell for disk. The flow pressure was set as 100 mbar for all the measurements. The zeta potential results of different membrane surfaces at pH = 7.4 were obtained via adjusting the pH of the solution by NaOH solution (0.1 M). The surface zeta potential ζ was obtained by the Helmholtz-Smoluchowski equation:

$$\zeta = \frac{\Delta E}{\Delta P}\frac{\eta\kappa}{\varepsilon} \tag{5.2}$$

where ΔE is the streaming potential, ΔP is the applied pressure, ε is the permittivity, η and κ are the viscosity and the conductivity of the solution, respectively.

5.2.6 Dynamic Protein Filtration Tests

Dynamic protein filtration was implemented to evaluate the protein antifouling property of the membrane, which was carried out by a solvent resistant stirred cell (Millipore XFUF04701). The membrane sample with an effective membrane area of 15 cm^2 was fixed on the sample holder after wetted with DI water. The dead-end filtration cell was fully clamped to ensure a properly sealed condition and connected with a compressed nitrogen gas cylinder for the following operating

procedure as shown in Figure 5.1.

The membrane was firstly compacted under 0.3 MPa for 20 min at 25 ℃. Then the pure water flux J_{w1} (L m^{-2} h^{-1}) was measured at 0.1 Mpa until a stable value and calculated by the equation (5.3) below:

$$J = \frac{V}{A\Delta t} \tag{5.3}$$

where V (L) is the permeated volume, A (m^2) is the effective membrane area, and Δt (h) is the permeation time. BSA was chosen as the protein model to investigate the protein-resistant performance. The concentration of BSA was 1 mg mL^{-1} in PBS buffer solution (0.01 M, pH = 7.4). The cell was placed centrally on a magnetic stirrer to avoid the concentration polarization of BSA with a stirring speed of 100 rpm. After measuring the flux of BSA solution J_{BSA} (L m^{-2} h^{-1}) at 0.10 Mpa, the membrane was cleaned with DI water in a beaker shaking at 140 rpm for 30 min. The cleaning water was changed every 5 min. And then the pure water flux J_{w2} (L m^{-2} h^{-1}) of the cleaned membrane was tested again at 0.10 Mpa to observe the flux recovery of the membrane. In order to assess the antifouling property of the membranes, the relative flux reduction (RFR), flux recovery ratio (FRR), reversible fouling ratio (F_r), and irreversible fouling ratio (F_{ir}) were calculated as follows:

$$\text{RFR}\ (\%) = \left(1 - \frac{J_{BSA}}{J_{w1}}\right) \times 100 \tag{5.4}$$

$$\text{FRR}\ (\%) = \frac{J_{w2}}{J_{w1}} \times 100 \tag{5.5}$$

$$F_r\ (\%) = \frac{J_{w2} - J_{BSA}}{J_{w1}} \times 100 \tag{5.6}$$

$$F_{ir}\ (\%) = \frac{J_{w1} - J_{w2}}{J_{w1}} \times 100 \tag{5.7}$$

The lower RFR and higher FRR values indicate the better antifouling property of membrane. The reversible fouling ratio (F_r) shows the flux reduction due to the formation of protein cake layer

on the surface, which can be easily rinsed off by hydraulic cleaning. On the other hand, the irreversible fouling ratio (F_{ir}) shows the flux decline caused by the adsorption and entrapment of protein on the surface and in the pores, which are hard to be removed by hydraulic cleaning solely.[43]

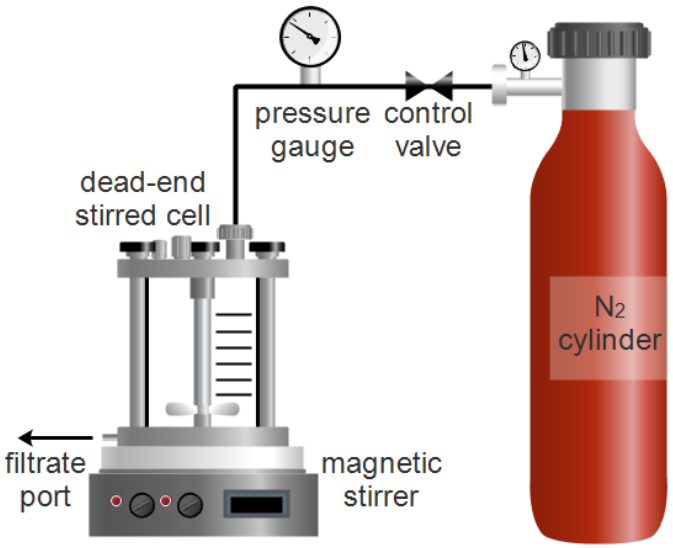

Figure 5.1 Dead-end filtration setup for dynamic protein filtration tests.

5.2.7 Static Protein Adsorption Tests

To investigate the capacity of static protein resistance, the membranes were cut to small pieces with the same area of 1 × 2 cm^2. Each of the samples was immersed in BSA solution (10 mL, 0.01 M PBS buffer solution, pH = 7.4) under shaking at 100 rpm for 4 h at room temperature to reach the adsorption equilibrium. And then each sample was taken out of the vial by a tweezer and washed with 10 mL PBS solution (pH = 7.4) using a syringe to remove the non-adsorbed protein residue. The wash-off solution was directly added into the vial. The concentrations of the initial and final BSA solutions were detected by the UV-vis-NIR spectrometer at the wavelength of 278 nm, and calculated according to the calibration curve (C = 0.7593X - 0.0007), where X is the value

of UV adsorption of the solution. The weight of BSA adsorbed on the membrane surface per unit area (A_{BSA}, μg cm^{-2}) can be described by the equation (5.8):

$$A_{BSA}=\frac{C_0V_0 - C_{BSA}V}{S}\times 1000 \quad (5.8)$$

where C_0 (mg mL^{-1}) and V_0 (mL) are the actual concentration and volume of the initial BSA solution, respectively. C_{BSA} (mg mL^{-1}) and V (mL) are the concentration and volume of the final BSA solution, respectively. S (cm^2) is the area of sample.

5.3 Results and Discussion

5.3.1 Deposition Densities and Surface Morphologies of Different Membranes

The deposition of PDA on the substrate largely depends on the temperature, concentration of dopamine, pH condition, reaction time and additional oxidant.[6] In our experiments, the temperature and the concentration of dopamine were chosen to be 25 ℃ and 2 mg mL^{-1}, respectively. In order to investigate the impact of reaction time, oxidant and pH value, the deposition density was obtained by measuring the weight increment per unit area of the membrane after modification.

As indicated in Figure 5.2, the deposition density of the PDA-O_2-Tris was only 0.0654 ± 0.0266 mg cm^{-2}. However, the oxidant-induced membranes showed an obvious increase of the deposition density, which became even larger along with the reaction time. For PDA-SP-0.5h, the deposition density was 0.3037 ± 0.0643 mg cm^{-2}, about five times larger than that of the pure PDA deposition in a much shorter reaction time. Moreover, the deposition density of the PDA-SP-2h reached 0.5075 ± 0.0305 mg cm^{-2}, revealing a high formation rate of the thick PDA layer on the membrane while sodium periodate was used as the oxidant.

Figure 5.3 displayed the surface morphologies of the membranes obtained by the FESEM.

Figure 5.3g and Figure 5.3h apparently demonstrated that the membrane pores of PDA-SP-2h were severely obstructed due to the formation of a great deal of PDA nanoparticles, which were in a good agreement with the deposition density result in Figure 5.2. This morphology may lead to the flowing hindrance and flux decline through the porous membrane. Whereas, the images of the rapid oxidant-induced modification with a reaction time of 0.5 h (Figure 5.3e and Figure 5.3f) indicated that smaller nanoparticles were deposited on the surfaces and channels without obvious pore blocking, and thereby the original porous conformation of the pristine membrane was maintained, ensuring the permeability of the modified membrane. For PDA-O_2-Tris, no PDA nanoparticles can be observed in Figure 5.3c and Figure 5.3d, revealing the low deposition efficiency of the conventional method.

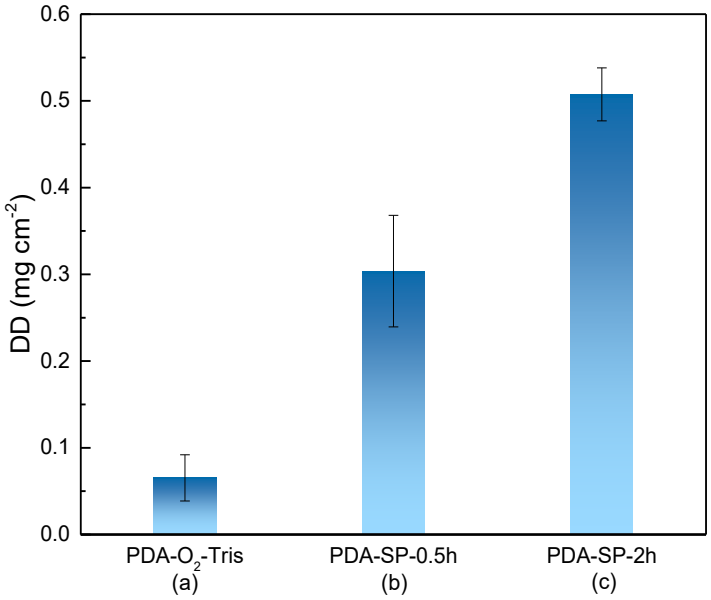

Figure 5.2 The deposition density of the (a) dopamine/O_2-modified PVDF membrane (pH = 8.5, 2 h), and dopamine/sodium periodate-modified PVDF membrane (pH = 5.0) for (b) 0.5 h and (c) 2 h.

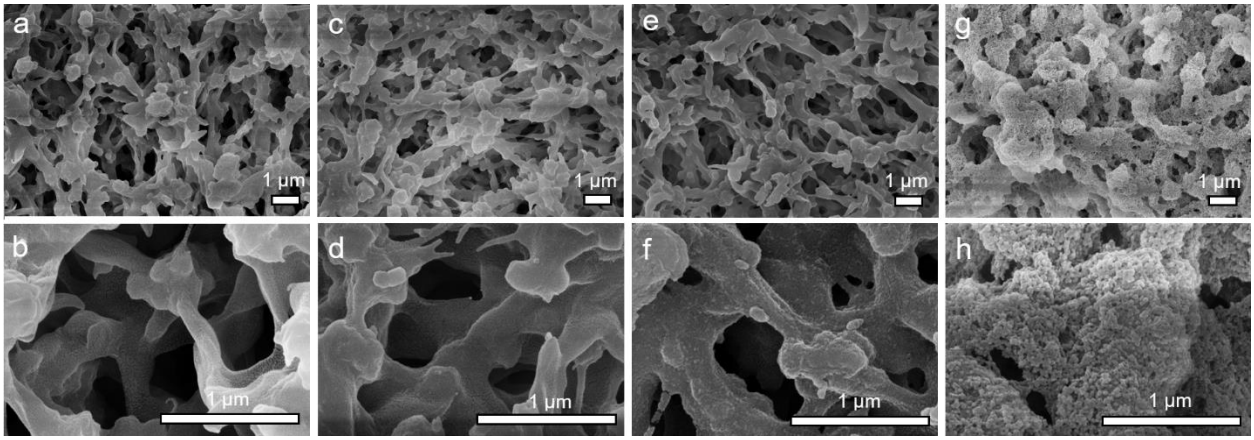

Figure 5.3 FESEM top-view images of the (a, b) pristine PVDF membrane, (c, d) dopamine/O_2-modified PVDF membrane (pH = 8.5, 2 h), (e, f) dopamine/sodium periodate-modified PVDF membrane (pH = 5.0, 0.5 h), and (g, h) dopamine/sodium periodate-modified PVDF membrane (pH = 5.0, 2 h). The scale bars are 1 μm in all images at different magnifications of 10k (a, c, e, g) and 50k (b, d, f, h).

5.3.2 Surface Chemistry and Wettability

In our previous work, we have emphasized the formation of carboxyl groups on the substrate via the ATR-FTIR and XPS tests.[42] From the ATR-FTIR spectra of nascent and modified membranes (pore size 0.22 μm) in Figure 5.4, both PDA-SP-0.5h and PDA-SP-2h showed the characteristic peak of carboxyl groups around 1717 cm^{-1}. Their percent atomic concentrations of O 1s were higher than that of PDA-O_2-Tris according to the surface elemental composition measured by XPS.[42] The time-dependent measurements of water contact angles of the membranes were presented in Figure 5.5. The water contact angle of the pristine PVDF membrane was about 131°, showing the intrinsic hydrophobic property of the nascent membrane. By contrast, after the high-efficient deposition of PDA with the oxidation effect of sodium periodate, the PDA-SP-0.5h and PDA-SP-2h displayed instant contact angles about 13° and 10°, respectively. Once contacted with the surface, the water droplets spread and permeated through the membrane completely in

about 10 s to reach a contact angle of 0°, indicating the superhydrophilicity feature of the modified membranes.

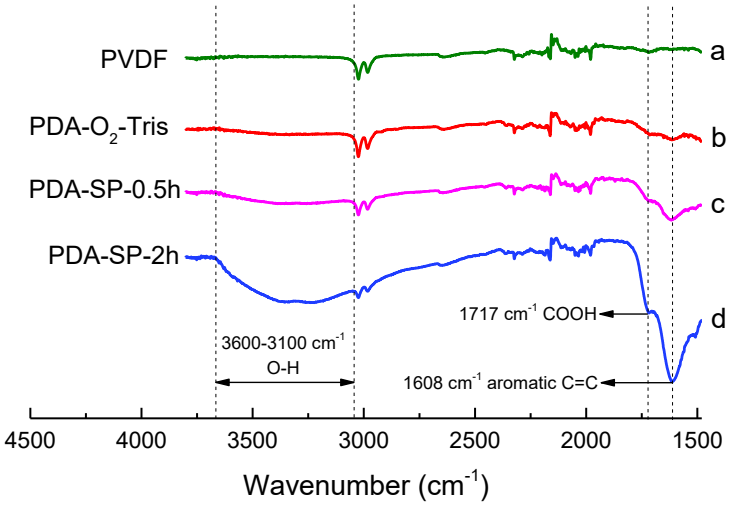

Figure 5.4 ATR-FTIR spectra of (a) PVDF membrane (pore size 0.22 μm), (b) dopamine/O_2-modified PVDF membrane (pH = 8.5, 2 h), and dopamine/sodium periodate-modified PVDF membrane (pH = 5.0) for (c) 0.5 h, and (d) 2 h.

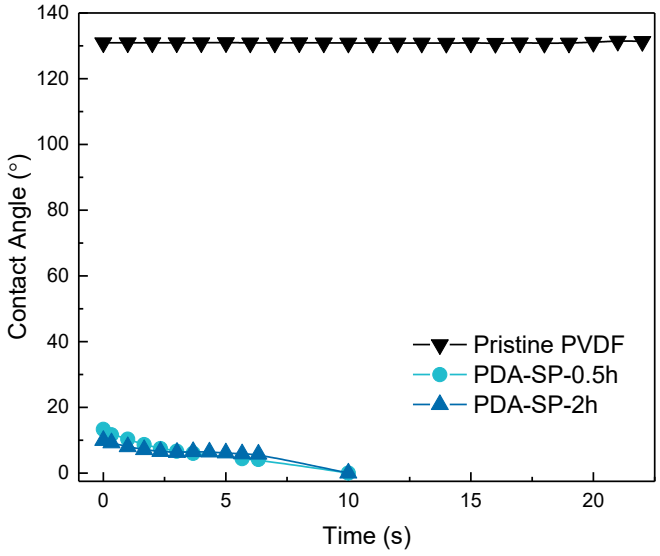

Figure 5.5 Water contact angles in air of the pristine PVDF membrane, and the dopamine/sodium

periodate-modified PVDF membrane (pH = 5.0) for 0.5 h and 2 h.

5.3.3 Surface Zeta Potential

The zeta potential results of the pristine and the modified membranes were displayed in Figure 5.6, demonstrating that the surfaces of all the membranes were negatively charged at pH = 7.4. It is noted that the surface charge of the modified membranes became more negative than that of the pristine one because of the formation of carboxyl groups on the surface under sodium periodate oxidation at acidic pH. PDA-SP-2h was more negatively charged than PDA-SP-0.5h ascribed to the denser PDA layer with more carboxyl groups on its substrate with the increasing reaction time.

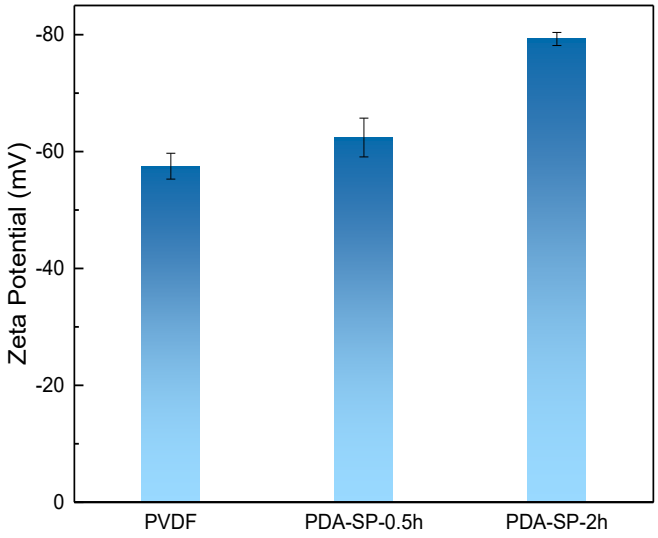

Figure 5.6 Zeta potential of the pristine PVDF membrane, and the dopamine/sodium periodate-modified PVDF membrane (pH = 5.0) for 0.5 h and 2 h.

5.3.4 Antifouling Performance

The structural characteristics of protein change with the pH condition, which strongly affect the adsorption mechanism between BSA and membrane.[3] At a neutral condition (pH = 7.4 > IEP),

BSA is negatively charged in PBS buffer solution because of the deprotonation.[40] Dynamic protein filtration test was adopted to investigate the antifouling capacity of different membranes using BSA solution (pH = 7.4). Figure 5.7 showed the time-dependent flux measurements of a recycle process including three steps: permeation of DI water, permeation of BSA solution, and permeation of DI water again. During the first stage, the water fluxes of PDA-SP-0.5h and PDA-SP-2h were higher than that of the pristine PVDF membrane, which were about 1040 L m^{-2} h^{-1} and 780 L m^{-2} h^{-1} at 0.1 MPa, respectively. However, the water flux of the PDA-SP-2h was slightly lower than that of the PDA-SP-0.5h because the denser PDA coating caused pore blocking and thickness increasing of the membrane.

As shown in Table 5.1, the RFR of the pristine PVDF membrane was 64.91%, which means the membrane was blocked due to the protein adsorption arising from the hydrophobic interaction between protein and hydrophobic membrane. In contrast, PDA-SP-0.5h displayed a lower RFR (43.27%), which was ascribed to the enhanced hydrophilicity and the more negatively charged surface resulted from the deprotonation of carboxyl groups on the membrane. The water molecule layer formed on the membrane surface and the improved electrostatic repulsion between the protein and membrane can effectively inhibit the protein adsorption and therefore reduce fouling. However, PDA-SP-2h showed a higher RFR (69.23%) indicating that the formation of a denser and thicker PDA coating led to an undesirable reduction of pore size, thus resulting in an obvious flowing hindrance of BSA solution.

Additionally, PDA-SP-0.5h showed the highest FRR (84.62%) indicating the relatively high flux recovery after hydraulic cleaning and thus reflecting the relatively excellent antifouling performance. Whereas, the FRR of PDA-SP-2h (56.41%) was lower than that of the PDA-SP-0.5h because of the rather thick and excessive PDA nanoparticles forming in the pores. The decline of

flux was caused by the pore blockage because of the entrapment of protein molecules in pores when proteins were forced to pass through the membrane under pressure, which significantly deteriorated the antifouling performance of the membrane.[44, 45]

The flux decline is caused by the total fouling of the membrane, which is composed of the reversible fouling and the irreversible fouling. For PDA-SP-0.5h, the percentage of the reversible fouling in the total fouling (F_r/RFR) was about 64.44%, which was relatively higher than those of the pristine membrane and PDA-SP-2h. Besides, the percentage of irreversible fouling in the total fouling (F_{ir}/RFR) was about 35.56%, which was apparently lower than those of other membranes. This conspicuous feature of the PDA-SP-0.5h indicated that the reversible fouling induced by protein cake layer was dominant in the fouling behavior. In contrary, the higher F_{ir}/RFR and lower F_r/RFR of the PDA-SP-2h demonstrated that the irreversible fouling caused by the protein entrapment in the pores had a mainly negative influence on the antifouling characteristic due to the severe reduction of the pore size.

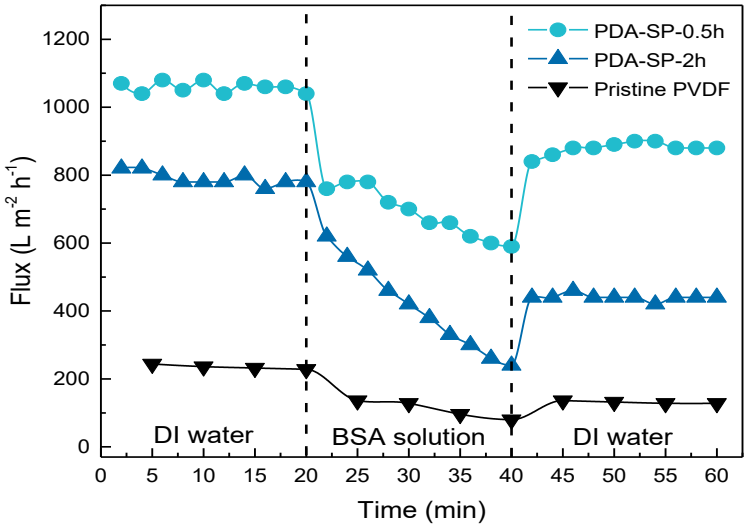

Figure 5.7 The dynamic protein filtration tests of the pristine PVDF membrane, and the dopamine/sodium periodate-modified PVDF membrane (pH = 5.0) for 0.5 h and 2 h.

Table 5.1 The Relative Flux Reduction (RFR), Flux Recovery Ratio (FRR), Reversible Fouling Ratio (F_r), Irreversible Fouling Ratio (F_{ir}), Percentage of Reversible Fouling in Total Fouling (F_r/RFR), and Percentage of Irreversible Fouling in Total Fouling (F_{ir}/RFR) of Different Membranes

	RFR (%)	FRR (%)	F_r (%)	F_{ir} (%)	F_r/RFR (%)	F_{ir}/RFR (%)
PVDF	64.91	56.14	21.05	43.86	32.43	67.57
PDA-SP-0.5h	43.27	84.62	27.88	15.38	64.44	35.56
PDA-SP-2h	69.23	56.41	25.64	43.59	37.04	62.96

Static protein adsorption tests were also conducted to evaluate the antifouling property of the rapid modified membrane compared with that of the pristine PVDF membrane. Table 5.2 displayed the UV absorbance values at the wavelength of 278 nm of the BSA solutions obtained eventually of different membranes. The actual concentration of the initial BSA was about 0.9903 mg mL^{-1}. It can be seen from Figure 5.8 and Table 5.2, after being immersed in BSA solution (10 mL, pH = 7.4) for 4 h, the amount of BSA adsorbed on the pristine PVDF membrane was much higher than that of the modified membrane. By comparison, A_{BSA} value of the PDA-SP-0.5h indicated the excellent static protein resistance because of the superhydrophilicity and the more negatively charged surface of the membrane, which was in a good agreement with the results of contact angle measurements and surface zeta potential tests.

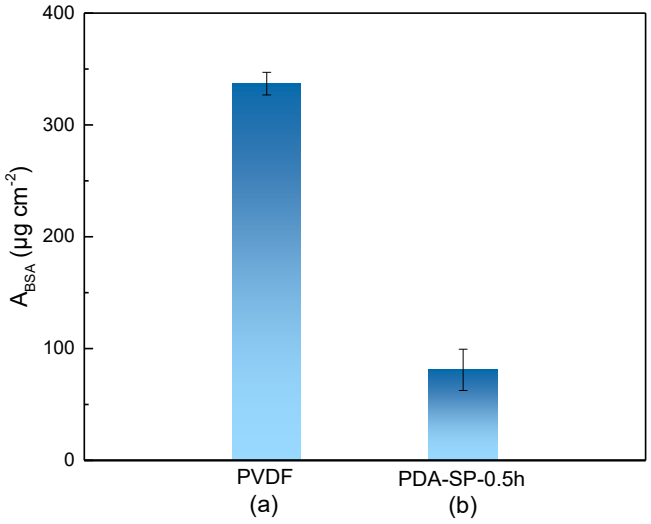

Figure 5.8 The amount of BSA adsorbed on the surface and pores of the (a) pristine PVDF membrane, and (b) dopamine/sodium periodate-modified PVDF membrane (pH = 5.0) for 0.5 h.

Table 5.2 The UV Absorbance Values at the Wavelength of 278 nm of Diluted BSA Solutions, and the Amounts of BSA Adsorbed on the Membranes Per Unit Area (A_{BSA}, μg cm^{-2})

	Absorbance	A_{BSA} (μg cm^{-2})
PVDF	0.3497 ± 0.0008	336.93 ±10.13
PDA-SP-0.5h	0.3691 ± 0.0014	81.00 ± 18.44

5.4 Conclusions

We investigated the antifouling property of the sodium periodate-induced PDA deposition on the PVDF membrane in an extreme short reaction time of 0.5 h. This dramatically rapid deposition can maintain the conformation of the porous membrane without pore blocking due to the uniform and thin coating layer of small nanoparticles. In contrast with the pristine PVDF membrane, the optimized membrane showed better antifouling property because of the formation of hydrophilic

carboxyl group on the surface, which resulted in the more hydrophilic and more negatively charged surface, and hence effectively inhibited the BSA deposition and adsorption. This work proposes a high-efficient pathway of PDA coating via chemical oxidation to promote the antifouling property of hydrophobic membranes.

5.5 References

(1) Saxena, A.; Tripathi, B. P.; Kumar, M.; Shahi, V. K. Membrane-Based Techniques for the Separation and Purification of Proteins: An Overview. *Adv. Colloid Interface Sci.* **2009***, 145*, 1-22.

(2) Jhaveri, J. H.; Murthy, Z. A Comprehensive Review on Anti-Fouling Nanocomposite Membranes for Pressure Driven Membrane Separation Processes. *Desalination* **2016***, 379*, 137-154.

(3) Boributh, S.; Chanachai, A.; Jiraratananon, R. Modification of PVDF Membrane by Chitosan Solution for Reducing Protein Fouling. *J. Membr. Sci.* **2009***, 342*, 97-104.

(4) Shannon, M. A.; Bohn, P. W.; Elimelech, M.; Georgiadis, J. G.; Marias, B. J.; Mayes, A. M. Science and Technology for Water Purification in the Coming Decades. *Nature* **2008***, 452*, 301-310.

(5) Pi, J.; Yang, H.; Wan, L.; Wu, J.; Xu, Z. Polypropylene Microfiltration Membranes Modified with TiO_2 Nanoparticles for Surface Wettability and Antifouling Property. *J. Membr. Sci.* **2016***, 500*, 8-15.

(6) Zhang, C.; Li, H.; Du, Y.; Ma, M.; Xu, Z. $CuSO_4/H_2O_2$-Triggered Polydopamine/Poly (sulfobetaine methacrylate) Coatings for Antifouling Membrane Surfaces. *Langmuir* **2017***, 33*, 1210-1216.

(7) Rana, D.; Matsuura, T. Surface Modifications for Antifouling Membranes. *Chem. Rev.* **2010***, 110*, 2448-2471.

(8) Meng, F.; Chae, S.; Drews, A.; Kraume, M.; Shin, H.; Yang, F. Recent Advances in Membrane Bioreactors (MBRs): Membrane Fouling and Membrane Material. *Water Res.* **2009***, 43*, 1489-1512.

(9) Hilal, N.; Ogunbiyi, O. O.; Miles, N. J.; Nigmatullin, R. Methods Employed for Control of Fouling in MF and UF Membranes: A Comprehensive Review. *Sep. Sci. Technol.* **2005***, 40*, 1957-2005.

(10) Chen, S.; Li, L.; Zhao, C.; Zheng, J. Surface Hydration: Principles and Applications Toward Low-Fouling/Nonfouling Biomaterials. *Polymer* **2010***, 51*, 5283-5293.

(11) Zheng, J.; Li, L.; Tsao, H.; Sheng, Y.; Chen, S.; Jiang, S. Strong Repulsive Forces Between Protein and Oligo (ethylene glycol) Self-Assembled Monolayers: A Molecular Simulation Study. *Biophys. J.* **2005***, 89*, 158-166.

(12) Herrwerth, S.; Eck, W.; Reinhardt, S.; Grunze, M. Factors that Determine the Protein Resistance of Oligoether Self-Assembled Monolayers−Internal Hydrophilicity, Terminal Hydrophilicity, and Lateral Packing Density. *J. Am. Chem. Soc.* **2003***, 125*, 9359-9366.

(13) Vatanpour, V.; Madaeni, S. S.; Khataee, A. R.; Salehi, E.; Zinadini, S.; Monfared, H. A. TiO_2 Embedded Mixed Matrix PES Nanocomposite Membranes: Influence of Different Sizes and Types of Nanoparticles on Antifouling and Performance. *Desalination* **2012***, 292*, 19-29.

(14) Hyun, J.; Jang, H.; Kim, K.; Na, K.; Tak, T. Restriction of Biofouling in Membrane Filtration Using a Brush-Like Polymer Containing Oligoethylene Glycol Side Chains. *J. Membr. Sci.* **2006***, 282*, 52-59.

(15) Bae, T.; Tak, T. Effect of TiO_2 Nanoparticles on Fouling Mitigation of Ultrafiltration Membranes for Activated Sludge Filtration. *J. Membr. Sci.* **2005***, 249*, 1-8.

(16) Boricha, A. G.; Murthy, Z. Preparation, Characterization and Performance of Nanofiltration

Membranes for the Treatment of Electroplating Industry Effluent. *Sep. Purif. Technol.* **2009***, 65*, 282-289.

(17) Saljoughi, E.; Mohammadi, T. Cellulose Acetate (CA)/Polyvinylpyrrolidone (PVP) Blend Asymmetric Membranes: Preparation, Morphology and Performance. *Desalination* **2009***, 249*, 850-854.

(18) Jayalakshmi, A.; Rajesh, S.; Kim, I. C.; Senthilkumar, S.; Mohan, D.; Kwon, Y. Poly (isophthalamide) Based Graft Copolymer for the Modification of Cellulose Acetate Ultrafiltration Membranes and a Fouling Study by AFM Imaging. *J. Membr. Sci.* **2014***, 465*, 117-128.

(19) Nguyen, T. P. N.; Yun, E.; Kim, I.; Kwon, Y. Preparation of Cellulose Triacetate/Cellulose Acetate (CTA/CA)-Based Membranes for Forward Osmosis. *J. Membr. Sci.* **2013***, 433*, 49-59.

(20) Zhao, Z.; Wang, Z.; Wang, S. Formation, Charged Characteristic and BSA Adsorption Behavior of Carboxymethyl Chitosan/PES Composite MF Membrane. *J. Membr. Sci.* **2003***, 217*, 151-158.

(21) Zhao, Z.; Wang, Z.; Ye, N.; Wang, S. A Novel N, O-Carboxymethyl Amphoteric Chitosan/Poly (ethersulfone) Composite MF Membrane and Its Charged Characteristics. *Desalination* **2002***, 144*, 35-39.

(22) Gohil, G. S.; Nagarale, R. K.; Binsu, V. V.; Shahi, V. K. Preparation and Characterization of Monovalent Cation Selective Sulfonated Poly (ether ether ketone) and Poly (ether sulfone) Composite Membranes. *J. Colloid Interface Sci.* **2006***, 298*, 845-853.

(23) Belfer, S.; Fainchtain, R.; Purinson, Y.; Kedem, O. Surface Characterization by FTIR-ATR Spectroscopy of Polyethersulfone Membranes-Unmodified, Modified and Protein Fouled. *J. Membr. Sci.* **2000***, 172*, 113-124.

(24) Reddy, A.; Trivedi, J. J.; Devmurari, C. V.; Mohan, D. J.; Singh, P.; Rao, A. P.; Joshi, S. V.;

Ghosh, P. K. Fouling Resistant Membranes in Desalination and Water Recovery. *Desalination* **2005***, 183*, 301-306.

(25) Pieracci, J.; Wood, D. W.; Crivello, J. V.; Belfort, G. UV-Assisted Graft Polymerization of N-vinyl-2-pyrrolidinone onto Poly (ether sulfone) Ultrafiltration Membranes: Comparison of Dip Versus Immersion Modification Techniques. *Chem. Mater.* **2000***, 12*, 2123-2133.

(26) Higuchi, A.; Iwata, N.; Tsubaki, M.; Nakagawa, T. Surface‐Modified Polysulfone Hollow Fibers. *J. Appl. Polym. Sci.* **1988***, 36*, 1753-1767.

(27) Nabe, A.; Staude, E.; Belfort, G. Surface Modification of Polysulfone Ultrafiltration Membranes and Fouling by BSA Solutions. *J. Membr. Sci.* **1997***, 133*, 57-72.

(28) Higuchi, A.; Mishima, S.; Nakagawa, T. Separation of Proteins by Surface Modified Polysulfone Membranes. *J. Membr. Sci.* **1991***, 57*, 175-185.

(29) Fang, B.; Ling, Q.; Zhao, W.; Ma, Y.; Bai, P.; Wei, Q.; Li, H.; Zhao, C. Modification of Polyethersulfone Membrane by Grafting Bovine Serum Albumin on the Surface of Polyethersulfone/Poly (acrylonitrile-co-acrylic acid) Blended Membrane. *J. Membr. Sci.* **2009***, 329*, 46-55.

(30) Bae, T.; Tak, T. Preparation of TiO_2 Self-Assembled Polymeric Nanocomposite Membranes and Examination of Their Fouling Mitigation Effects in a Membrane Bioreactor System. *J. Membr. Sci.* **2005***, 266*, 1-5.

(31) Mansourpanah, Y.; Madaeni, S. S.; Rahimpour, A.; Farhadian, A.; Taheri, A. H. Formation of Appropriate Sites on Nanofiltration Membrane Surface for Binding TiO_2 Photo-Catalyst: Performance, Characterization and Fouling-Resistant Capability. *J. Membr. Sci.* **2009***, 330*, 297-306.

(32) Lee, H.; Dellatore, S. M.; Miller, W. M.; Messersmith, P. B. Mussel-Inspired Surface

Chemistry for Multifunctional Coatings. *Science* **2007***, 318*, 426-430.

(33) Jiang, J.; Zhu, L.; Zhu, L.; Zhang, H.; Zhu, B.; Xu, Y. Antifouling and Antimicrobial Polymer Membranes Based on Bioinspired Polydopamine and Strong Hydrogen-Bonded Poly (N-vinyl pyrrolidone). *ACS Appl. Mater. Interfaces* **2013***, 5*, 12895-12904.

(34) Cai, T.; Li, X.; Wan, C.; Chung, T. Zwitterionic Polymers Grafted Poly (ether sulfone) Hollow Fiber Membranes and Their Antifouling Behaviors for Osmotic Power Generation. *J. Membr. Sci.* **2016***, 497*, 142-152.

(35) Zhu, L.; Liu, F.; Yu, X.; Gao, A.; Xue, L. Surface Zwitterionization of Hemocompatible Poly (lactic acid) Membranes for Hemodiafiltration. *J. Membr. Sci.* **2015***, 475*, 469-479.

(36) Kang, S. M.; Ryou, M.; Choi, J. W.; Lee, H. Mussel-and Diatom-Inspired Silica Coating on Separators Yields Improved Power and Safety in Li-Ion Batteries. *Chem. Mater.* **2012***, 24*, 3481-3485.

(37) Shao, L.; Wang, Z. X.; Zhang, Y. L.; Jiang, Z. X.; Liu, Y. Y. A Facile Strategy to Enhance PVDF Ultrafiltration Membrane Performance via Self-Polymerized Polydopamine Followed by Hydrolysis of Ammonium Fluotitanate. *J. Membr. Sci.* **2014***, 461*, 10-21.

(38) Yang, H.; Chen, Y.; Ye, C.; Jin, Y.; Li, H.; Xu, Z. Polymer Membrane with a Mineral Coating for Enhanced Curling Resistance and Surface Wettability. *Chem. Commun.* **2015***, 51*, 12779-12782.

(39) Liu, Y.; Chang, C.; Sun, T. Dopamine-Assisted Deposition of Dextran for Nonfouling Applications. *Langmuir* **2014***, 30*, 3118-3126.

(40) Zhou, R.; Ren, P.; Yang, H.; Xu, Z. Fabrication of Antifouling Membrane Surface by Poly (sulfobetaine methacrylate)/Polydopamine Co-Deposition. *J. Membr. Sci.* **2014***, 466*, 18-25.

(41) Yang, H.; Wu, M.; Li, Y.; Chen, Y.; Wan, L.; Xu, Z. Effects of Polyethyleneimine Molecular

Weight and Proportion on the Membrane Hydrophilization by Codepositing with Dopamine. *J. Appl. Polym. Sci.* **2016***, 133*.

(42) Luo, C.; Liu, Q. Oxidant-Induced High-Efficient Mussel-Inspired Modification on PVDF Membrane with Superhydrophilicity and Underwater Superoleophobicity Characteristics for Oil/Water Separation. *ACS Appl. Mater. Interfaces* **2017***, 9*, 8297-8307.

(43) Zhu, L.; Zhu, L.; Jiang, J.; Yi, Z.; Zhao, Y.; Zhu, B.; Xu, Y. Hydrophilic and Anti-Fouling Polyethersulfone Ultrafiltration Membranes with Poly (2-hydroxyethyl methacrylate) Grafted Silica Nanoparticles as Additive. *J. Membr. Sci.* **2014***, 451*, 157-168.

(44) Peng, J.; Su, Y.; Shi, Q.; Chen, W.; Jiang, Z. Protein Fouling Resistant Membrane Prepared by Amphiphilic Pegylated Polyethersulfone. *Bioresour. Technol.* **2011***, 102*, 2289-2295.

(45) Pieracci, J.; Crivello, J. V.; Belfort, G. Increasing Membrane Permeability of UV-Modified Poly (ether sulfone) Ultrafiltration Membranes. *J. Membr. Sci.* **2002***, 202*, 1-16.

Chapter 6 Conclusions and Contributions

6.1 Major Conclusions

This thesis is composed of two parts. The first part was to prepare a high-efficient PDA coating on PVDF membrane under the oxidation of sodium periodate in a slightly acidic condition (pH = 5.0). The optimally designed membrane exhibited outstanding ability to achieve oil/water separation. The other part was to investigate the protein-resistant property of the modified membrane via a rapid deposition. With an extreme short reaction time of 0.5 h, the modified membrane showed better antifouling performance against BSA than that of the pristine membrane. The major conclusions are summarized as follows:

1. This facile one-step mussel-inspired approach can effectively modify hydrophobic PVDF microfiltration membrane with superhydrophilicity and underwater superoleophobicity because of the significant improvement of hydrophilicity and the micro/nano-hierarchical structure on the surface and pore walls.

2. Chemical characterizations of the modified membranes via FTIR and XPS indicated the carboxyl groups on the substrate were generated by the oxidation effect of sodium periodate at acidic pH.

3. For the microfiltration PVDF membrane with a pore size of 0.45 μm, the morphology result of the PDA-SP-2h obtained by FESEM demonstrated the micro/nano-structured coating on the surface and inner pores, as well as the negligible pore blocking. The EDS mappings and the spectra also indicated the homogeneous distribution of the hydrophilic PDA nanoparticles. These prerequisite conditions endowed the membrane with the ultrahigh pure water flux and the high-efficient oil/water separation capability.

4. By the measurements of water contact angle before and after chemical and physical

treatments, the PDA-SP-2h exhibited excellent chemical stability of coating after rinsed by the neutral (pH = 7), strong acidic (pH = 2), and strong basic (pH = 12) solution for 12 h, and the outstanding mechanical stability after the destructive disturbance of 1 min sonication for twice.

5. The excellent oil antifouling performance and reusability of the PDA-SP-2h were evaluated through the three-cyclic filtration experiment using SDS-stabilized petroleum ether-in-water emulsion under 0.038 MPa. The water flux decreased sharply at the beginning because of the oil accumulation, but the flux can be easily recovered to the initial level after rinsing by DI water.

6. The dramatically rapid deposition of PDA coating on PVDF membrane oxidized by sodium periodate for only 0.5 h also showed the superhydrophilic property. From the FESEM results, a thin layer of small nanoparticles formed on the porous membrane without pore blocking.

7. The formation of the hydrophilic carboxyl group during the PDA deposition process led to the more hydrophilic and more negatively charged surface of the modified membrane, and thus diminished the BSA deposition and adsorption on the membrane surface because of the combined-water layer and the electrostatic repulsion, resulting in the improvement of the antifouling performance against negatively charged proteins.

6.2 Contributions to the Original Knowledge

The PDA coating suffers from the low-efficiency of polymerization, limited hydrophilicity, and instability, which greatly restrict its application on coating modification. For the aspects of oil/water separation and antifouling improvement, previous researches mainly focused on the two-step modification utilizing the reactivity of PDA as an intermediate layer for post-modification, or the addition of other reactants such as polymer, inorganic nanoparticles, coupling agent, etc. for the single-step modification. However, those methods are relatively complex and time-consuming. In this work, the one-step oxidant-induced approach of the PDA deposition on hydrophobic

membrane greatly improves the hydrophilicity and stability, and meanwhile dramatically shortens the reaction time. This oxidant-assisted method provides a pathway to broaden the application of PDA coating on various fields beyond membrane modification.

Chapter 7 Future Work

1. To investigate the protein-resistant property of the negatively charged membrane, the representative protein used in this work is BSA because it is negatively charged at the neutral condition. However, the addition of zwitterionic charged material could be a more effective way to resist different charged proteins. The overall electrically neutral surface could be achieved by grafting the zwitterionic polymeric additives onto the PDA-decorated membrane, or obtained by the codeposition with dopamine facilitated by chemical oxidation.

2. The dead-end stirred cell utilized in this study has a maximum capacity of 75 mL. In order to increase the volume capacity, a reservoir and a selector valve between the reservoir and the stirred cell could be installed to extend its application on protein permeation or nanofiltration with a larger treatment capacity.

3. Janus membrane composed of two sides with opposite wettability leads to the special transport behaviors. The hydrophilic side of the Janus membrane could be fabricated by the method mentioned in this study via the floated deposition. The other side could be grafted with hydrophobic polymers. This type of Janus membrane may be used in the separation of both water-in-oil emulsions and oil-in-water emulsions. Besides, it may also be employed in the water-to-oil and oil-to-water emulsification process. Or it could be applied for fine bubble aeration.

Bibliography

Adamson, A. W.; Gast, A. P. *Physical Chemistry of Surfaces*; Interscience Publishers: New York, 1967.

Akbari, A.; Derikvandi, Z.; Rostami, S. M. M. Influence of Chitosan Coating on the Separation Performance, Morphology and Anti-Fouling Properties of the Polyamide Nanofiltration Membranes. *J. Ind. Eng. Chem.* **2015***, 28*, 268-276.

Al-Obeidani, S.; Al-Hinai, H.; Goosen, M.; Sablani, S.; Taniguchi, Y.; Okamura, H. Chemical Cleaning of Oil Contaminated Polyethylene Hollow Fiber Microfiltration Membranes. *J. Membr. Sci.* **2008***, 307*, 299-308.

Ayyavoo, J.; Nguyen, T. P. N.; Jun, B.; Kim, I.; Kwon, Y. Protection of Polymeric Membranes with Antifouling Surfacing via Surface Modifications. *Colloids Surf. Physicochem. Eng. Aspects* **2016***, 506*, 190-201.

Bae, T.; Tak, T. Effect of TiO_2 Nanoparticles on Fouling Mitigation of Ultrafiltration Membranes for Activated Sludge Filtration. *J. Membr. Sci.* **2005***, 249*, 1-8.

Bae, T.; Tak, T. Preparation of TiO_2 Self-Assembled Polymeric Nanocomposite Membranes and Examination of Their Fouling Mitigation Effects in a Membrane Bioreactor System. *J. Membr. Sci.* **2005***, 266*, 1-5.

Belfer, S.; Fainchtain, R.; Purinson, Y.; Kedem, O. Surface Characterization by FTIR-ATR Spectroscopy of Polyethersulfone Membranes-Unmodified, Modified and Protein Fouled. *J. Membr. Sci.* **2000***, 172*, 113-124.

Boributh, S.; Chanachai, A.; Jiraratananon, R. Modification of PVDF Membrane by Chitosan Solution for Reducing Protein Fouling. *J. Membr. Sci.* **2009***, 342*, 97-104.

Boricha, A. G.; Murthy, Z. Preparation, Characterization and Performance of Nanofiltration

Membranes for the Treatment of Electroplating Industry Effluent. *Sep. Purif. Technol.* **2009***, 65*, 282-289.

Cai, T.; Li, X.; Wan, C.; Chung, T. Zwitterionic Polymers Grafted Poly (ether sulfone) Hollow Fiber Membranes and Their Antifouling Behaviors for Osmotic Power Generation. *J. Membr. Sci.* **2016***, 497*, 142-152.

Cassie, A.; Baxter, S. Wettability of Porous Surfaces. *Trans. Faraday Soc.* **1944***, 40*, 546-551.

Chan, C. C.; Lam, H.; Zhang, X. *Practical Approaches to Method Validation and Essential Instrument Qualification*; John Wiley & Sons: 2011.

Charcosset, C. Ultrafiltration, Microfiltration, Nanofiltration and Reverse Osmosis in Integrated Membrane Processes. In *Integrated Membrane Systems and Processes;* John Wiley & Sons: 2015; pp 1.

Charlot, A.; Sciannama, V.; Lenoir, S.; Faure, E.; Jrme, R.; Jrme, C.; Van De Weerdt, C.; Martial, J.; Archambeau, C.; Willet, N. All-in-One Strategy for the Fabrication of Antimicrobial Biomimetic Films on Stainless Steel. *J. Mater. Chem.* **2009***, 19*, 4117-4125.

Chen, J.; Li, J.; Chen, C. Surface Modification of Polyvinylidene Fluoride (PVDF) Membranes by Low-Temperature Plasma with Grafting Styrene. *Plasma Sci. Technol.* **2009***, 11*, 42.

Chen, S.; Li, L.; Zhao, C.; Zheng, J. Surface Hydration: Principles and Applications Toward Low-Fouling/Nonfouling Biomaterials. *Polymer* **2010***, 51*, 5283-5293.

Chen, W.; Su, Y.; Peng, J.; Zhao, X.; Jiang, Z.; Dong, Y.; Zhang, Y.; Liang, Y.; Liu, J. Efficient Wastewater Treatment by Membranes through Constructing Tunable Antifouling Membrane Surfaces. *Environ. Sci. Technol.* **2011***, 45*, 6545-6552.

Chu, P. K.; Chen, J. Y.; Wang, L. P.; Huang, N. Plasma-Surface Modification of Biomaterials. *Mater. Sci. Eng. R Rep.* **2002***, 36*, 143-206.

Chu, Z.; Feng, Y.; Seeger, S. Oil/Water Separation with Selective Superantiwetting/Superwetting Surface Materials. *Angew. Chem., Int. Ed.* **2015***, 54*, 2328-2338.

Coping with Water Scarcity. Challenge of the Twenty-First Century; United Nations (UN) Water. Food and Agricultural Association (FAO): 2007.

Dreyer, D. R.; Miller, D. J.; Freeman, B. D.; Paul, D. R.; Bielawski, C. W. Elucidating the Structure of Poly (dopamine). *Langmuir* **2012**, *28*, 6428-6435.

Drioli, E.; Romano, M. Progress and New Perspectives on Integrated Membrane Operations for Sustainable Industrial Growth. *Ind. Eng. Chem. Res.* **2001***, 40*, 1277-1300.

Du, J. R.; Peldszus, S.; Huck, P. M.; Feng, X. Modification of Poly (vinylidene fluoride) Ultrafiltration Membranes with Poly (vinyl alcohol) for Fouling Control in Drinking Water Treatment. *Water Res.* **2009***, 43*, 4559-4568.

Elimelech, M.; Chen, W. H.; Waypa, J. J. Measuring the Zeta (Electrokinetic) Potential of Reverse Osmosis Membranes by a Streaming Potential Analyzer. *Desalination* **1994***, 95*, 269-286.

Elimelech, M.; Zhu, X.; Childress, A. E.; Hong, S. Role of Membrane Surface Morphology in Colloidal Fouling of Cellulose Acetate and Composite Aromatic Polyamide Reverse Osmosis Membranes. *J. Membr. Sci.* **1997***, 127*, 101-109.

Fakhru'l-Razi, A.; Pendashteh, A.; Abdullah, L. C.; Biak, D. R. A.; Madaeni, S. S.; Abidin, Z. Z. Review of Technologies for Oil and Gas Produced Water Treatment. *J. Hazard. Mater.* **2009***, 170*, 530-551.

Fang, B.; Ling, Q.; Zhao, W.; Ma, Y.; Bai, P.; Wei, Q.; Li, H.; Zhao, C. Modification of Polyethersulfone Membrane by Grafting Bovine Serum Albumin on the Surface of Polyethersulfone/Poly (acrylonitrile-co-acrylic acid) Blended Membrane. *J. Membr. Sci.* **2009***, 329*, 46-55.

Feng, L.; Zhang, Z.; Mai, Z.; Ma, Y.; Liu, B.; Jiang, L.; Zhu, D. A Super-Hydrophobic and Super-Oleophilic Coating Mesh Film for the Separation of Oil and Water. *Angew. Chem., Inter. Ed.* **2004***, 43*, 2012-2014.

Fontananova, E.; Jansen, J. C.; Cristiano, A.; Curcio, E.; Drioli, E. Effect of Additives in the Casting Solution on the Formation of PVDF Membranes. *Desalination* **2006***, 192*, 190-197.

Fritt-Rasmussen, J.; Wegeberg, S.; Gustavson, K. Review on Burn Residues from In Situ Burning of Oil Spills in Relation to Arctic Waters. *Water Air Soil Pollut.* **2015***, 226*, 329.

Gao, H.; Sun, Y.; Zhou, J.; Xu, R.; Duan, H. Mussel-Inspired Synthesis of Polydopamine-Functionalized Graphene Hydrogel as Reusable Adsorbents for Water Purification. *ACS Appl. Mater. Interfaces* **2013***, 5*, 425-432.

Gao, X.; Xu, L.; Xue, Z.; Feng, L.; Peng, J.; Wen, Y.; Wang, S.; Zhang, X. Dual‐Scaled Porous Nitrocellulose Membranes with Underwater Superoleophobicity for Highly Efficient Oil/Water Separation. *Adv. Mater.* **2014***, 26*, 1771-1775.

Genzer, J.; Efimenko, K. Recent Developments in Superhydrophobic Surfaces and Their Relevance to Marine Fouling: A Review. *Biofouling* **2006***, 22*, 339-360.

Gohil, G. S.; Nagarale, R. K.; Binsu, V. V.; Shahi, V. K. Preparation and Characterization of Monovalent Cation Selective Sulfonated Poly (ether ether ketone) and Poly (ether sulfone) Composite Membranes. *J. Colloid Interface Sci.* **2006***, 298*, 845-853.

Guiver, M. D.; Robertson, G. P. Chemical Modification of Polysulfones: A Facile Method of Preparing Azide Derivatives from Lithiated Polysulfone Intermediates. *Macromolecules* **1995***, 28*, 294-301.

Herrwerth, S.; Eck, W.; Reinhardt, S.; Grunze, M. Factors that Determine the Protein Resistance of Oligoether Self-Assembled Monolayers−Internal Hydrophilicity, Terminal

Hydrophilicity, and Lateral Packing Density. *J. Am. Chem. Soc.* **2003***, 125*, 9359-9366.

Higuchi, A.; Iwata, N.; Tsubaki, M.; Nakagawa, T. Surface‐Modified Polysulfone Hollow Fibers. *J. Appl. Polym. Sci.* **1988***, 36*, 1753-1767.

Higuchi, A.; Mishima, S.; Nakagawa, T. Separation of Proteins by Surface Modified Polysulfone Membranes. *J. Membr. Sci.* **1991***, 57*, 175-185.

Hilal, N.; Ogunbiyi, O. O.; Miles, N. J.; Nigmatullin, R. Methods Employed for Control of Fouling in MF and UF Membranes: A Comprehensive Review. *Sep. Sci. Technol.* **2005***, 40*, 1957-2005.

Hiraoka, Y.; Sedat, J. W.; Agard, D. A. The Use of a Charge-Coupled Device for Quantitative Optical Microscopy of Biological Structures. *Science* **1987**, 36-41.

Hong, S.; Na, Y. S.; Choi, S.; Song, I. T.; Kim, W. Y.; Lee, H. Non‐Covalent Self-Assembly and Covalent Polymerization Co-Contribute to Polydopamine Formation. *Adv. Funct. Mater.* **2012***, 22*, 4711-4717.

Hsu, C. S. Infrared Spectroscopy. In *Handbook of Instrumental Techniques for Analytical Chemistry;* Prentice Hall: Englewood Cliffs, NJ, 1997; pp 247-283.

Huisman, I. H.; Prádanos, P.; Hernández, A. The Effect of Protein–Protein and Protein–Membrane Interactions on Membrane Fouling in Ultrafiltration. *J. Membr. Sci.* **2000***, 179*, 79-90.

Hyun, J.; Jang, H.; Kim, K.; Na, K.; Tak, T. Restriction of Biofouling in Membrane Filtration Using a Brush-Like Polymer Containing Oligoethylene Glycol Side Chains. *J. Membr. Sci.* **2006***, 282*, 52-59.

Ito, S.; Wakamatsu, K. Chemical Degradation of Melanins: Application to Identification of Dopamine‐Melanin. *Pigm. Cell Res.* **1998***, 11*, 120-126.

Ivshina, I. B.; Kuyukina, M. S.; Krivoruchko, A. V.; Elkin, A. A.; Makarov, S. O.; Cunningham,

C. J.; Peshkur, T. A.; Atlas, R. M.; Philp, J. C. Oil Spill Problems and Sustainable Response Strategies through New Technologies. *Environ. Sci.: Processes Impacts* **2015***, 17*, 1201-1219.

Jayalakshmi, A.; Rajesh, S.; Kim, I. C.; Senthilkumar, S.; Mohan, D.; Kwon, Y. Poly (isophthalamide) Based Graft Copolymer for the Modification of Cellulose Acetate Ultrafiltration Membranes and a Fouling Study by AFM Imaging. *J. Membr. Sci.* **2014***, 465*, 117-128.

Jayalakshmi, A.; Rajesh, S.; Mohan, D. Fouling Propensity and Separation Efficiency of Epoxidated Polyethersulfone Incorporated Cellulose Acetate Ultrafiltration Membrane in the Retention of Proteins. *Appl. Surf. Sci.* **2012***, 258*, 9770-9781.

Jayalakshmi, A.; Rajesh, S.; Senthilkumar, S.; Mohan, D. Epoxy Functionalized Poly (ether-sulfone) Incorporated Cellulose Acetate Ultrafiltration Membrane for the Removal of Chromium Ions. *Sep. Purif. Technol.* **2012***, 90*, 120-132.

Jhaveri, J. H.; Murthy, Z. A Comprehensive Review on Anti-Fouling Nanocomposite Membranes for Pressure Driven Membrane Separation Processes. *Desalination* **2016***, 379*, 137-154.

Jiang, J.; Zhu, L.; Zhu, L.; Zhang, H.; Zhu, B.; Xu, Y. Antifouling and Antimicrobial Polymer Membranes Based on Bioinspired Polydopamine and Strong Hydrogen-Bonded Poly (N-vinyl pyrrolidone). *ACS Appl. Mater. Interfaces* **2013***, 5*, 12895-12904.

Joss, A.; Zabczynski, S.; Gbel, A.; Hoffmann, B.; Lffler, D.; McArdell, C. S.; Ternes, T. A.; Thomsen, A.; Siegrist, H. Biological Degradation of Pharmaceuticals in Municipal Wastewater Treatment: Proposing a Classification Scheme. *Water Res.* **2006***, 40*, 1686-1696.

Ju, J.; Wang, T.; Wang, Q. Superhydrophilic and Underwater Superoleophobic PVDF Membranes via Plasma-Induced Surface PEGDA for Effective Separation of Oil-in-Water Emulsions. *Colloids Surf., A* **2015**, *481*, 151-157.

Juang, R.; Huang, C.; Hsieh, C. Surface Modification of PVDF Ultrafiltration Membranes by Remote Argon/Methane Gas Mixture Plasma for Fouling Reduction. *J. Taiwan Inst. Chem. Eng.* **2014***, 45*, 2176-2186.

Kaeselev, B.; Pieracci, J.; Belfort, G. Photoinduced Grafting of Ultrafiltration Membranes: Comparison of Poly (ether sulfone) and Poly (sulfone). *J. Membr. Sci.* **2001***, 194*, 245-261.

Kang, G.; Cao, Y. Application and Modification of Poly (vinylidene fluoride) (PVDF) Membranes-A Review. *J. Membr. Sci.* **2014***, 463*, 145-165.

Kang, S. M.; Hwang, N. S.; Yeom, J.; Park, S. Y.; Messersmith, P. B.; Choi, I. S.; Langer, R.; Anderson, D. G.; Lee, H. One-Step Multipurpose Surface Functionalization by Adhesive Catecholamine. *Adv. Funct. Mater.* **2012***, 22*, 2949-2955.

Kang, S. M.; Ryou, M.; Choi, J. W.; Lee, H. Mussel-and Diatom-Inspired Silica Coating on Separators Yields Improved Power and Safety in Li-Ion Batteries. *Chem. Mater.* **2012***, 24*, 3481-3485.

Kang, S.; Asatekin, A.; Mayes, A. M.; Elimelech, M. Protein Antifouling Mechanisms of PAN UF Membranes Incorporating PAN-g-PEO Additive. *J. Membr. Sci.* **2007***, 296*, 42-50.

Khulbe, K.; Hamad, F.; Feng, C.; Matsuura, T.; Khayet, M. Study of the Surface of the Water Treated Cellulose Acetate Membrane by Atomic Force Microscopy. *Desalination* **2004***, 161*, 259-262.

Kim, I.; Lee, K. Dyeing Process Wastewater Treatment Using Fouling Resistant Nanofiltration and Reverse Osmosis Membranes. *Desalination* **2006***, 192*, 246-251.

Kim, K. J.; Fane, A. G.; Fell, C. The Performance of Ultrafiltration Membranes Pretreated by Polymers. *Desalination* **1988***, 70*, 229-249.

Kleindienst, S.; Paul, J. H.; Joye, S. B. Using Dispersants after Oil Spills: Impacts on the

Composition and Activity of Microbial Communities. *Nat. Rev. Micro.* **2015***, 13*, 388.

Kota, A. K.; Kwon, G.; Choi, W.; Mabry, J. M.; Tuteja, A. Hygro-Responsive Membranes for Effective Oil-Water Separation. *Nat. Commun.* **2012***, 3*, 1025-1030.

Kwon, G.; Kota, A.; Li, Y.; Sohani, A.; Mabry, J. M.; Tuteja, A. On-Demand Separation of Oil-Water Mixtures. *Adv. Mater.* **2012***, 24*, 3666-3671.

Lahann, J. Environmental Nanotechnology: Nanomaterials Clean Up. *Nature Nanotech.* **2008***, 3*, 320-321.

Lee, H.; Dellatore, S. M.; Miller, W. M.; Messersmith, P. B. Mussel-Inspired Surface Chemistry for Multifunctional Coatings. *Science* **2007***, 318*, 426-430.

Lei, J.; Ulbricht, M. Macroinitiator-Mediated Photoreactive Coating of Membrane Surfaces with Antifouling Hydrogel Layers. *J. Membr. Sci.* **2014***, 455*, 207-218.

Li, J.; Xu, Z.; Yang, H.; Yu, L.; Liu, M. Effect of TiO_2 Nanoparticles on the Surface Morphology and Performance of Microporous PES Membrane. *Appl. Surf. Sci.* **2009***, 255*, 4725-4732.

Li, J.; Yan, L.; Zhao, Y.; Zha, F.; Wang, Q.; Lei, Z. One-Step Fabrication of Robust Fabrics with Both-Faced Superhydrophobicity for the Separation and Capture of Oil from Water. *Phys. Chem. Chem. Phys.* **2015***, 17*, 6451-6457.

Liebscher, J.; Mrówczyński, R.; Scheidt, H. A.; Filip, C.; Hădade, N. D.; Turcu, R.; Bende, A.; Beck, S. Structure of Polydopamine: A Never-Ending Story? *Langmuir* **2013***, 29*, 10539-10548.

Liu, F.; Du, C.; Zhu, B.; Xu, Y. Surface Immobilization of Polymer Brushes onto Porous Poly (vinylidene fluoride) Membrane by Electron Beam to Improve the Hydrophilicity and Fouling Resistance. *Polymer* **2007***, 48*, 2910-2918.

Liu, F.; Hashim, N. A.; Liu, Y.; Abed, M. M.; Li, K. Progress in the Production and Modification

of PVDF Membranes. *J. Membr. Sci.* **2011***, 375*, 1-27.

Liu, M.; Wang, S.; Wei, Z.; Song, Y.; Jiang, L. Bioinspired Design of a Superoleophobic and Low Adhesive Water/Solid Interface. *Adv. Mater.* **2009***, 21*, 665-669.

Liu, N.; Chen, Y.; Lu, F.; Cao, Y.; Xue, Z.; Li, K.; Feng, L.; Wei, Y. Straightforward Oxidation of a Copper Substrate Produces an Underwater Superoleophobic Mesh for Oil/Water Separation. *ChemPhysChem* **2013***, 14*, 3489-3494.

Liu, Y.; Ai, K.; Lu, L. Polydopamine and Its Derivative Materials: Synthesis and Promising Applications in Energy, Environmental, and Biomedical Fields. *Chem. Rev.* **2014***, 114*, 5057-5115.

Liu, Y.; Chang, C.; Sun, T. Dopamine-Assisted Deposition of Dextran for Nonfouling Applications. *Langmuir* **2014***, 30*, 3118-3126.

Luo, C.; Liu, Q. Oxidant-Induced High-Efficient Mussel-Inspired Modification on PVDF Membrane with Superhydrophilicity and Underwater Superoleophobicity Characteristics for Oil/Water Separation. *ACS Appl. Mater. Interfaces* **2017***, 9*, 8297-8307.

Luo, M.; Zhao, J.; Tang, W.; Pu, C. Hydrophilic Modification of Poly (ether sulfone) Ultrafiltration Membrane Surface by Self-Assembly of TiO_2 Nanoparticles. *Appl. Surf. Sci.* **2005***, 249*, 76-84.

Ma, Q.; Cheng, H.; Fane, A. G.; Wang, R.; Zhang, H. Recent Development of Advanced Materials with Special Wettability for Selective Oil/Water Separation. *Small* **2016***, 12*, 2186-2202.

Makhlouf, C.; Marais, S.; Roudesli, S. Graft Copolymerization of Acrylic Acid onto Polyamide Fibers. *Appl. Surf. Sci.* **2007***, 253*, 5521-5528.

Malaisamy, R.; Mahendran, R.; Mohan, D.; Rajendran, M.; Mohan, V. Cellulose Acetate and Sulfonated Polysulfone Blend Ultrafiltration Membranes. I. Preparation and

Characterization. *J. Appl. Polym. Sci.* **2002***, 86*, 1749-1761.

Mansourpanah, Y.; Madaeni, S. S.; Rahimpour, A.; Farhadian, A.; Taheri, A. H. Formation of Appropriate Sites on Nanofiltration Membrane Surface for Binding TiO_2 Photo-Catalyst: Performance, Characterization and Fouling-Resistant Capability. *J. Membr. Sci.* **2009***, 330*, 297-306.

Masuelli, M.; Marchese, J.; Ochoa, N. A. SPC/PVDF Membranes for Emulsified Oily Wastewater Treatment. *J. Membr. Sci.* **2009***, 326*, 688-693.

Maximous, N.; Nakhla, G.; Wan, W.; Wong, K. Preparation, Characterization and Performance of Al_2O_3/PES Membrane for Wastewater Filtration. *J. Membr. Sci.* **2009***, 341*, 67-75.

Meng, F.; Chae, S.; Drews, A.; Kraume, M.; Shin, H.; Yang, F. Recent Advances in Membrane Bioreactors (MBRs): Membrane Fouling and Membrane Material. *Water Res.* **2009***, 43*, 1489-1512.

Mueller, J.; Davis, R. H. Protein Fouling of Surface-Modified Polymeric Microfiltration Membranes. *J. Membr. Sci.* **1996***, 116*, 47-60.

Muppalla, R.; Rana, H. H.; Devi, S.; Jewrajka, S. K. Adsorption of pH-Responsive Amphiphilic Copolymer Micelles and Gel on Membrane Surface as an Approach for Antifouling Coating. *Appl. Surf. Sci.* **2013***, 268*, 355-367.

Nabe, A.; Staude, E.; Belfort, G. Surface Modification of Polysulfone Ultrafiltration Membranes and Fouling by BSA Solutions. *J. Membr. Sci.* **1997***, 133*, 57-72.

Nagendran, A.; Arockiasamy, D. L.; Mohan, D. Cellulose Acetate and Polyetherimide Blend Ultrafiltration Membranes, I: Preparation, Characterization, and Application. *Mater. Manuf. Process.* **2008***, 23*, 311-319.

Nakao, S.; Osada, H.; Kurata, H.; Tsuru, T.; Kimura, S. Separation of Proteins by Charged

Ultrafiltration Membranes. *Desalination* **1988***, 70*, 191-205.

Nguyen, T. P. N.; Yun, E.; Kim, I.; Kwon, Y. Preparation of Cellulose Triacetate/Cellulose Acetate (CTA/CA)-Based Membranes for Forward Osmosis. *J. Membr. Sci.* **2013***, 433*, 49-59.

Nystrm, M. Fouling of Unmodified and Modified Polysulfone Ultrafiltration Membranes by Ovalbumin. *J. Membr. Sci.* **1989***, 44*, 183-196.

Ochoa, N.; Masuelli, M.; Marchese, J. Effect of Hydrophilicity on Fouling of an Emulsified Oil Wastewater with PVDF/PMMA Membranes. *J. Membr. Sci.* **2003***, 226*, 203-211.

Oh, S.; Kim, N.; Lee, Y. Preparation and Characterization of PVDF/TiO_2 Organic-Inorganic Composite Membranes for Fouling Resistance Improvement. *J. Membr. Sci.* **2009***, 345*, 13-20.

Padaki, M.; Murali, R. S.; Abdullah, M. S.; Misdan, N.; Moslehyani, A.; Kassim, M. A.; Hilal, N.; Ismail, A. F. Membrane Technology Enhancement in Oil–Water Separation. A Review. *Desalination* **2015***, 357*, 197-207.

Peng, J.; Su, Y.; Shi, Q.; Chen, W.; Jiang, Z. Protein Fouling Resistant Membrane Prepared by Amphiphilic Pegylated Polyethersulfone. *Bioresour. Technol.* **2011***, 102*, 2289-2295.

Perkampus, H.; Grinter, H. *UV-VIS Spectroscopy and Its Applications*; Springer: 1992.

Pi, J.; Yang, H.; Wan, L.; Wu, J.; Xu, Z. Polypropylene Microfiltration Membranes Modified with TiO_2 Nanoparticles for Surface Wettability and Antifouling Property. *J. Membr. Sci.* **2016***, 500*, 8-15.

Pieracci, J.; Crivello, J. V.; Belfort, G. Increasing Membrane Permeability of UV-Modified Poly (ether sulfone) Ultrafiltration Membranes. *J. Membr. Sci.* **2002***, 202*, 1-16.

Pieracci, J.; Wood, D. W.; Crivello, J. V.; Belfort, G. UV-Assisted Graft Polymerization of N-vinyl-2-pyrrolidinone onto Poly (ether sulfone) Ultrafiltration Membranes: Comparison of

Dip Versus Immersion Modification Techniques. *Chem. Mater.* **2000***, 12*, 2123-2133.

Ponzio, F.; Barthes, J.; Bour, J.; Michel, M.; Bertani, P.; Hemmerlé, J.; d'Ischia, M.; Ball, V. Oxidant Control of Polydopamine Surface Chemistry in Acids: A Mechanism-Based Entry to Superhydrophilic-Superoleophobic Coatings. *Chem. Mater.* **2016***, 28*, 4697-4705.

Raaman, N. *Phytochemical Techniques*; New India Publishing: 2006.

Rana, D.; Matsuura, T. Surface Modifications for Antifouling Membranes. *Chem. Rev.* **2010***, 110*, 2448-2471.

Reddy, A.; Trivedi, J. J.; Devmurari, C. V.; Mohan, D. J.; Singh, P.; Rao, A. P.; Joshi, S. V.; Ghosh, P. K. Fouling Resistant Membranes in Desalination and Water Recovery. *Desalination* **2005***, 183*, 301-306.

Reichelt, R. Scanning Electron Microscopy. In *Science of Microscopy;* Springer: 2007; pp 133-272.

Saljoughi, E.; Mohammadi, T. Cellulose Acetate (CA)/Polyvinylpyrrolidone (PVP) Blend Asymmetric Membranes: Preparation, Morphology and Performance. *Desalination* **2009***, 249*, 850-854.

Saxena, A.; Tripathi, B. P.; Kumar, M.; Shahi, V. K. Membrane-Based Techniques for the Separation and Purification of Proteins: An Overview. *Adv. Colloid Interface Sci.* **2009***, 145*, 1-22.

Schmidt, C. K.; Brauch, H. N, N-dimethylsulfamide as Precursor for N-nitrosodimethylamine (NDMA) Formation upon Ozonation and Its Fate during Drinking Water Treatment. *Environ. Sci. Technol.* **2008***, 42*, 6340-6346.

Schrope, M. Deep Wounds. *Nature* **2011***, 472*, 152-154.

Shang, J.; Flury, M.; Harsh, J. B.; Zollars, R. L. Comparison of Different Methods to Measure

Contact Angles of Soil Colloids. *J. Colloid Interface Sci.* **2008***, 328*, 299-307.

Shannon, M. A.; Bohn, P. W.; Elimelech, M.; Georgiadis, J. G.; Marias, B. J.; Mayes, A. M. Science and Technology for Water Purification in the Coming Decades. *Nature* **2008***, 452*, 301-310.

Shao, L.; Wang, Z. X.; Zhang, Y. L.; Jiang, Z. X.; Liu, Y. Y. A Facile Strategy to Enhance PVDF Ultrafiltration Membrane Performance via Self-Polymerized Polydopamine Followed by Hydrolysis of Ammonium Fluotitanate. *J. Membr. Sci.* **2014***, 461*, 10-21.

Shen, L.; Xu, Z.; Liu, Z.; Xu, Y. Ultrafiltration Hollow Fiber Membranes of Sulfonated Polyetherimide/Polyetherimide Blends: Preparation, Morphologies and Anti-Fouling Properties. *J. Membr. Sci.* **2003***, 218*, 279-293.

Shi, H.; He, Y.; Pan, Y.; Di, H.; Zeng, G.; Zhang, L.; Zhang, C. A Modified Mussel-Inspired Method to Fabricate TiO_2 Decorated Superhydrophilic PVDF Membrane for Oil/Water Separation. *J. Membr. Sci.* **2016***, 506*, 60-70.

Stamm, M. *Polymer Surfaces and Interfaces*; Springer: 2008.

Sugimura, Y.; Suzuki, Y. A High-Temperature Catalytic Oxidation Method for the Determination of Non-Volatile Dissolved Organic Carbon in Seawater by Direct Injection of a Liquid Sample. *Mar. Chem.* **1988***, 24*, 105-131.

Sui, Y.; Gao, X.; Wang, Z.; Gao, C. Antifouling and Antibacterial Improvement of Surface-Functionalized Poly (vinylidene fluoride) Membrane Prepared via Dihydroxyphenylalanine-Initiated Atom Transfer Radical Graft Polymerizations. *J. Membr. Sci.* **2012***, 394*, 107-119.

Sun, T.; Feng, L.; Gao, X.; Jiang, L. Bioinspired Surfaces with Special Wettability. *Acc. Chem. Res.* **2005***, 38*, 644-652.

Susanto, H.; Ulbricht, M. Photografted Thin Polymer Hydrogel Layers on PES Ultrafiltration

Membranes: Characterization, Stability, and Influence on Separation Performance. *Langmuir* **2007***, 23*, 7818-7830.

Tang, C.; Ye, S.; Liu, H. Electrospinning of Poly (styrene-co-maleic anhydride) (SMA) and Water-Swelling Behavior of Crosslinked/Hydrolyzed SMA Hydrogel Nanofibers. *Polymer* **2007***, 48*, 4482-4491.

Ulbricht, M.; Richau, K.; Kamusewitz, H. Chemically and Morphologically Defined Ultrafiltration Membrane Surfaces Prepared by Heterogeneous Photo-Initiated Graft Polymerization. *Colloids Surfaces A: Physicochem. Eng. Aspects* **1998***, 138*, 353-366.

Van der Bruggen, B. Chemical Modification of Polyethersulfone Nanofiltration Membranes: A Review. *J. Appl. Polym. Sci.* **2009***, 114*, 630-642.

Vatanpour, V.; Madaeni, S. S.; Khataee, A. R.; Salehi, E.; Zinadini, S.; Monfared, H. A. TiO_2 Embedded Mixed Matrix PES Nanocomposite Membranes: Influence of Different Sizes and Types of Nanoparticles on Antifouling and Performance. *Desalination* **2012***, 292*, 19-29.

Wang, B.; Liang, W.; Guo, Z.; Liu, W. Biomimetic Super-Lyophobic and Super-Lyophilic Materials Applied for Oil/Water Separation: A New Strategy Beyond Nature. *Chem. Soc. Rev.* **2015***, 44*, 336-361.

Wang, F.; Lei, S.; Xue, M.; Ou, J.; Li, C.; Li, W. Superhydrophobic and Superoleophilic Miniature Device for the Collection of Oils from Water Surfaces. *J. Phys. Chem. C* **2014***, 118*, 6344-6351.

Wang, J.; Chen, Y. Oil-Water Separation Capability of Superhydrophobic Fabrics Fabricated via Combining Polydopamine Adhesion with Lotus-Leaf-Like Structure. *J. Appl. Polym. Sci.* **2015***, 132*, 42614.

Wang, Z.; Jiang, X.; Cheng, X.; Lau, C. H.; Shao, L. Mussel-Inspired Hybrid Coatings that

Transform Membrane Hydrophobicity into High Hydrophilicity and Underwater Superoleophobicity for Oil-in-Water Emulsion Separation. *ACS Appl. Mater. Interfaces* **2015**, *7*, 9534-9545.

Watts, J. F. X-Ray Photoelectron Spectroscopy. *Vacuum* **1994**, *45*, 653-671.

Wei, H.; Ren, J.; Han, B.; Xu, L.; Han, L.; Jia, L. Stability of Polydopamine and Poly (DOPA) Melanin-Like Films on the Surface of Polymer Membranes under Strongly Acidic and Alkaline Conditions. *Colloids Surf., B* **2013**, *110*, 22-28.

Wenzel, R. N. Resistance of Solid Surfaces to Wetting by Water. *Ind. Eng. Chem.* **1936**, *28*, 988-994.

Werner, C.; Krber, H.; Zimmermann, R.; Dukhin, S.; Jacobasch, H. Extended Electrokinetic Characterization of Flat Solid Surfaces. *J. Colloid Interface Sci.* **1998**, *208*, 329-346.

Xi, Z.; Xu, Y.; Zhu, L.; Wang, Y.; Zhu, B. A Facile Method of Surface Modification for Hydrophobic Polymer Membranes Based on the Adhesive Behavior of Poly (DOPA) and Poly (dopamine). *J. Membr. Sci.* **2009**, *327*, 244-253.

Xiang, Y.; Liu, F.; Xue, L. Under Seawater Superoleophobic PVDF Membrane Inspired by Polydopamine for Efficient Oil/Seawater Separation. *J. Membr. Sci.* **2015**, *476*, 321-329.

Xu, Z.; Huang, X.; Wan, L. *Surface Engineering of Polymer Membranes*; Springer Science & Business Media: 2009.

Xue, C.; Ji, P.; Zhang, P.; Li, Y.; Jia, S. Fabrication of Superhydrophobic and Superoleophilic Textiles for Oil-Water Separation. *Appl. Surf. Sci.* **2013**, *284*, 464-471.

Xue, Z.; Cao, Y.; Liu, N.; Feng, L.; Jiang, L. Special Wettable Materials for Oil/Water Separation. *J. Mater. Chem. A* **2014**, *2*, 2445-2460.

Xue, Z.; Wang, S.; Lin, L.; Chen, L.; Liu, M.; Feng, L.; Jiang, L. A Novel Superhydrophilic and

Underwater Superoleophobic Hydrogel-Coated Mesh for Oil/Water Separation. *Adv. Mater.* **2011***, 23*, 4270-4273.

Yamato, N.; Kimura, K.; Miyoshi, T.; Watanabe, Y. Difference in Membrane Fouling in Membrane Bioreactors (MBRs) Caused by Membrane Polymer Materials. *J. Membr. Sci.* **2006***, 280*, 911-919.

Yang, H.; Chen, Y.; Ye, C.; Jin, Y.; Li, H.; Xu, Z. Polymer Membrane with a Mineral Coating for Enhanced Curling Resistance and Surface Wettability. *Chem. Commun.* **2015***, 51*, 12779-12782.

Yang, H.; Lan, Y.; Zhu, W.; Li, W.; Xu, D.; Cui, J.; Shen, D.; Li, G. Polydopamine-Coated Nanofibrous Mats as a Versatile Platform for Producing Porous Functional Membranes. *J. Mater. Chem.* **2012***, 22*, 16994-17001.

Yang, H.; Liao, K.; Huang, H.; Wu, Q.; Wan, L.; Xu, Z. Mussel-Inspired Modification of a Polymer Membrane for Ultra-High Water Permeability and Oil-in-Water Emulsion Separation. *J. Mater. Chem. A* **2014***, 2*, 10225-10230.

Yang, H.; Luo, J.; Lv, Y.; Shen, P.; Xu, Z. Surface Engineering of Polymer Membranes via Mussel-Inspired Chemistry. *J. Membr. Sci.* **2015***, 483*, 42-59.

Yang, H.; Pi, J.; Liao, K.; Huang, H.; Wu, Q.; Huang, X.; Xu, Z. Silica-Decorated Polypropylene Microfiltration Membranes with a Mussel-Inspired Intermediate Layer for Oil-in-Water Emulsion Separation. *ACS Appl. Mater. Interfaces* **2014***, 6*, 12566-12572.

Yang, H.; Wu, M.; Li, Y.; Chen, Y.; Wan, L.; Xu, Z. Effects of Polyethyleneimine Molecular Weight and Proportion on the Membrane Hydrophilization by Codepositing with Dopamine. *J. Appl. Polym. Sci.* **2016***, 133*.

Yang, J.; Zhang, Z.; Xu, X.; Zhu, X.; Men, X.; Zhou, X. Superhydrophilic–Superoleophobic

Coatings. *J. Mater. Chem.* **2012***, 22*, 2834-2837.

Yang, L.; Phua, S. L.; Toh, C. L.; Zhang, L.; Ling, H.; Chang, M.; Zhou, D.; Dong, Y.; Lu, X. Polydopamine-Coated Graphene as Multifunctional Nanofillers in Polyurethane. *RSC Adv.* **2013***, 3*, 6377-6385.

Yang, X.; Zhang, B.; Liu, Z.; Deng, B.; Yu, M.; Li, L.; Jiang, H.; Li, J. Preparation of the Antifouling Microfiltration Membranes from Poly (N, N-dimethylacrylamide) Grafted Poly (vinylidene fluoride) (PVDF) Powder. *J. Mater. Chem.* **2011***, 21*, 11908-11915.

Yang, Y.; Li, Y.; Li, Q.; Wan, L.; Xu, Z. Surface Hydrophilization of Microporous Polypropylene Membrane by Grafting Zwitterionic Polymer for Anti-Biofouling. *J. Membr. Sci.* **2010***, 362*, 255-264.

Yao, X.; Song, Y.; Jiang, L. Applications of Bio‐Inspired Special Wettable Surfaces. *Adv. Mater.* **2011***, 23*, 719-734.

You, I.; Kang, S. M.; Byun, Y.; Lee, H. Enhancement of Blood Compatibility of Poly (urethane) Substrates by Mussel-Inspired Adhesive Heparin Coating. *Bioconjug. Chem.* **2011***, 22*, 1264-1269.

Yu, H.; He, X.; Liu, L.; Gu, J.; Wei, X. Surface Modification of Polypropylene Microporous Membrane to Improve Its Antifouling Characteristics in an SMBR: N_2 Plasma Treatment. *Water Res.* **2007***, 41*, 4703-4709.

Yu, H.; Hu, M.; Xu, Z.; Wang, J.; Wang, S. Surface Modification of Polypropylene Microporous Membranes to Improve Their Antifouling Property in MBR: NH_3 Plasma Treatment. *Sep. Purif. Technol.* **2005***, 45*, 8-15.

Yu, H.; Liu, L.; Tang, Z.; Yan, M.; Gu, J.; Wei, X. Surface Modification of Polypropylene Microporous Membrane to Improve Its Antifouling Characteristics in an SMBR: Air Plasma

Treatment. *J. Membr. Sci.* **2008***, 311*, 216-224.

Yu, H.; Xie, Y.; Hu, M.; Wang, J.; Wang, S.; Xu, Z. Surface Modification of Polypropylene Microporous Membrane to Improve Its Antifouling Property in MBR: CO_2 Plasma Treatment. *J. Membr. Sci.* **2005***, 254*, 219-227.

Yu, L.; Xu, Z.; Shen, H.; Yang, H. Preparation and Characterization of PVDF–SiO_2 Composite Hollow Fiber UF Membrane by Sol–Gel Method. *J. Membr. Sci.* **2009***, 337*, 257-265.

Zhang, C.; Li, H.; Du, Y.; Ma, M.; Xu, Z. $CuSO_4/H_2O_2$-Triggered Polydopamine/Poly (sulfobetaine methacrylate) Coatings for Antifouling Membrane Surfaces. *Langmuir* **2017***, 33*, 1210-1216.

Zhang, C.; Yang, H.; Wan, L.; Liang, H.; Li, H.; Xu, Z. Polydopamine-Coated Porous Substrates as a Platform for Mineralized β-FeOOH Nanorods with Photocatalysis under Sunlight. *ACS Appl. Mater. Interfaces* **2015***, 7*, 11567-11574.

Zhang, F.; Zhang, W. B.; Shi, Z.; Wang, D.; Jin, J.; Jiang, L. Nanowire‐Haired Inorganic Membranes with Superhydrophilicity and Underwater Ultralow Adhesive Superoleophobicity for High‐Efficiency Oil/Water Separation. *Adv. Mater.* **2013***, 25*, 4192-4198.

Zhang, J.; Huang, W.; Han, Y. A Composite Polymer Film with Both Superhydrophobicity and Superoleophilicity. *Macromol. Rapid Commun.* **2006***, 27*, 804-808.

Zhang, R.; Liu, Y.; He, M.; Su, Y.; Zhao, X.; Elimelech, M.; Jiang, Z. Antifouling Membranes for Sustainable Water Purification: Strategies and Mechanisms. *Chem. Soc. Rev.* **2016***, 45*, 5888-5924.

Zhang, W.; Shi, Z.; Zhang, F.; Liu, X.; Jin, J.; Jiang, L. Superhydrophobic and Superoleophilic PVDF Membranes for Effective Separation of Water-in-Oil Emulsions with High Flux. *Adv.*

Mater. **2013**, *25*, 2071-2076.

Zhang, W.; Zhu, Y.; Liu, X.; Wang, D.; Li, J.; Jiang, L.; Jin, J. Salt-Induced Fabrication of Superhydrophilic and Underwater Superoleophobic PAA-g-PVDF Membranes for Effective Separation of Oil-in-Water Emulsions. *Angew. Chem., Int. Ed.* **2014**, *53*, 856-860.

Zhao, Z.; Wang, Z.; Wang, S. Formation, Charged Characteristic and BSA Adsorption Behavior of Carboxymethyl Chitosan/PES Composite MF Membrane. *J. Membr. Sci.* **2003***, 217*, 151-158.

Zhao, Z.; Wang, Z.; Ye, N.; Wang, S. A Novel N, O-Carboxymethyl Amphoteric Chitosan/Poly (ethersulfone) Composite MF Membrane and Its Charged Characteristics. *Desalination* **2002***, 144*, 35-39.

Zheng, J.; Li, L.; Tsao, H.; Sheng, Y.; Chen, S.; Jiang, S. Strong Repulsive Forces Between Protein and Oligo (ethylene glycol) Self-Assembled Monolayers: A Molecular Simulation Study. *Biophys. J.* **2005***, 89*, 158-166.

Zhou, R.; Ren, P.; Yang, H.; Xu, Z. Fabrication of Antifouling Membrane Surface by Poly (sulfobetaine methacrylate)/Polydopamine Co-Deposition. *J. Membr. Sci.* **2014***, 466*, 18-25.

Zhu, L.; Liu, F.; Yu, X.; Gao, A.; Xue, L. Surface Zwitterionization of Hemocompatible Poly (lactic acid) Membranes for Hemodiafiltration. *J. Membr. Sci.* **2015***, 475*, 469-479.

Zhu, L.; Zhu, L.; Jiang, J.; Yi, Z.; Zhao, Y.; Zhu, B.; Xu, Y. Hydrophilic and Anti-Fouling Polyethersulfone Ultrafiltration Membranes with Poly (2-hydroxyethyl methacrylate) Grafted Silica Nanoparticles as Additive. *J. Membr. Sci.* **2014***, 451*, 157-168.

Zhu, Y.; Wang, D.; Jiang, L.; Jin, J. Recent Progress in Developing Advanced Membranes for Emulsified Oil/Water Separation. *NPG Asia Mater.* **2014**, *6*, e101.

Zhu, Y.; Zhang, F.; Wang, D.; Pei, X. F.; Zhang, W.; Jin, J. A Novel Zwitterionic Polyelectrolyte

Grafted PVDF Membrane for Thoroughly Separating Oil from Water with Ultrahigh Efficiency. *J. Mater. Chem. A* **2013***, 1*, 5758-5765.